

**IMPLICATIONS OF AN INTERACTION BETWEEN PINK1 AND VCP FOR
PARKINSON'S DISEASE PATHOGENESIS**

by

Erin Kay Steer

B.A. in Biology, Concordia College, 2010

Submitted to the Graduate Faculty of
The School of Medicine in partial fulfillment
of the requirements for the degree of
Ph.D. in Cellular and Molecular Pathology

University of Pittsburgh

2015

UNIVERSITY OF PITTSBURGH
SCHOOL OF MEDICINE

This dissertation was presented

by

Erin Kay Steer

It was defended on

November 24, 2015

and approved by

Scott M. Kulich, MD, PhD, Associate Professor

Jeffrey L. Brodsky, PhD, Professor

Kirill Kiselyov, PhD, Associate Professor

Yoram Vodovotz, PhD, Professor

Dissertation Advisor: Charleen T. Chu, MD, PhD, Professor

Copyright © by Erin Kay Steer

2015

IMPLICATIONS OF AN INTERACTION BETWEEN PINK1 AND VCP FOR PARKINSON'S DISEASE PATHOGENESIS

Erin Kay Steer, PhD

University of Pittsburgh, 2015

Parkinson's disease (PD) is the most common neurodegenerative movement disorder, and affects approximately 950 per 100,000 people in North America. The etiology of PD remains unknown, but a small percentage of affected individuals have heritable forms of the disease with known genetic causes. Study of the proteins encoded by these genes has provided tremendous insight into molecular pathways that underlie PD-associated neurodegeneration. Mutations in the gene encoding PTEN-induced kinase 1 (PINK1) have been identified as the cause of an autosomal, recessively inherited parkinsonism. PINK1 is a serine/threonine kinase, uniquely localized to both the cytosol and mitochondrion. The profound effect of PINK1 on mitochondrial homeostasis has been extensively investigated, but far less is understood about its function in the cytosol. This project aimed to identify cytosolic PINK1 interacting proteins and characterize the functional consequences of the association. Using an unbiased proteomic screen, valosin-containing protein (VCP), an AAA+ ATPase, was identified as a PINK1 interactor. Upon discovery that the physical association does not require mitochondrial localization, the role of VCP in previously identified functions of the cytosolic pool of PINK1 was examined. These studies discovered a PINK1-VCP pathway that promotes neurite extension and complexity, and contributes to the maturation and maintenance of synapses. Further, PINK1 and VCP were shown to co-regulate autophagy and the accumulation of high molecular weight ubiquitination

products. These results indicate that the PINK1-VCP interaction plays a key role in dendritic arbor maintenance, synapse preservation, and autophagy regulation. These three processes are commonly impaired in sporadic and familial PD as well as other neurodegenerative diseases, indicating that treatments targeting components of the PINK1-VCP signaling hub may have broad therapeutic applications.

TABLE OF CONTENTS

PREFACE.....	XIV
1.0 INTRODUCTION	1
1.1 PARKINSON’S DISEASE	2
1.1.1 Treatment of PD.....	3
1.1.2 Synaptic pathology in PD	4
1.1.3 Autophagy in PD.....	5
1.2 PTEN-INDUCED KINASE 1	7
1.2.1 Domains	8
1.2.2 Mitochondrial import and processing	9
1.2.3 PINK1 protects against apoptosis induced by parkinsonian injury.	12
1.2.4 Mitochondrial functions of PINK1	12
1.2.4.1 Energized mitochondria.....	12
1.2.4.2 Depolarized mitochondria	14
1.2.5 Role of PINK1 in neurite maintenance and synaptic function.....	17
1.2.6 Role of PINK1 in autophagy regulation	18
1.3 VALOSIN CONTAINING PROTEIN IN NEURODEGENERATION	20

1.4	FUNCTIONS OF NEUROFIBROMIN 1 IN THE CENTRAL NERVOUS SYSTEM	23
1.5	COLLAPSIN RESPONSE MEDIATOR PROTEIN 2 IN NEURONAL MORPHOGENESIS	26
2.0	RATIONALE AND HYPOTHESIS	29
3.0	MATERIALS AND METHODS	30
3.1	PINK1 KO MICE	30
3.2	CELL CULTURE	30
3.2.1	Mouse primary neuron isolation	30
3.2.2	Human and mouse cell culture	31
3.2.3	Pharmacological treatments	32
3.2.4	Plasmids, siRNA, and transfections	32
3.3	BIOCHEMICAL ANALYSES	34
3.3.1	Cell lysis	34
3.3.2	Immunoprecipitations	34
3.3.3	Mass spectrometry for protein identification	35
3.3.4	Immunoblotting	36
3.3.5	Two-dimensional gel electrophoresis	38
3.4	IMAGE ANALYSES	39
3.4.1	Immunocytochemistry	39
3.4.2	Neurite length	40
3.4.3	Primary dendrite analysis	40
3.4.4	Sholl analysis	41

3.4.5	Dendritic spine analysis	41
3.4.6	Autophagosome number	42
3.5	STATISTICAL ANALYSES	42
4.0	RESULTS	43
4.1	PINK1 PROMOTES NEURONAL DIFFERENTIATION	43
4.2	PINK1 INTERACTS WITH VCP.....	45
4.2.1	Mass spectrometric identification of PINK1-VCP interaction	45
4.2.2	Immunoblot validation of PINK1-VCP interaction	46
4.2.3	Mitochondrial localization is not required for PINK1-VCP binding.....	47
4.2.4	PINK1 does not regulate post-translational modification of VCP.....	50
4.3	VCP ACTS DOWNSTREAM OF PINK1 TO PROMOTE NEURITE EXTENSION AND DENDRITIC COMPLEXITY	51
4.3.1	VCP overexpression protects against PINK1 KD induced neurite retraction..	51
4.3.2	PINK1 requires VCP expression to promote dendrite complexity	53
4.3.3	PINK1 interacts with the D1 domain of VCP	55
4.3.4	PINK1 requires NF1 to promote neurite outgrowth and dendrite complexity.	57
4.3.5	VCP binding is impaired in two PD-associated PINK1 mutants.....	60
4.4	PINK1 INTERACTS WITH CRMP2	62
4.4.1	PINK1 regulates CRMP2 phosphorylation.....	64
4.4.2	PINK1 does not affect CRMP2-Tubulin binding	67
4.5	PINK1 REGULATES SYNAPSES	68
4.6	PINK1 AND VCP CO-REGULATE AUTOPHAGY	71

4.6.1	PINK1 expression modulates sensitivity to autophagy induced by chemical inhibition of VCP	71
4.6.2	VCP protects against autophagosome accumulation induced by PINK1 knockdown	73
4.6.3	Role of autophagy in PINK1-induced neurite extension	74
4.6.4	PKA phosphorylation of LC3 in PINK1 overexpressing cells	75
4.6.5	PINK1 overexpression promotes accumulation of high molecular weight ubiquitinated proteins	78
5.0	DISCUSSION	81
5.1	PINK1-VCP-NF1-CRMP2 AS A SIGNALING HUB THAT REGUALTES NEURONAL MORPHOLOGY	82
5.2	REGULATION OF SYNAPSES BY PINK1	84
5.3	PINK1 AND VCP COOPERATE TO REGULATE AUTOPHAGY	87
5.4	LIMITATIONS TO DATA INTERPRETATION	93
6.0	FUTURE DIRECTIONS.....	94
6.1	PINK1 AND SYNAPTIC CALCIUM	94
6.2	REGULATION OF CRMP2 PHOSPHORYLATION BY PINK1.....	96
6.3	PINK1 AND CRMP2 IN REGULATION OF MITOCHONDRIAL TRAFFICKING	98
6.4	REGULATION OF UBIQUITINATED PROTEINS BY PINK1-VCP.....	99
6.5	CRMP2 PHOSPHORYLATION IN PD, IBMPFD, AND NEUROFIBROMATOSIS	102
7.0	SUMMARY	104

BIBLIOGRAPHY..... 107

LIST OF TABLES

Table 1: Antibodies and dilutions used for immunoblotting.	37
Table 2: Antibodies and dilutions used for immunocytochemistry	40
Table 3: PINK1 interacting proteins identified by mass spectrometry.....	45

LIST OF FIGURES

Figure 1: Spine morphology	4
Figure 2: Domain structure of PTEN-induced putative kinase 1 (PINK1) and homology of autophosphorylation sites.....	8
Figure 3: Mitochondrial import of PINK1.....	11
Figure 4: PINK1 substrates on depolarized mitochondria.....	16
Figure 5: Dual functions of PINK1.....	19
Figure 6: Regulation of neuronal morphogenesis by NF1	26
Figure 7: Neuronal morphology analysis.....	41
Figure 8: PINK1 promotes neurite extension and dendritic complexity	44
Figure 9: Sequence coverage of PINK1 and VCP in PINK1-GFP IP products.....	46
Figure 10: Immunoblot validation of PINK1-VCP interaction	47
Figure 11: Mitochondrial localization is not required for PINK1-VCP interaction	49
Figure 12. PINK1 overexpression does not alter isoelectric focusing of VCP.....	50
Figure 13. VCP overexpression prevents neurite shortening induced by PINK1 knockdown.....	52
Figure 14: PINK1 requires VCP to promote dendritic complexity	54
Figure 15. Interaction of VCP with PINK1 requires the D1 domain.....	55

Figure 16: Overexpression of PINK1-binding domain of VCP blocks the effect of PINK1 overexpression on neurites.....	56
Figure 17: PINK1 requires NF1 expression to promote dendritic complexity.....	59
Figure 18: G309D- and G409V-PINK1-GFP co-immunoprecipitate less VCP and fail to promote neurite extension.....	61
Figure 19: PINK1 interacts with CRMP2.....	63
Figure 20: PINK1 overexpression promotes phosphorylation of CRMP2 at Ser522.....	65
Figure 21: Phosphorylation of CRMP2 at Ser522 is reduced in PINK1 KO mice.....	66
Figure 22: PINK1 does not alter CRMP2 binding to tubulin.	67
Figure 23: Expression of synaptic markers is unaltered at 3 months in PINK1 KO mice	69
Figure 24: Expression of synaptic markers is decreased at 6 months in PINK1 KO mice.....	70
Figure 25: PINK1 promotes dendritic spinogenesis.....	71
Figure 26: PINK1 modulates sensitivity to VCP inhibition	72
Figure 27: VCP overexpression protects against autophagy induced by PINK1 knockdown.....	73
Figure 28: ATG7 knockdown abrogates neurite length differences between SH-SY5Ys expressing GFP and PINK1–GFP.....	75
Figure 29: LC3 phosphorylation at Ser12 in PINK1 overexpressing cells.....	77
Figure 30: PKA inhibition prevents accumulation of high molecular weight phospho-LC3	78
Figure 31. PINK1 overexpression promotes accumulation of poly-ubiquitinated proteins	80
Figure 32: Proposed model of PINK1-VCP-NF1-CRMP2 signaling in regulation of neuronal morphology.....	106

PREFACE

ACKNOWLEDGEMENTS

I am extraordinarily grateful that my mentor, Charleen Chu, allowed me to join her lab. My graduate school experience was immeasurably enriched because I was lucky enough to work for an individual committed to helping me develop as a scientist. Even when I was largely inexperienced, she challenged me to generate and test my own hypotheses, while providing patient guidance when I encountered problems. Charleen is an incredibly creative, thoughtful, and enthusiastic scientist and it has truly been a privilege to learn from her.

I also want to thank past and present members of the Chu and Oury labs. Sam, thank you for taking me under your wing when I had little to no idea what I was doing. You were instrumental to my success as a graduate student. Jason Callio, thank you for preparing countless neuronal cultures, this project would have taken me twice as long without your efforts. I also want to thank Lily Francis for collecting the PINK1 dendritic spine data presented in this dissertation. Aaron, Anthony, Beth, Ed, Gina, Jason, Jason, Jeffrey, Kent, Lily, Pavle, Manish, Ruben, Sam, Tim, and Vivek it has genuinely been a pleasure working with you. Thanks for tolerating my temper tantrums when experiments failed, helping me troubleshoot technical problems, and brainstorming ideas. I'm not sure I will ever again be lucky enough to work in

such a congenial environment. I also want to extend my gratitude to Christine Wu, Nicholas Bateman, and Scott Goulding for their help in performing the mass spectrometry experiments described here.

I also would like to thank the members of my committee: Drs. Jeff Brodsky, Kirill Kiselyov, Scott Kulich, and Yoram Vodovotz. You helped me to remove my blinders when I was overly focused on certain aspects of my project. My committee meetings were always positive experiences, and your advice never failed to move my research in a more productive direction. Thank you for agreeing to guide me through this process.

Finally, I want to thank my family and friends. To my parents, John and Candi, I want to thank you for your endless support and unconditional love. Your unwavering confidence that I will accomplish whatever goal I set out to achieve has enabled me to push past limits that I thought I had. To my sister Jami, thank you for always being a distraction when I needed one. No one entertains or understands me quite as well as you do, and our conversations are always a morale boost. I'm also incredibly thankful to the members of my extended family. Your interest and encouragement have allowed me to return to the bench with a fresh perspective. To all of my friends, thank you for making graduate school bearable. You have injected humor into difficult situations and helped (sometimes forced) me to take time to enjoy myself.

LIST OF ABBREVIATIONS

6-OHDA	6-hydroxydopamine
AC	Adenylate cyclase
AKT	RAC-alpha serine/threonine-protein kinase
AMBRA	Autophagy/Beclin-1 Regulator
ANOVA	Analysis of variance
ATP	Adenosine triphosphate
Bcl-XL	B-cell lymphoma-extra large
BSA	Bovine serum albumin
cAMP	Cyclic adenosine mono-phosphate
CaV2.2	Voltage gated calcium channel 2.2
CCCP	Carbonyl cyanide m-chlorophenyl hydrazone
CDC37	Cell division cycle 37
Cdk5	Cyclin-dependentkinase 5
CNS	Central nervous system
Co-IPed	Co-immunoprecipitated
CRMP2	Collapsin response mediator protein 2
DBS	Deep brain stimulation
DMEM	Dulbecco's Modified Eagle Medium
DNA	Deoxyribonucleic Acid
DPBS	Dulbecco's phosphate buffered saline
DRP1	Dynamin related protein 1
DTT	Dithiothreitol
ETC	Electron transport chain
FBS	Fetal Bovine Serum
FCCP	Carbonyl cyanide-p-trifluoromethoxyphenylhydrazone
GAPDH	Glyceraldehyde 3-phosphate dehydrogenase
GFP	Green fluorescent protein
GSK3-β	Glycogen-synthase kinase 3-β
H89	N-[2-(p-Bromocinnamylamino)ethyl]- 5-isoquinolinesulfonamide dihydrochloride
HSC70	Heat shock cognate protein 70
HSP90	Heat shock protein 90
IBMPFD	Inclusion body myopathy with Paget's disease and frontotemporal dementia
IMM	Inner mitochondrial membrane
IP	Immunoprecipitation
IPed	Immunoprecipitated
IPG	Immobilized pH gradient
KD	Knockdown

KI	Knock-in
KO	Knockout
L-DOPA	L-3,4-dihydroxyphenylalanine
LAMP2A	Lysosomal associated protein 2A
LC3	Microtubule associated protein light chain 3
LTP	Long-term potentiation
MAP	Microtubule-associated protein
MCU	Mitochondrial calcium uniporter
Mfn1/2	Mitofusin 1/2
MPP	Mitochondrial processing peptidase
mPTP	Mitochondrial permeability transition pore
MPTP	1-methyl-4-phenyl-1, 2, 3, 6- tetrahydropyridine
MSN	Medium spiny neuron
mTOR	Mammalian target of rapamycin
mTORC2	Mammalian target of rapamycin complex 2
MTS	Mitochondrial targeting sequence
NBR1	Neighbor of BRCA gene 1
NCLX	Mitochondrial sodium/calcium exchanger
NF1	Neurofibromin1
NMDA	N-methyl D-aspartate
OMM	Outer mitochondrial membrane
Opa1	Optic atrophy protein
OPTN	Optineurin
PARL	Presenilin-associated rhomboid-like protein
PARP1	Poly (ADP-ribose) polymerase 1
PD	Parkinson's disease
PINK1	PTEN-induced kinase 1
PKA	cAMP-dependentprotein kinase
PNS	Peripheral nervous system
PSD95	Post-synaptic density 95
PTDINS3K	Phosphatidylinositol 3 kinase
RhoK	Rho kinase
SDS-PAGE	Sodium dodecyl sulfate polyacrylamide gel electrophoresis
shRNA	Short hairpin RNA
siRNA	Small interfering RNA
SNAP	Soluble NSF attachment protein
SNARE	Soluble NSF attachment protein receptor
Snc	Substantia nigra pars compacta
Sra	Specifically Rac1-associated protein-1
SYN	Synaptophysin
TCA	Tricarboxylic acid

TIM	Translocase of the inner membrane
TOLLIP	Toll interacting protein
TOM	Translocase of the outer membrane
TRAP1	TNF receptor associated protein 1
Ub	Ubiquitin
ULK1/2	Unc-like kinase 1/2
UVRAG	UV Radiation Resistance-Associated Gene Protein
VCP	Valosin containing protein
VGLUT1	Vesicular glutamate transporter
Vms1	VCP/Cdc48-associated mitochondrial stress-responsive 1
WAVE	WASP family verprolin-homologous protein-1
WT	Wild-type

1.0 INTRODUCTION

Nearly a decade ago, the serine/threonine kinase PTEN-induced kinase 1 (PINK1) was linked to a recessively inherited parkinsonism [1]. There is a growing body of evidence that PINK1 has unique functions depending on its subcellular localization. While accumulation of full-length PINK1 on the outer mitochondrial membrane (OMM) is a signal of mitochondrial dysfunction [2-5], the release of mitochondrial processed PINK1 into the cytosol of neuronal cells may act as a sensor of healthy mitochondria to promote differentiation [6] and survival [7, 8]. Considerable progress has been made in elucidating the mitochondrial functions of PINK1, but few studies have investigated its neurotrophic functions in the cytosol. As an early step in understanding the biology of cytosolic PINK1, this project aimed to identify cytosolic proteins that interact with PINK1 and contribute to its effects on dendrites. During the course of this work, valosin-containing protein (VCP), an AAA+ ATPase molecular motor that remodels client proteins targeted for degradation, was identified as a PINK1 interactor. Further, VCP and neurofibromin-1 (NF1), a VCP-interacting protein and key regulator of Ras and PKA signaling in neurons, expression is required for dendritic complexity promoted by PINK1. This study also discovered that collapsin response mediator protein 2 (CRMP2), a NF1-interacting protein and important regulator of neuritic, cytoskeletal dynamics and synaptic calcium influx, also associates with

PINK1. The interactions between these proteins, and their roles in promoting neuronal health will be explored in greater depth below.

1.1 PARKINSON'S DISEASE

Parkinson's disease (PD) is the second most common neurodegenerative disorder, affecting approximately 950 per 100,000 people in North America [9]. James Parkinson first described the disorder in his 1817 work entitled "An Essay on Shaking Palsy", identifying bradykinesia (slowness to initiate movement), resting tremor, rigidity, and postural instability as definitive features of the disease. These motor impairments arise from a loss of 50-60% of the dopaminergic neurons from the substantia nigra pars compacta (SNc) leading to an 80-90% reduction in striatal dopamine levels [10-12]. Proteinaceous cytoplasmic inclusions predominantly comprised of alpha-synuclein, ubiquitin, and neurofilament called Lewy Bodies are frequently found in the surviving neurons of the SNc [13]. Lewy pathology has also been observed in other neuronal populations, including the: cerebral cortex (especially limbic cortices), raphe nuclei and locus coeruleus of the pons, olfactory bulb, nucleus basalis of Meynert of the basal forebrain, and dorsal motor nucleus of the vagus of the medulla oblongata [14]. Neuronal injury or degeneration from these affected brain regions may contribute to the onset of non-motor symptoms of PD such as disrupted sleep/wake cycles, mood disturbances, hyposmia, cognitive impairment, and pain [15-17].

1.1.1 Treatment of PD

The dopamine precursor, L-3,4-dihydroxyphenylalanine (L-dopa) has been the gold standard treatment for PD for over four decades [18]. L-dopa is particularly efficacious at treating motor symptoms in early stages of the disease, but does nothing to prevent degeneration of the dopaminergic neurons of the SNc [19]. As a result, higher doses of the drug are needed to alleviate motor impairments. Eventually, even high doses are unable to manage these symptoms, and many patients develop dyskinesias or fluctuate between periods of symptom control and ineffective treatment. Dopamine receptor agonists or monoamine oxidase type B inhibitors have been used in early stages of PD to delay the L-dopa toxicity suspected to contribute to these long-term complications [20-22], though a recent study suggests that postponing initiation of L-dopa treatment does not have a long-term benefit [21].

Deep brain stimulation (DBS) of the globus pallidus or subthalamic nucleus is a fairly recent addition to the arsenal of PD therapeutics. This surgical intervention is designed to restore inhibitory input to the thalamus, which is dramatically reduced by degeneration of SNc neurons. DBS is typically offered while patients are still responsive to L-dopa. Despite the dramatic benefit for some patients, there are still significant drawbacks to this procedure [23]. Like dopamine replacement strategies, DBS does not prevent SNc neuronal loss and is primarily used to treat motor impairments. Additionally, there is some evidence of post-operative cognitive decline in a minority of patients, with onset of dementia being reported a few months after surgery [24]. Further, most individuals still require L-dopa to effectively manage their symptoms, albeit at lower, potentially less toxic doses [25].

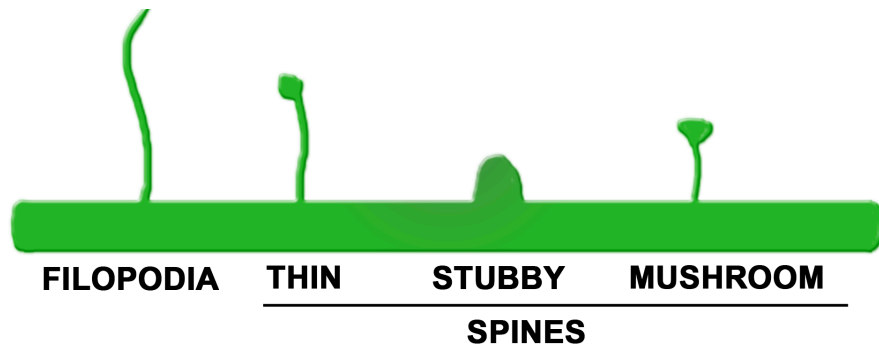


Figure 1: Spine morphology. Schematic representation of the thin filamentous dendritic spine precursor (filopodia) and examples of the various spine morphologies, including: thin, stubby, and mushroom.

1.1.2 Synaptic pathology in PD

Dendritic spines are small protrusion along the dendritic membrane where synaptic input is concentrated and integrated. Mature dendritic spines are comprised of a spine head connected to the dendritic shaft through a narrow neck. Spine morphology is variable, and often divided into three subgroups: stubby, thin, and mushroom ([26]; Fig. 1). Long, thin protrusions along the dendritic shaft called filopodia are the precursor structure to mature spines [27, 28]. Numerous studies have elucidated an important correlation between spine morphology and synaptic function [29]. In general, increased synaptic strength is associated with a larger spine head volume. Thus, spine number and morphology alterations observed in neurodegenerative diseases, including Parkinson's disease, may underlie dysfunctional neural circuits.

Medium spiny neurons (MSNs), the majority neuronal population in the striatum, are densely studded with dendritic spines. Dopaminergic axons projecting from the SNc synapse on the neck of MSN spines, while glutamatergic neurons synapse on the spine head [30]. Loss of dendritic spines from MSNs has been widely observed in post-mortem tissue from PD patients [31-34]. It has been further demonstrated that the loss of dendritic spines in MSNs is tightly

linked to a reduction in complexity and size of the dendritic tree [32-35]. Additionally, reduction of spine number, decreased dendrite length, and dendritic beading of dopaminergic SNc neurons have been reported in a small cohort of PD patients [36]. Calcium dyshomeostasis is the prevailing hypothetical cause of these pathologies [34, 37], but more experimental evidence is needed to elucidate the underlying mechanism.

1.1.3 Autophagy in PD

Autophagy is highly conserved, catabolic process by which cytosolic components and organelles are targeted for degradation by the lysosome. Three types of autophagy have been defined based on their mechanism of sequestering cargo into lysosomes [38]. Proteins containing a consensus sequence recognized by heat shock cognate protein 70 (HSC70) are targeted for chaperone-mediated autophagy. Cargo degraded by this mechanism is translocated into the lysosome through an interaction with the lysosome associated membrane protein 2a (LAMP2a). Microautophagy occurs when cytosolic components become engulfed by the lysosome through membrane involution, without intervening components. Macroautophagy, hereafter referred to as autophagy, is accomplished by engulfment of cargo into a double-membraned vesicle called an autophagosome that then fuses with a lysosome.

Canonical autophagy is a complex process initiated upon inactivation of mammalian target of rapamycin (mTOR) [39]. This suppression results in the dephosphorylation and activation of complex comprised of UNC-like kinase 1 and 2 (ULK1/2), Autophagy like protein (Atg) 13, and FIP200. Following activation of the ULK complex, phagophore nucleation is initiated by recruitment of a membrane bound class III phosphatidylinositol 3-kinase (PtdIns3K)

complex to the phagophore assembly site [40]. This complex consisting of hVps34, Beclin-1, p150 and mutually exclusive binding partners Atg14L/AMBRA or UVRAG/Rubicon, generates phosphatidylinositol 3-phosphate (PI3P), the autophagosomal membrane lipid. Proposed sources of the autophagosome membrane include the: endoplasmic reticulum, Golgi apparatus, ER-Golgi intermediate compartment, recycling endosomes, and mitochondria-associated ER membranes [reviewed in [41]]. Two ubiquitin-like conjugation systems act to elongate and expand the phagophore. One arm of this process involves the conjugation of Atg5 to Atg12 through an Atg7 and Atg10-dependent mechanism [42]. Atg5 and Atg12 are subsequently conjugated to Atg16L. Simultaneously, microtubule-associated protein light chain 3 (LC3) is conjugated to phosphatidylethanolamine by Atg7 and Atg3. These two pathways converge as the Atg5-Atg12-Atg16L complex determines the membrane site for this LC3 lipidation. Following closure of the phagophore, the autophagosome is delivered to the lysosome by the microtubule motor dynein [43]. Autophagosome maturation occurs when the membrane of the autophagosome fuses with endolysosomal compartments in a process mediated by a soluble NSF attachment protein (SNAP) receptor (SNARE) complex [44, 45].

It is becoming increasingly clear that ubiquitin-dependent selective autophagy plays a key role in maintaining proteostasis. Ubiquitinated proteins in this pathway are recognized by ubiquitin binding domains of autophagy receptors that interact with autophagosomes through a LC3-interaction motif [46]. There is a growing body of evidence that protein aggregates are targeted for degradation by this process [47-50]. The autophagy receptors p62, optineurin (OPTN), neighbor of BRCA gene 1 (NBR1), toll-interacting protein (TOLLIP), and Cue5 can all mediate this mode of degradation, called aggrephagy [46].

Autophagy is implicated in a wide range of neurodegenerative diseases by histological analysis of post-mortem tissue. Nearly two decades ago, autophagosomes were observed in the SNc of PD patients, but not controls [51]. Shortly after, phospho-ERK1/2 was shown to accumulate on early autophagosomes in the SNc of individuals with Lewy body pathologies [52]. Basal autophagy is relatively efficient in neurons [53], suggesting that the observed accumulation of these structures arises from perturbed autophagy regulation in PD. It remains unclear whether this buildup is caused by hyperactivation of autophagy, failure in autophagic flux, or a combination of these processes. Further, Lewy body formation is the pathological hallmark of PD [13]. Failure to clear these aggregates of ubiquitinated alpha-synuclein may point to a role for ubiquitin-dependent selective autophagy in PD, though evidence of enhanced or arrested autophagy in post-mortem PD brain has not yet been reported in the literature.

1.2 PTEN-INDUCED KINASE 1

The etiology of PD remains unknown, but a small percentage of affected individuals have heritable forms of the disease with known genetic causes. Mutations in the gene that encodes PTEN-induced kinase 1 (PINK1) are responsible for the second most common cause of autosomal recessive parkinsonism [54]. The early-onset parkinsonism caused by pathogenic PINK1 mutations was first identified in 2004 [55], and is characterized clinically by earlier age of onset (range of 9-52 years), long disease duration, and sustained response to levodopa treatment [55-58]. Either reduced kinase activity or decreased protein stability has been reported for many of the identified mutations, suggesting that loss of PINK1 function is pathogenic.

1.2.1 Domains

PINK1 is a ubiquitously expressed serine/threonine kinase with homology to the calcium/calmodulin family. Eleven conserved subdomains have been described within the kinase domain (Fig. 2; [59]) Subdomains I–IV orient and dock ATP, while subdomains VI–XI bind substrates to facilitate phosphotransfer to the targeted peptide. Two evolutionarily conserved autophosphorylation sites within the kinase domain have been shown to promote kinase activity [60]. Phosphorylation at Thr313, a residue that is pathogenic when mutated to methionine, also augments PINK1 kinase activity [61]. The kinase domain is flanked by a regulatory tail on the C-terminus, a canonical, N-terminal mitochondrial targeting sequence (MTS), and putative transmembrane domain.

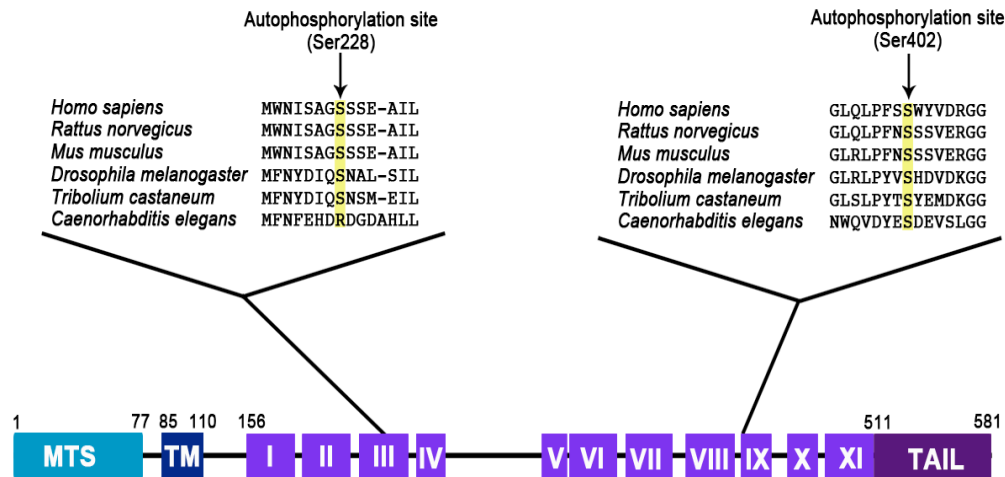


Figure 2: Domain structure of PTEN-induced putative kinase 1 (PINK1) and homology of autophosphorylation sites. PINK1 is composed of a canonical N-terminal mitochondrial targeting sequence, putative transmembrane domain, serine/threonine kinase domain, and a C-terminal regulatory tail. Eleven conserved subdomains have been described within the kinase domain. Subdomains I–IV coordinate the orientation and docking of ATP, whereas the subdomains VI–XI are responsible for detection of target peptides and phosphotransfer. Two evolutionarily conserved, activating autophosphorylation sites within the kinase domain have been identified.

1.2.2 Mitochondrial import and processing

Virtually all nuclear-encoded mitochondrial proteins are imported across the outer mitochondrial membrane (OMM) via the translocase of the outer membrane (TOM) complex [62]. Two receptor subunits of this complex, TOM20 and TOM22 recognize N-terminal mitochondrial targeting sequences (MTS) and initiate transport through the β -barrel pore of TOM40. Because PINK1 has a predicted N-terminal MTS, and complexes with TOM20, 22, and 40 on depolarized mitochondria [63], it is likely to be transported across the OMM through this pathway. However, a recent study found that PINK1 import can also occur in the absence of TOM40, through a mechanism that requires TOM70 [64]. TOM70 is a receptor subunit of the TOM complex that detects internal mitochondrial localization signals [62]. Cytosolic chaperones, including known PINK1 interactors, specifically interact with TOM70 to initiate transport of proteins that contain internal mitochondrial localization signals [65]. This finding provides insight into how trace amounts of PINK1 constructs lacking the predicted N-terminal MTS may be imported into the mitochondria as detected by protease protection assays [66, 67], and why interaction with CDC37/Hsp90 increases mitochondrial localization of PINK1 [68, 69]. Nevertheless, as only trace levels of overexpressed N-terminal deletions of PINK1 can be detected in mitochondria, the major pathway for PINK1 mitochondrial import likely occurs via the canonical MTS.

The import and insertion of PINK1 into the inner mitochondrial membrane (IMM) is presumed to occur through the translocase of the inner membrane 23 (TIM23) complex in a process driven by $\Delta\Psi_m$. In general, proteins that are imported through the TOM complex are recognized by TIM50, which acts to guide the MTS through TIM23 [62]. Proteins destined for the IMM generally have a hydrophobic sequence following the MTS that acts as a stop transfer

signal. Upon sequence analysis of PINK1, a putative transmembrane domain that could act as a stop transfer signal has been identified [67, 70].

The submitochondrial localization of PINK1, and its concurrent processing by mitochondrial proteases, occurs through a $\Delta\Psi_m$ -dependent mechanism. An interference RNA (RNAi) screen suggested that the mitochondrial processing peptidase (MPP) processes PINK1, as it does many other mitochondrial proteins containing a N-terminal MTS [71]. Sim et al. have identified two conserved regions of PINK1, corresponding to amino acids 8-18 and 67-77 of human PINK1, that contain potential MPP cleavage motifs [70]. However, it has recently been shown that PINK1 processing was unaffected in isolated mitochondria treated with a divalent ion chelator to inhibit MPP [64, 66], and recombinant MPP did not cleave PINK1 in an *in vitro* assay [64]. The processing of the PINK1 precursor (~60 kDa band) into its ΔN_1 form (~50 kDa) by presenilin-associated rhomboid-like protein (PARL) has been well characterized [71-74].

This integral IMM protease cleaves PINK1 between the alanine-103 and phenylalanine-104 residues, a site within the putative transmembrane domain [74]. The resultant product is likely targeted for proteasomal degradation [75], if not retained in the mitochondria, stabilized in a complex with other proteins or further processed by other peptidases. The protease responsible for producing the ΔN_2 fragment (~45 kDa band) has not been identified. Following mitochondrial processing, PINK1 is released into the cytosol through an unidentified mechanism.

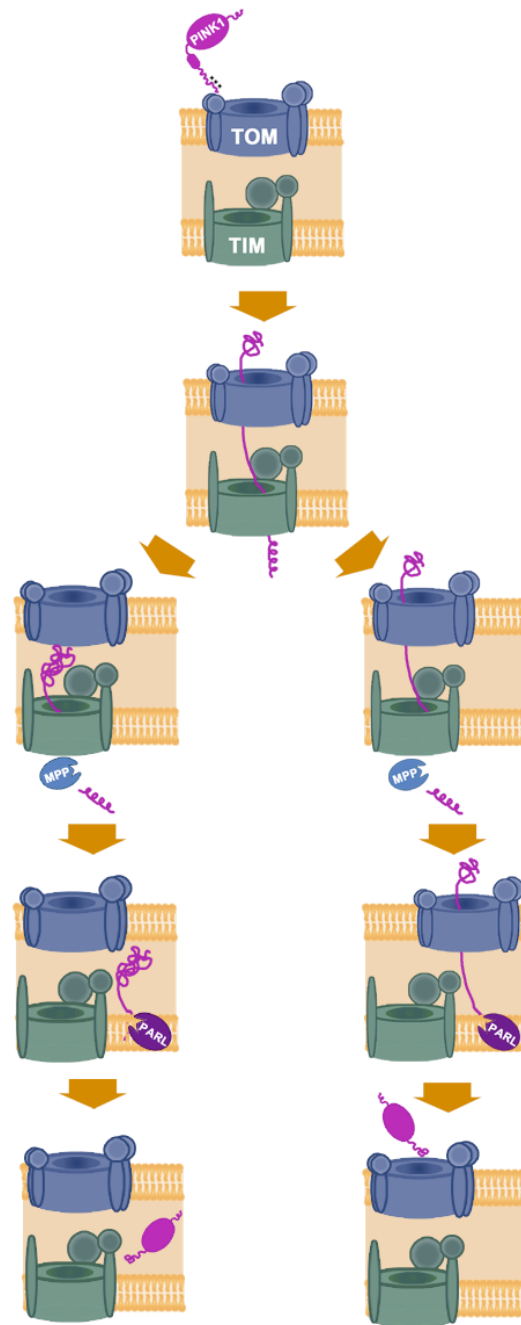


Figure 3: Mitochondrial import of PINK1. In mitochondria with intact mitochondrial membrane potential, PINK1 is imported through the traditional TOM/TIM pathway before being processed by several mitochondrial proteases, including MPP and PARL. After processing, a portion of PINK1 remains in the mitochondrial inner membrane space to promote mitochondrial complex I activity and contribute to the maintenance of mitochondrial membrane potential. A pool of PINK1 is also released into the cytosol. This processed form of PINK1 is neuroprotective, but is rapidly degraded by the proteasome in non-neuronal cells.

1.2.3 PINK1 protects against apoptosis induced by parkinsonian injury

Overexpression of PINK1 protects against a number of apoptotic stimuli with relevance to PD-associated injury, including oxidative stress [76], proteasomal inhibition [55], mitochondrial depolarization [77], and ETC complex I inhibition [78]. Additionally, PINK1 depletion sensitizes cells to apoptosis induced by complex I inhibitors [78, 79] and mitochondrial depolarization [77]. PINK1-dependent phosphorylation of the mitochondrial chaperone TNF receptor-associated protein 1 (TRAP1) [76], and anti-apoptotic protein Bcl-x1 ([77], Fig. 4) have been shown to protect against cell death induced by oxidative stress and mitochondrial depolarization respectively.

1.2.4 Mitochondrial functions of PINK1

1.2.4.1 Energized mitochondria A growing body of evidence has made it increasingly clear that mitochondrial dysfunction is a key feature of PD pathogenesis. Compromised function of the electron transport chain (ETC) has been observed both in PD patient tissue, and genetic and toxin models of PD [80, 81]. The unique bioenergetic demands of neurons make maintenance of mitochondrial homeostasis crucial for their health and survival. Interestingly, impaired respiration, decreased mitochondrial membrane potential ($\Delta\Psi_m$) and reduced levels of ATP have also been reported in PINK1 deficient mammalian cells and animal models. A study employing mitochondria isolated from PINK1 knockout mouse embryonic fibroblasts (MEFs) found that a reduction in substrate oxidation, rather than proton leak, was responsible for the loss of $\Delta\Psi_m$ [82]. This finding is consistent with reports of reduced ETC complex I [82-85] and II [82, 84,

85] linked respiration in PINK1 deficient neurons and MEFs. However, increased opening of the mitochondrial permeability transition pore (mPTP) [85], and deficient activity of the mitochondrial $\text{Na}^+/\text{Ca}^{2+}$ exchanger (NCLX) [86, 87] have also been shown to contribute to loss of $\Delta\Psi_m$ and impaired respiration observed in PINK1 knockout cells. Further, PINK1 deficiency also affects substrate availability [86] and activity of aconitase [84], an enzymatic component of the tricarboxylic acid (TCA) cycle. While the mechanism underlying disruption of normal ETC function and ATP production caused by PINK1 deficiency remains unclear, Vitamin K_2 is able to reverse ATP deficiencies in PINK1 null flies by its action as an ETC electron transporter [88]. This finding has not yet been validated in mammalian systems, but may suggest that improving the efficiency of the ETC is sufficient to overcome some bioenergetic consequences of the loss of PINK1 function.

In addition to energy production, the mitochondria's ability to buffer calcium is crucial to neuronal function. This is especially true of neurons that are exposed to frequent and sustained elevations in intracellular calcium concentration, such as the vulnerable populations in PD (reviewed in [89]). Cytosolic calcium is transported across the IMM into the matrix via the $\Delta\Psi_m$ activity of the mitochondrial calcium uniporter (MCU) [90], and efflux of calcium from the mitochondria occurs through the $\text{Na}^+/\text{Ca}^{2+}$ exchanger (NCLX) [91]. Dysregulation of mitochondrial calcium handling has been reported in PINK1 deficient cells [85-87, 92]. Elevated levels of calcium in the mitochondrial matrix have been observed in PINK1 deficient neuronal cells and MEFs [85, 86]. Gandhi et al. found that mitochondrial calcium extrusion in response to sodium was impaired in PINK1 deficient neurons, and reasoned that accumulation of calcium in the matrix was likely due to diminished efflux activity of NCLX [86]. Phosphorylation of NCLX by PKA at Ser258 has recently been shown to prevent this calcium

overload, preserve mitochondrial membrane potential, and promote neuronal survival of PINK1 KO neurons [87]. Failure to extrude calcium may lead to the elevation in mitochondrial matrix calcium levels reported to increase susceptibility to opening of the mPTP and cell death in PINK1 knockout MEFs [85].

1.2.4.2 Depolarized mitochondria In healthy cells, the processes of mitochondrial fission, fusion, and mitochondrial degradation by macroautophagy (mitophagy) are balanced in a dynamic equilibrium necessary for maintaining a healthy mitochondrial network. This is particularly important in neurons, which are dependent on oxidative phosphorylation and require extensive mitochondrial transport among dendrites and axons. Fusion events, mediated by the mitofusins (Mfn1 and 2) and optic atrophy protein (Opa1), allow for sharing of components. Fusion is often followed by fission events, mediated by Drp1, which allow for detachment of mitochondria from the network for transport as well as separation of damaged components for degradation [93]. A fraction of fission events may result in daughter mitochondria with different mitochondrial membrane potentials [94]; the daughter with the decreased $\Delta\Psi_m$ is targeted for mitophagy [95]. When damaged or dysfunctional mitochondria are unable to repair themselves or undergo fusion, they are also targeted for mitophagy. However, the exact mechanism by which mitochondria are targeted to the autophagosome is an emerging area of research.

In some model systems, PINK1 itself has been identified as a trigger for Parkin-dependent mitochondrial degradation [96, 97]. Treatment of mammalian cells with the protonophore CCCP causes mitochondrial depolarization, which leads to cessation of import and intramitochondrial processing of PINK1 and results in accumulation of full-length PINK1 on the outer mitochondrial membrane (OMM). Parkin, an E3 ubiquitin ligase, is recruited to the

mitochondrion and facilitates its degradation by mitophagy [71, 98, 99]. Recently, it has been discovered that PINK1 phosphorylates both ubiquitin and parkin to promote parkin recruitment to the mitochondria in this experimental paradigm [4, 100, 101]. PINK1-activated parkin then builds ubiquitin chains on OMM proteins and recruits the autophagy receptors optineurin and NDP52 [102, 103].

As previously reviewed by Van Laar and Berman [104], the mitophagic pathway seems to vary by the bioenergetic state and morphology of the cell, and the type of stressor. The CCCP-PINK-Parkin process occurs robustly in non-neuronal, glycolytic cells to result in complete or near-complete mitochondrial clearance. In neuronal and oxidative phosphorylation-dependent cells, CCCP treatment does not induce Parkin translocation [104] until after 24 hours of treatment [105]. Rotenone and 6-OHDA toxin models did not show accumulation of PINK or Parkin translocation, unlike CCCP [106]. The induction of mitophagy in PINK1-deficient animals and cells, dependent on increased superoxide and Drp-mediated fission, suggests additional mechanisms of PINK1-independent mitophagy [107]. This may involve externalization of cardiolipin (CL), an inner mitochondrial membrane phospholipid, to the mitochondrial surface, which was shown to occur in rotenone-treated cortical neurons. CL then interacts with microtubule-associated-protein-1-light chain-3 (LC3) on autophagic membranes to mediate mitophagy of the damaged mitochondrion [106].

PINK1 has been shown to form a complex with Miro, an outer mitochondrial membrane Rho GTPase, and Milton in *Drosophila*, proteins involved in trafficking of mitochondria [108]. PINK1, in cooperation with Parkin, downregulates Miro protein levels in *Drosophila*, leading to a decrease in mitochondrial trafficking in axons [109]. RNAi knockdown of Miro in CCCP-treated HeLa cells leads to increased Parkin-mediated mitophagy [109]. As postulated by Van

Laar et al. (2013), the ability of PINK1/Parkin to decrease mitochondrial trafficking in axons could isolate the damaged mitochondria from the functional network, prevent the accumulation of damaged mitochondria in high-energy demand areas, such as axon terminals, and allow the mitochondria to be degraded [104].

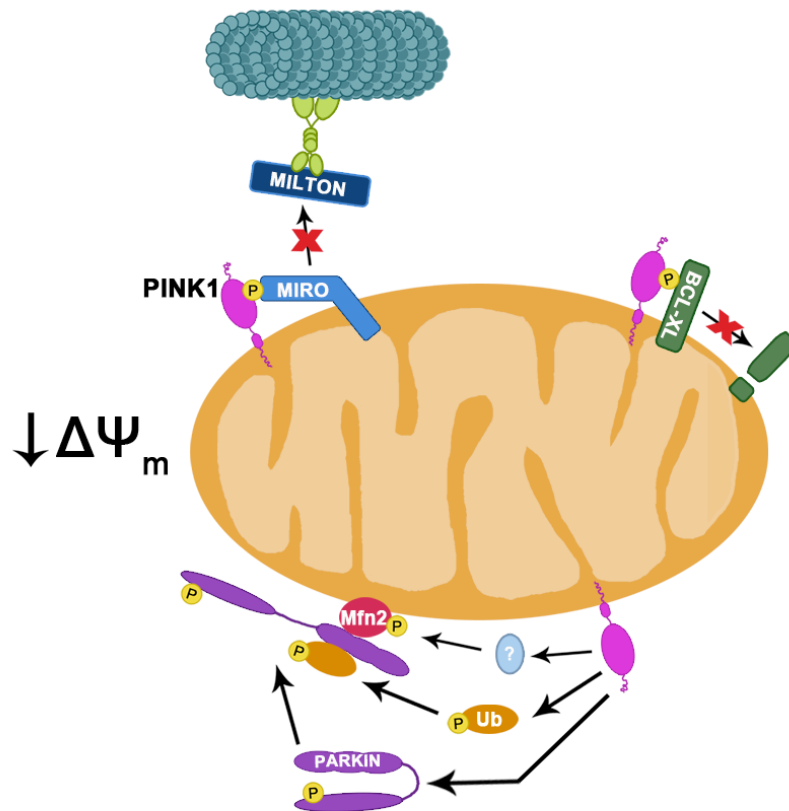


Figure 4: PINK1 substrates on depolarized mitochondria. Import of mitochondrial proteins is impaired in depolarized mitochondria, resulting in the accumulation of unprocessed PINK1 on the mitochondrial surface. Localization of this species of PINK1 to the OMM of damaged mitochondria activates multiple signaling cascades. OMM-tethered PINK1 phosphorylates both ubiquitin and Parkin to promote mitochondrial recruitment of Parkin. PINK1 also regulates the phosphorylation and subsequent degradation of the mitochondrial fusion protein Mitofusin 2 and the mitochondrial transport adaptor Miro in this experimental paradigm. Loss of these proteins readies a mitochondrion for mitophagy by promoting mitochondrial fission and inactivating axonal trafficking. Following mitochondrial depolarization, PINK1 phosphorylates Bcl-XL and inhibits apoptosis by blocking its cleavage.

1.2.5 Role of PINK1 in neurite maintenance and synaptic function

While a large body of literature describes the chemically induced accumulation of full-length PINK1 on the mitochondrial surface, far less is understood about the potential signaling function(s) of correctly processed PINK1. Given that healthy mitochondria process and release PINK1 to the cytosol, PINK1 could also serve as a sensor for mitochondrial function. In this capacity, correctly processed PINK1 may be released from healthy mitochondria to regulate other cellular functions.

The cytosolic pool of PINK1 has been shown to regulate neurite morphology through a kinase-dependent mechanism [110]. Knockout of PINK1 in primary cortical and midbrain neurons reduces neurite length and complexity. Overexpression of either full length or Δ N-PINK1 is able to rescue neurite morphology in these cells. A PINK1 construct targeted to the OMM, despite being able to partially reverse the effects of PINK1 deficiency on mitochondrial homeostasis, had no effect on neurite length. Although the mechanism has not been completely elucidated, PKA signaling amplifies the neurite outgrowth promoted by cytosolic PINK1 [110], suggesting that PINK1 and PKA signaling pathways converge to co-regulate neurite extension just as they do for mitochondrial calcium extrusion [87].

PINK1 rodent models have phenotypes that parallel those purportedly resulting from synaptic pathology in PD patients. Basal dopamine levels in the striatum and dopaminergic SNc neuron number are unaltered in young PINK1 KO and G309D-PINK1 knock-in (KI) mice (PD-associated mutation) [111-113]. Despite the lack of SNc neurodegeneration, evoked release of catecholamines and long-term potentiation (LTP) is reduced in the striatum of 2-3 month old PINK1 KO mice [113]. Similarly, LTP failure that could be rescued by chemically induced

dopamine release was also reported in heterozygous PINK1 KO mice [114]. By 9 months, G309D-PINK1-KI mice have a reduction in basal levels of striatal dopamine that is exacerbated at 22-24 months [111]. Further, reduced expression of the D₂ dopamine receptor has been reported in the striatum of PINK1 rats, a finding consistent with early-stage idiopathic PD [115]. These discoveries, when considered in combination with the role of PINK1 in neuronal morphology, point to a potential regulatory role of PINK1 in synaptic function.

1.2.6 Role of PINK1 in autophagy regulation

In addition to its widely investigated role in mitophagy, a small number of studies have implicated PINK1 in regulation of autophagy. PINK1 has been shown to interact with Beclin1 and promote autophagosome accumulation [116]. Dissimilarly, overexpression of PINK1 promotes resistance to LC3 puncta accrual induced by treatment with the PD-associated toxin 6-hydroxydopamine in a neuronal cell line [117]. Further, increased LC3 lipidation has been reported in PINK1 deficient dopaminergic neuronal cell lines [117, 118] and the striatum of mice injected with PINK1 shRNA lentivirus [118]. PINK1 has also been shown to promote cell survival through mTORC2/Akt activation [8, 119], a pathway known to negatively regulate autophagy [120]. As discussed above, PINK1 has recently been shown to directly phosphorylate ubiquitin at Ser65 (p-Ser65-Ub) to promote autophagic clearance of mitochondria. Interestingly, cytoplasmic p-Ser65-Ub granules have been recently reported to surround Lewy bodies in the brain of idiopathic PD patients [121]. This finding implicates PINK1 in regulation of ubiquitin-dependent autophagy, but further study is required to understand the mechanism underlying this exciting discovery.

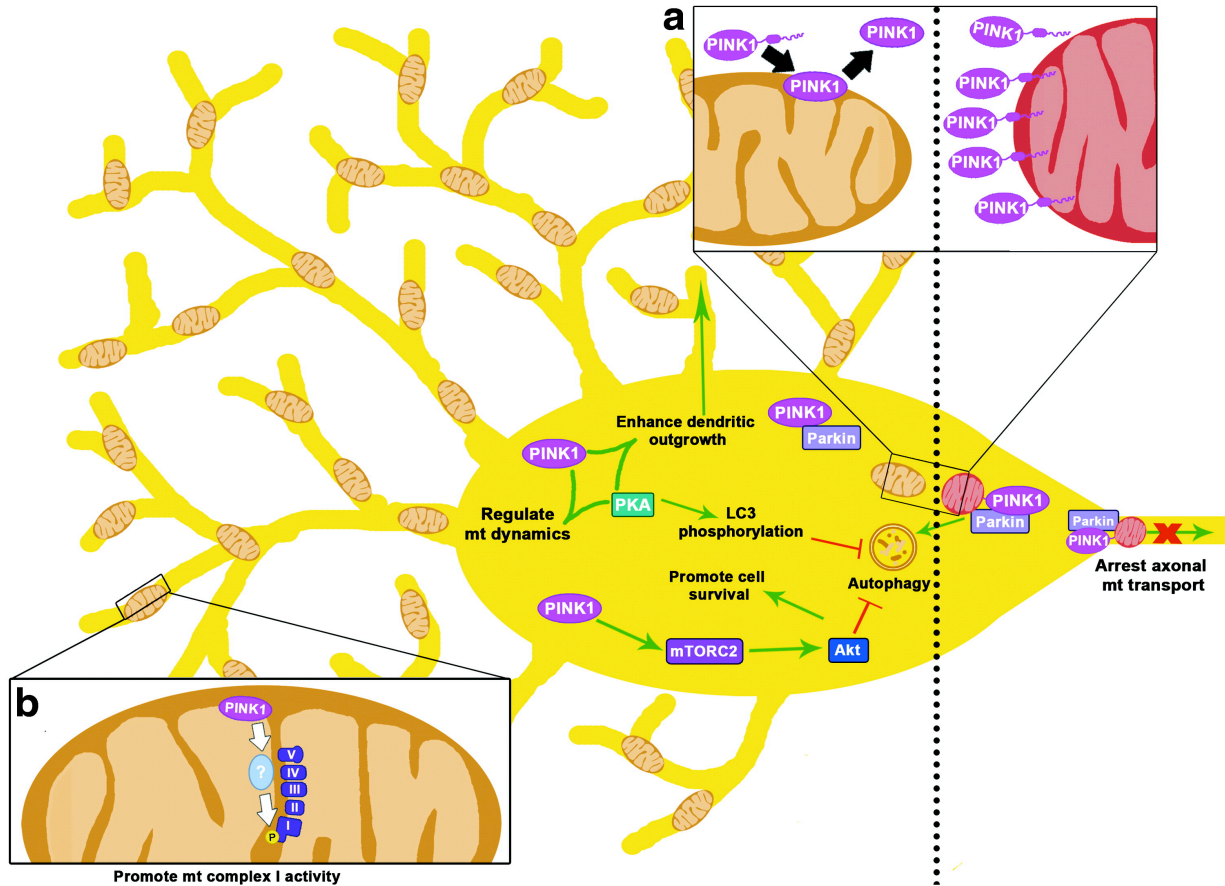


Figure 5: Dual functions of PINK1. In healthy mitochondria, PINK1 is imported through the TOM/TIM complexes and processed by several mitochondrial proteases before being released back into the cytosol (inset a). This cytosolic pool of PINK1 may serve as a signal to the cell that the integrity of its mitochondrial network remains intact. Processed PINK1 promotes complex I activity (inset b), regulates mitochondrial calcium homeostasis, suppresses autophagy/mitophagy, fosters neurite extension, enhances mitochondrial trafficking into dendrites, and activates survival and differentiation signaling pathways. When mitochondria lose their membrane potential, full length PINK1 accumulates on the OMM (inset a). As a result, axonal transport of mitochondria is arrested and the damaged mitochondrion becomes a target for degradation mediated by parkin.

1.3 VALOSIN CONTAINING PROTEIN IN NEURODEGENERATION

Valosin-containing protein/p97 (VCP) belongs to a family of homohexameric AAA+ ATPases with diverse cellular functions [122]. Powered by ATP hydrolysis, VCP acts as a molecular motor to unfold ubiquitinated substrate proteins. This structural remodeling allows for substrates to be extracted from organellar membranes and isolated from binding partners. Many client proteins are targeted for autophagic or proteasomal degradation, but VCP also mediates membrane fusion and trafficking. Each monomer contains two ATPase domains, D1 and D2 that are assembled as stacked rings [123, 124]. Hexamerization of VCP requires the D1 domain, while the D2 domain is largely responsible for generating mechanical force [125]. VCP activity is targeted to distinct pathways by interaction with co-factors (reviewed in [126]). Over 40 VCP co-factors have been identified in the mammalian system, the majority of which bind to the N-terminal domain.

Missense mutations in the gene encoding VCP are the cause of a rare autosomal dominant disorder called inclusion body myopathy and Paget's disease with frontotemporal dementia (IBMPFD), and have been linked to a small percentage of cases of familial amyotrophic lateral sclerosis [127-129]. These mutations are concentrated at the interface between the N and D1 domains, indicating that this site modulates an important function of VCP that is disrupted by pathogenic mutants. Some, but not all, VCP pathogenic mutants augment the ATP hydrolytic activity of the D2 domain [130]. Arg155 is the amino acid most often

mutagenized in IBMPFD which is responsible for disease onset in approximately 50% of affected families [127]. Tissue degeneration begins earlier and occurs more rapidly in individuals harboring an Ala232 mutation, giving rise to a more severe clinical presentation. Thus, transgenic models of IBMPFD generally harbor one of these two mutations.

Like many neurodegenerative diseases, accumulation of ubiquitinated protein aggregates has been observed in the brains of IBMPFD patients [131, 132]. This finding indicates that impaired protein degradation contributes to IBMPFD pathology. Proteasomal degradation seems to be largely preserved in cells expressing IBMPFD-associated VCP mutants [133, 134], though some endoplasmic reticulum-associated degradation clients may be affected [135, 136]. Conversely, expression of VCP pathogenic mutants results in a dramatic impairment of maturation of autophagosomes containing ubiquitinated proteins and aggregates [133, 137, 138]. Additionally, VCP has been detected in neuronal nuclear inclusion of multiple polyglutamine diseases, eosinophilic nuclear inclusions in the aged, and particularly relevant to this work, Lewy bodies of PD subjects [139]. This physical association with aggregates of varied composition suggests that VCP may be a component of a degradation pathway commonly perturbed in neurodegenerative disease.

Abnormal mitochondrial morphology has been observed in two recently generated mouse models of IBMPFD. Enlarged mitochondria with disrupted cristae accumulate in the brain of homozygous and heterozygous VCP mutant (R155H) knock-in mice [140, 141]. Further, mitochondrial membrane potential is diminished and ATP production reduced in VCP deficient and VCP mutant expressing neuronal cells [142, 143]. Translocation of the yeast homolog of VCP, CDC48, with its co-factor VCP/Cdc48-associated mitochondrial stress-responsive 1 (Vms1), preserves mitochondrial respiratory function in oxidatively stressed cells [144, 145].

Therefore, failure to degrade VCP-Vms1 mitochondrial substrates may result in impaired mitochondrial function. There may be some redundancy in this pathway, as parkin, a PD-associated protein, recruits VCP to chemically depolarized mitochondria [146, 147]. VCP-dependent, proteasomal degradation of mitochondrial fusion proteins precedes parkin-mediated mitophagy in this experimental paradigm. The role of PINK1 in mitochondrial recruitment of VCP is less clear, but VCP overexpression ameliorates the mitochondrial morphology phenotype and protects against muscle degeneration in PINK1 knockdown flies [147].

Formation and maintenance of appropriate synaptic connections is essential for brain function. Degeneration and dysfunction of neurons from the frontotemporal lobe give rise to cognitive impairments observed in approximately one-third of patients with IBMPFD [127]. These cognitive phenotypes are reflected in aged R155H- [148] and A232E-VCP [149] transgenic mice. Accumulation of aggregated proteins in the brains of these mice was simultaneously reported, though more mechanistic studies are needed to determine whether this is the primary insult leading to neurodegeneration. VCP is also a key regulator of dendritic pruning in flies through proteolytic [150] and non-proteolytic [151] mechanisms. Inactivation of VCP in this context caused a dramatic simplification of dendritic arbors, while a milder phenotype was observed in flies expressing R155H-VCP [150]. Recently, an elegant study described the role of VCP in regulation of dendritic spine density [152]. Through an interaction with neurofibromin-1 (NF1), a cytosolic protein that modulates Ras and adenylate cyclase (AC) activity, VCP promotes dendritic spinogenesis. Dendritic spine density is reduced in neurons expressing IBMPFD-disease associated VCP mutants that disrupt the association between NF1 and VCP. Interestingly, expression of NF1 is unaffected by VCP knockdown either in the presence or absence of a proteasomal inhibitor. This suggests that NF1 is not targeted for

degradation through its association with VCP. Cumulatively, these studies indicate that VCP plays an important role in neuronal morphogenesis, and disruption of this function may directly contribute to dementia onset in IBMPFD patients.

1.4 FUNCTIONS OF NEUROFIBROMIN 1 IN THE CENTRAL NERVOUS SYSTEM

Neurofibromin 1 (NF1) is a large, multi-domain protein predominantly localized to the cytosol [153]. The 2818 amino acid protein is comprised of a cysteine-serine rich domain, tubulin-binding domain, GTPase-activating protein related domain, Sec14 homology/leucine rich (phospholipid binding) domain, pleckstrin homology domain, and C-terminal domain. Mutations in NF1 cause neurofibromatosis type I, a prevalent autosomal, dominant tumor predisposition syndrome. Approximately 1 in 2,700 people are born with neurofibromatosis 1 [154]. Though the disease is fully penetrant, clinical presentation is widely varied in affected individuals [155]. Atypical skin pigmentation (café-au-lait macules, skin-fold freckling), and development of tumors in the peripheral nerve sheath (schwannomas, neurofibromas) and optical pathway are among the diagnostic criteria for neurofibromatosis-1 [153].

Cognitive impairment is a common co-morbidity in neurofibromatosis patients [156, 157]. Approximately 50% of children with neurofibromatosis-1 have formally diagnosed learning disabilities [158], a dramatic increase from the estimated 10% of the general population of children in the United States [159]. Inactivation of a single NF1 allele produces learning and memory phenotypes in mice, associated with impairment of LTP in the hippocampus [160]. Additionally, reduced cortical thickness has been observed in mice with conditional knockout of

NF1 in neuroglial progenitor cells (NF1-Cre^{BLBP}) [161]. Anatomical orientation and number of neurons in the cortex of NF1-Cre^{BLBP} mice are unaffected. Rather, the decrease in cortical thickness was attributed to simplified dendritic arbors and shortened neurites.

Attention problems are also prevalent in individuals harboring pathogenic NF1 mutations, with 38-50% meeting the diagnostic criteria for attention deficit disorder [158]. Learning and memory are impaired in heterozygous NF1 knockout mice, but they do not recapitulate attention deficits in these patients [162]. However, the attention phenotype is modeled in NF1 +/- mice with complete knock out of NF1 in astrocytes (NF1 +/-^{GFAP-CKO}). The observed reduction in attentive behaviors coincided with reduced dopaminergic innervation to the striatum. Treatments that increase the availability of dopamine in the striatum ameliorated the attention abnormalities in NF1 +/-^{GFAP-CKO} mice. Though dopamine depletion has not been reported in children with neurofibromatosis-1, attention deficit is effectively treated with dopamine reuptake inhibitors in these individuals [163]. Additionally, neurite length is reduced in dopaminergic neurons of the ventral midbrain from NF1 +/- mice [162]. Collectively, these studies in mouse models of neurofibromatosis 1 with disease-associated neurological symptoms suggests that NF1 plays an important role neuronal differentiation. In vitro studies have identified three mechanisms by which NF1 regulates neuronal morphology: inactivation of Ras, activation of AC/PKA signaling, and interaction with collapsin-response mediating protein (CRMP2).

NF1 includes a Ras-GTPase activating protein (Ras-GAP) domain that is crucial to its activity as a tumor suppressor [153]. Finely tuned Ras activation in response to calcium influx is also necessary for appropriate synapse formation and maturation [164, 165]. Recently, NF1 was identified as the major Ras inactivator in dendritic spines [166]. Prolonged Ras activation

impairs formation and maintenance of functional excitatory synapses in NF1 deficient rat cortical neurons. This study complemented earlier work that identified a role for NF1 inactivation of Ras in neurotrophic factor induced neuronal differentiation of a neuroblastic cell line (PC-12) [167].

Ras-overactivation has been observed in neurons derived from both the central nervous system (CNS) and peripheral nervous system (PNS), of NF1 +/- mice [168, 169]. Interestingly, NF1 haploinsufficiency does not affect neurite length of PNS neurons, but is dramatically reduced in CNS neurons. This neuritic phenotype in the CNS neurons correlates with a reduction in cyclic adenosine monophosphate (cAMP) production. Restoring PKA activation in these cells prevented the neurite shortening phenotype [169]. As described above, NF1 plays a role in the regulation of dendritic spinogenesis. While PKA activation alone is insufficient to promote spinogenesis [170, 171], it is required for dendritic filopodia formation induced by the synaptic protein syndecan-2 through its interaction with neurofibromin [170].

Another synaptic protein, collapsin response mediator 2 (CRMP2), also interacts with NF1 in neuronal cells [172, 173]. This association requires cyclin-dependent kinase 5 (Cdk5) activity [173], a kinase known to phosphorylate CRMP2 at Ser522 [174, 175]. Impaired neurite outgrowth and accumulation of highly phosphorylated species of CRMP2 was observed following transient knockdown of NF1 in PC-12 neuroblastic cells [172]. Interestingly, NF1 inhibits the phosphorylation of CRMP2 by Cdk5, GSK-3 β , and Rho kinase. Expression of the GAP-related domain of NF1 or pharmacological inhibition of Cdk5, GSK-3 β , and to a lesser extent RhoK reversed these neuritic phenotypes. It is unclear whether NF1 regulates upstream signaling cascades or simply acts as a physical barrier to inhibit CRMP2 phosphorylation by these kinases.

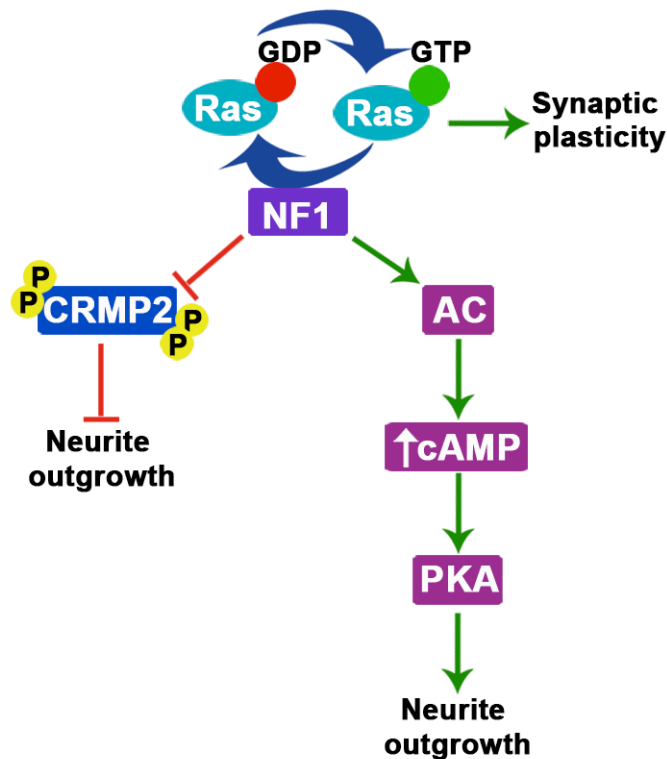


Figure 6: Regulation of neuronal morphogenesis by NF1. NF1 regulates neuronal morphology through three pathways: inactivation of Ras in dendritic spines to promote LTP, activation of AC activity to promote neurite outgrowth and dendritic filopodia formation. NF1 also binds CRMP2 to inhibit hyperphosphorylation. CRMP2 induced neurite outgrowth is impaired by hyperphosphorylation. Red lines indicate negative regulation and green arrows denote positive regulation.

1.5 COLLAPSIN RESPONSE MEDIATOR PROTEIN 2 IN NEURONAL MORPHOGENESIS

CRMP2 belongs to a family of five highly homologous, cytosolic proteins required for development and maintenance of CNS patterning. Of the five homologs, only CRMP2 is expressed at high levels in adult neurons and is particularly enriched in highly plastic regions of

the brain [176]. CRMP2 forms a quaternary complex as a homo- or hetero-tetramer with other members of the CRMP family [177]. By primary sequence analysis, CRMP2 is homologous to the enzyme dihydropyrimidinase [178]. Though CRMP2 enzymatic activity has not been described, divalent cations stabilize CRMP2 structure, just as they do in other members of the aminohydrolase family [179].

The canonical function of CRMP2 is regulation of microtubule dynamics. Overexpression of CRMP2 results in neurite, particularly axonal, lengthening in culture [180, 181]. This extension largely arises from the association of CRMP2 with the plus-end of microtubules. CRMP2 binding to tubulin promotes microtubule stability, leading to axonal elongation. Phosphorylation of CRMP2 at Thr509 and Thr514 by GSK3- β , which is preceded by a priming phosphorylation at Ser522 by Cdk5, disrupts this interaction. Perturbation of the CRMP2-tubulin interaction results in growth cone collapse and axonal retraction [174, 175, 182].

CRMP2 also binds the microtubule motor proteins dynein [183, 184] and kinesin [185]. In neuronal cells, binding of CRMP2 to dynein impairs retrograde transport [183]. Studies performed in non-neuronal cells suggest that this transport retardation may allow for optimized delivery to the endocytic recycling pool [184]. Conversely, CRMP2 acts as an adaptor protein that facilitates anterograde transport through its interaction with kinesin light chain [182, 186]. Through this interaction, CRMP2 promotes delivery of the neurotrophin receptor tyrosine kinase (TrkB) [186], and specifically Rac1-associated protein-1/WASP family verprolin-homologous protein-1 (Sra/WAVE) complex [182] to the distal axon. CRMP2-mediated trafficking of these proteins fosters actin remodeling in the growth cone. Phosphorylation of CRMP2 by GSK3- β results in dissolution of the CRMP2-kinesin interaction, leading to actin filament disorganization

in the growth cone. These studies indicate that multiple pathways contribute to the regulation of neuronal morphology by CRMP2.

While CRMP2 functional studies have largely investigated its regulation of cytoskeletal remodeling, CRMP2 also interacts with key regulators of pre- and post-synaptic calcium influx and buffering. Calmodulin, an EF hand protein that is a crucial integrator of synaptic signaling [187], binds to CRMP2 in a calcium dependent manner. The association of CRMP2 with calmodulin inhibits its cleavage by calpain [188]. Inhibition of this cleavage promotes neuronal survival following N-methyl-D-aspartate (NMDA) excitotoxicity [189]. CRMP2 also binds to the NR2B subunit of the NMDA receptor to promote post-synaptic calcium entry [190]. Additionally, CRMP2 regulates pre-synaptic calcium influx [191] and neurotransmitter release [192] through its interaction with the neuronal (N)-type voltage-gated calcium channel 2.2 (Cav2.2). Cav2.2 channels, act as the primary mediators of calcium induced neurotransmitter release in the axon terminals [193]. Phosphorylation of CRMP2 at Ser522 by Cdk5 promotes CRMP2-Cav2.2 binding and enhances Cav2.2 currents [194]. Mice with two alleles of an unphosphorylatable Ser522-CRMP2 mutant knocked in have severe deficits in spine density [195] and dendritic arbor patterning [196] of pyramidal neurons. Interestingly, neuronal activity suppresses GSK3- β activation in dendrites of cerebellar granule neurons [197]. This inhibition promotes dendritic outgrowth and complexity through a mechanism requiring CRMP2 expression. Cumulatively, these studies indicate that CRMP2 also regulates synaptic calcium levels with potential implications for dendritic morphology and spinogenesis.

2.0 RATIONALE AND HYPOTHESIS

The role of PINK1 in maintenance of mitochondrial homeostasis has been extensively investigated, but far less is understood about its function in the cytosol. Cytosolic PINK1 has regulates neurite length [110] and autophagy [117, 198], but the proteins with which it interacts to execute these functions are unknown. We identified VCP as a PINK1 interacting protein in a mass spectrometric screen of proteins that co-immunoprecipitated with PINK1. Most widely recognized as a key mediator of proteasomal degradation, VCP has also been implicated in autophagosome maturation and dendritic spinogenesis. Given these functional overlaps, I hypothesize that VCP and PINK1 act in concert to regulate autophagy and neuronal morphology. Further, I hypothesize that VCP and PINK1 have common downstream effectors, and perturbation of this signaling pathway would impair the ability of PINK1 to promote neurite outgrowth and suppress autophagy. The overarching aim of this work is to understand the contribution of the PINK1-VCP signaling network to the regulation of neuronal morphology and autophagy.

3.0 MATERIALS AND METHODS

3.1 PINK1 KO MICE

All animal studies were performed in accordance with protocols approved by the University of Pittsburgh Institutional Animal Care and Use Committee (IACUC). Dr. Chenjian Li kindly provided the PINK1 knockout (KO) mouse line, generated from C57/129_PINK1^{+/-} ES cells. The colony is maintained in house as a heterozygous line on a C57/129 background, crossing two heterozygotes to produce WT and KO littermates. KNS-25 (5'-ATG AGA TGG AGG GGA GTC-3'), KNS-27 (5'-GGA AGG AGG CCA TGG AAA TTG-3'), and Neo3a (5'-GCA GCG CAT CGC CTT CTA TC-3') primers are used to distinguish between WT, HET, and KO mice.

3.2 CELL CULTURE

3.2.1 Mouse primary neuron isolation

Mouse embryos (E16) were aseptically removed from the embryonic sac of timed pregnant mice (Charles River Laboratories, Wilmington, MA, USA) and placed in ice-cold Dulbecco's phosphate buffered saline (DPBS) (Gibco, Grand Island, NY, USA). A sterile scalpel was used

to decapitate the embryos and remove the brain. Subsequently, the meninges were gently peeled back from the brain and cortex dissected out. The cortex was then digested in 200 units of papain (Worthington Biochem. Corp. Lakewood, NJ, USA) in DPBS containing 2-3 grains of L-cysteine (Sigma-Aldrich Corp., St. Louis, MO, USA), and 500 units of DNase (Sigma-Aldrich Corp., St. Louis, MO, USA). The digestion was stopped by addition of two-three drops of a solution containing 2.5 mg/mL ovomucoid trypsin inhibitor (Worthington Biochem. Corp. Lakewood, NJ, USA), 500 units DNase, and 2.5 mg/mL BSA (Fisher Scientific, Pittsburgh, PA, USA) in Neurobasal media (Gibco, Grand Island, NY, USA) buffered with 10 mM HEPES (BioWhittaker, Walkersville, MD, USA). Fire-polished glass Pasteur Pipets were then used to triturate the resulting digests into a single cell suspension before being centrifuged at 200 x g to pellet. Neuronal pellets were resuspended in Neurobasal media containing 2% B-27 (Invitrogen, Carlsbad, CA, USA), and 2 mM Glutamax (Invitrogen, Carlsbad, CA, USA) and plated on poly-L-lysine coated 4-well Nunc LabTek 1.0 borosilicate glass chamber slides (VWR, Radnor, PA, USA).

3.2.2 Human and mouse cell culture

Human embryonic kidney 293 (HEK293) and human SH-SY5Y neuroblastoma cells were cultured in DMEM (Lonza Bioscience, Walkersville, MD, USA) with 10% fetal bovine serum (Fisher Scientific, Pittsburgh, PA, USA), 2 mM L-glutamine (BioWhittaker, Walkersville, MD, USA), and 10 mM HEPES. Mouse cortical neurons were cultured in Neurobasal media containing 2% B-27, and 2 mM Glutamax. Every third day, half of the media was replaced with fresh Neurobasal medium. All cells were cultured at 37°C with 5% CO₂.

PINK1-3xFLAG (#24) and empty vector (M14) stable cell lines were generated by transfecting pReceiver M14-PINK1-3xFLAG expression plasmid and the pReceiver M14 backbone into parental SH-SY5Y cells using 0.1% Lipofectamine (Invitrogen, Carlsbad, CA, USA). Transfected cells were selected using 1 mg/mL G418 (Promega Life Sciences, Madison, WI, USA) in the DMEM media described above for 24 days. Individual colonies were expanded, and maintained in 150 mg/mL G418.

3.2.3 Pharmacological treatments

FCCP (Sigma-Aldrich Corp., St. Louis, MO, USA), DBeQ (Millipore, Billerica, MA, USA), H89 (Merck KGaA, Darmstadt, Germany) and MG132 (Millipore, Billerica, MA, USA), were prepared in dimethyl sulfoxide (DMSO) (Fisher Scientific, Pittsburgh, PA, USA). Cells were treated with DBeQ at concentrations indicated in the text for 4 hours, 10 μ M FCCP for 2 hours, 10 μ M MG132 for 4 hours, or 250 nM H89 for 14 hours.

3.2.4 Plasmids, siRNA, and transfections

All plasmids used were prepared using the QIAGEN MaxiPrep Plasmid Purification kit (Qiagen, Venlo, Netherlands) according to the manufacturers' protocol. The eGFPc-1, VCP-GFP, pcDNA3.1, and WT-PINK1-GFP plasmids were purchased from Clontech, Addgene, Invitrogen, and Genecopoeia respectively. PLK0.5 and NF1shRNA-PLK0.5 plasmids were purchased from Sigma-Aldrich. Δ N-PINK1-GFP, OMM-PINK1-GFP, WT-LC3-HA, S12A-LC3-HA expression plasmids were previously generated by Dr. Ruben Dagda and Dr. Salvatore Cherra III while

members of Dr. Charleen Chu's laboratory [110, 199]. Dr. Yi-Ping Hsueh kindly provided the FL-VCP-MYC, N-VCP-MYC, D1-VCP-MYC, D2-VCP-MYC, ND1-VCP-MYC, D1D2-VCP-MYC, miRCTRL-GFP, and miRVCP-GFP plasmids. The OMM-GFP and PINK1-IRES-GFP plasmids were generous gifts from Dr. Stefan Strack and Dr. Dennis Selkoe respectively. PD-associated PINK1-GFP mutants (E240K-, G309D-, L347P-, G409V-, L489P-) and IRES-GFP (by mutagenizing to a stop codon before PINK1 coding sequence) plasmids were generated using the QuikChange site-directed mutagenesis II kit. Small interfering RNA (siRNA) targeting human ATG7 and PINK1 were purchased from Dharmacon and Sigma-Aldrich respectively. Mouse NF1 siRNA was also purchased from Sigma Aldrich.

All transfections were performed using Lipofectamine 2000 according to the manufacturers' protocol. Briefly, the required volume of OptiMEM I (Gibco, Grand Island, NY, USA) was divided into two tubes. Plasmids and siRNA were incubated in one tube for five minutes. An OptiMEM and Lipofectamine 2000 mixture was then added to the tube containing plasmid and/or siRNA. Lipofectamine was allowed to complex with the plasmid/siRNA for 20 minutes before being added drop wise to the media. When transfecting HEK293 or SH-SY5Y cells, DMEM media was changed immediately prior to transfection. Neurobasal medium was refreshed 12 hours following transfection of primary neurons. Lipofectamine 2000 was used at 0.2%, .02%, and .01% in HEK293, SH-SY5Y, and primary neurons respectively.

3.3 BIOCHEMICAL ANALYSES

3.3.1 Cell lysis

Media was aspirated from HEK293 cells, and they were washed once in DPBS. HEK293 cells were then collected by scraping in lysis buffer (Miltenyi Biotec, Auburn, CA, USA) containing 150 mM NaCl, 1% Triton. X-100, 50 mM Tris-HCl (pH 8.0) with a protease inhibitor cocktail (1:100) (Sigma-Aldrich Corp., St. Louis, MO, USA), 1 mM sodium orthovanadate (Sigma-Aldrich Corp., St. Louis, MO, USA), and 2mM sodium pyrophosphate (Sigma-Aldrich Corp., St. Louis, MO, USA). SH-SY5Y cells were collected in scraping buffer containing 25mM HEPES (pH 7.5) (ResearchOrganics, Inc., Cleveland, OH, USA), 50mM NaCl (Fisher Scientific, Pittsburgh, PA, USA), 5mM EDTA (Fisher Scientific, Pittsburgh, PA, USA). Cells were pelleted by centrifugation at 5,000 x g for 5 minutes. All cells were incubated on ice in lysis buffer for one hour. Lysates were pelleted by centrifugation at 15,000 x g for 15 at 4°C. Supernatants were then collected, and protein concentration was quantified by bicinchoninic acid (BCA) assay (Thermo Scientific, Rockford, IL, USA).

3.3.2 Immunoprecipitations

GFP, HA, and DYKDDDDK (FLAG) immunoprecipitations (IPs) were performed using the μ MACS Epitope Tag Protein Isolation Kit (Miltenyi Biotec, Auburn, CA, USA). Briefly, 50 μ L of microbeads were incubated with 0.5-1.0 mg of protein for 30 minutes on ice. Samples were then applied to the μ column on the μ MACS separator, and washed three times with 200 μ Ls of

Tris buffered saline (TBS). Microbeads were washed once with 20 mM Tris HCl (pH 7.5) before IP products were eluted in hot μ MACS elution buffer (Miltenyi Biotec, Auburn, CA, USA) containing 50 mM Tris HCl (pH 6.8), 50 mM DTT, 1% SDS, 1 mM EDTA, 0.005% bromphenol blue, and 10% glycerol.

IPs for endogenous proteins were performed by incubating 50 μ L of Protein A agarose beads (Invitrogen, Carlsbad, CA, USA), 2 μ g of indicated antibody, and 1 mg of cell lysate overnight at 4°C while rotating. Beads were collected by centrifugation at 4,500 x g for 2 minutes, and washed four times for five minutes with TBS. IP products were then eluted using hot μ MACS elution buffer described above.

3.3.3 Mass spectrometry for protein identification

Forty-eight hours after plating, HEK293 cells were transfected with EGFPc-1 or WT-PINK1-GFP. Two days following transfection, cells were harvested and GFP IPs performed as described above. IP products were briefly run into a stacking gel. Gel bands were excised and destained in 100 mM ammonium bicarbonate. Proteins were reduced in 5 mM DTT in 100 mM ammonium bicarbonate at 60°C for 30 minutes. Samples were cooled to room temperature before being alkylated in 15 mM iodoacetamide in the dark for 30 minutes. Solution was removed, and gel plug washed for 20 minutes in 50% acetonitrile/100 mM ammonium bicarbonate. Gel band was then incubated overnight in 0.05 μ g/ μ L trypsin in 100 mM ammonium bicarbonate at a 1:100 enzyme to protein ratio. Digested peptides were extracted in 60% acetonitrile/0.1% trifluoroacetic acid before being lyophilized and resuspended in 5% formic acid.

An EASY-nLC II liquid chromatography system coupled to an Orbitrap Elite Mass Spectrometer was used to collect data. High-resolution peptide precursor measurements were made in the Orbitrap ($R=60,000$ at $400m/z$) and low-resolution peptide fragment ion spectra were collected by collision-induced dissociation in a dual-linear ion trap. SEQUEST against a Uniprot-derived human protein database (downloaded 01/17/2011) amended with an entry for GFP was used to search data. Search parameters were: 10.0 ppm mass tolerance for peptide precursor measurements, 0.36 amu mass tolerance for fragmentation spectra, enzyme tolerance for trypsin, static modification of cysteine residues for carbamidomethylation (57.02 amu) and variable modifications on methionine oxidation (15.99amu). To enable analysis of “presence-absence” scenarios, Log_2 ratios were calculated for proteins identified by a minimum of two peptides by adding 0.5 to normalized spectral counts.

3.3.4 Immunoblotting

Equivalent amounts of protein were resolved by SDS-PAGE at 90 volts and transferred to 0.45 μm PVDF membranes (Millipore, Billerica, MA, USA) using the Trans-Blot® SD Semi-dry Transfer Cell (Bio-Rad, Hercules, CA, USA). Membranes were incubated in 5% milk in PBS with 0.3% Tween 20 (PBST) (Fisher Scientific, Pittsburgh, PA, USA), for one hour at room temperature. Subsequently, blots were incubated in primary antibodies at indicated concentrations (Table 1) overnight at 4°C . Following three washes in PBST, membranes were incubated for one hour in horseradish peroxidase conjugated secondary antibodies diluted 1:5000 in 5% milk in PBST at room temperature. Blots were then washed three times in PBST, developed using Luminata Western HRP Substrates (Millipore, Billerica, MA, USA) or

SuperSignal West Pico Chemiluminescent Substrate (Thermo Scientific, Rockford, IL, USA), and imaged using the LI-COR Odyssey Fc.

Densitometric analysis was performed using the LI-COR ImageStudio Lite software. Chemiluminescent signal of the protein of interest was normalized to GAPDH or β -actin signal. As previously described, biological replicates were normalized by dividing the signal of each sample by the summated signal of each sample in that biological replicate [200].

Table 1: Antibodies and dilutions used for immunoblotting.

Antigen	Dilution	Company
β -Tubulin III	1:5,000	Abcam, Cambridge, MA, USA
β -actin	1:5,000	Sigma-Aldrich Corp., St. Louis, MO, USA
CRMP2	1:2,500	Abcam, Cambridge, MA, USA
FLAG	1:2,000	Sigma-Aldrich Corp., St. Louis, MO, USA
GAPDH	1:10,000	Abcam, Cambridge, MA, USA
GFP	1:5,000	Invitrogen, Carlsbad, CA, USA
LC3	1:1,000	Novus Biologicals, Littleton, CO, USA
MYC	1:2,000	Cell Signaling Technology, Danvers, MA, USA
NF1	1:1,000	Bethyl Laboratories, Montgomery, TX, USA
PARP1	1:1,000	Cell Signaling Technology, Danvers, MA, USA
PINK1	1:500	Novus Biologicals, Littleton, CO, USA
pCRMP2 (Ser522)	1:1,000	ECM Biosciences, Versailles, KY, USA
pLC3 (Ser12)	1:500	Abgent Inc., San Diego, CA, USA
PSD95	1:500	Millipore, Billerica, MA, USA
SYN	1:1,000	Chemicon, Temecula CA, USA
Ub	1:1,000	Santa Cruz Biotechnology, Santa Cruz, CA, USA
VCP	1:2,000	Thermo Scientific, Rockford, IL, USA
VGLUT1	1:500	UC Davis/NIH NeuroMab Facility, Davis, CA, USA

3.3.5 Two-dimensional gel electrophoresis

Cells were lysed and protein quantified as described above. Four times the volume of ice-cold acetone (Fisher Scientific, Pittsburgh, PA, USA) was added to 50-75 μg of protein. Lysates were vortexed and incubated at -20°C for one hour. Precipitated proteins were then collected by centrifugation at $15,000 \times g$ for 15 minutes. The resulting supernatant was decanted and pellet dried at room temperature for 30 minutes. The pellet was then resolubilized in 250 μL s of rehydration buffer containing: 7 M urea (Invitrogen, Carlsbad, CA, USA), 2 M thiourea (Invitrogen, Carlsbad, CA, USA), 2% CHAPS (Sigma-Aldrich Corp., St. Louis, MO, USA), 50 mM DTT (Sigma-Aldrich Corp., St. Louis, MO, USA), and 5 μL of pH 3-11 ampholytes (GE Healthcare, Piscataway, NJ, USA).

The BioRad Protean IEF cell (Bio-Rad, Hercules, CA, USA) was used to perform active in-gel rehydration of IPG strips (pH 3-11) (GE Healthcare, Piscataway, NJ, USA) and isoelectric focusing. Following focusing, proteins were reduced by incubating IPG strips in equilibration buffer (375 mM Tris-HCl, pH 8.8, 6 M urea, 2% SDS) with 0.13 M DTT for 10 minutes, and alkylated in equilibration buffer plus 35 mg/mL iodoacetamide (Sigma-Aldrich Corp., St. Louis, MO, USA) for 10 minutes. Strips were then loaded into SDS-PAGE gels and resolved at 90 volts. Proteins were transferred and immunoblotted as described above.

3.4 IMAGE ANALYSES

3.4.1 Immunocytochemistry

Media was aspirated, and cells washed once in DPBS before fixation. When staining for endogenous LC3, cells were fixed in methanol (Fisher Scientific, Pittsburgh, PA, USA) for five minutes at -20°C. In all other experiments, cells were fixed in 4% paraformaldehyde (Sigma-Aldrich Corp., St. Louis, MO, USA) at room temperature for 15 minutes. The fixed cells were then washed twice with DPBS before being permeabilized in PBS containing 0.1% Triton-X (Fisher Scientific, Pittsburgh, PA, USA), for 30 minutes at room temperature. In some experiments, cells were incubated in rhodamine-phalloidin (1:5000) (Invitrogen, Carlsbad, CA, USA) for 15 minutes. Background staining was reduced by blocking in SuperBlock (Thermo Scientific, Rockford, IL, USA) for one hour at room temperature. Primary antibodies diluted in commercial antibody diluent at indicated concentrations (Table 2) were applied overnight at 4°C. Cells were then washed three times for five minutes before being incubated for one hour at room temperature in Alexa-488 or Alexa-546 secondary antibodies (Invitrogen, Carlsbad, CA, USA) diluted 1:1000. Following three more PBS washes, cells were imaged with an oil objective on an Olympus IX71 inverted or Nikon A1R Spectral confocal microscope.

Table 2: Antibodies and dilutions used for immunocytochemistry

Antigen	Dilution	Company
FLAG	1:1,000	Sigma-Aldrich Corp., St. Louis, MO, USA
GFP	1:5,000	Invitrogen, Carlsbad, CA, USA
HA	1:1,000	Invitrogen, Carlsbad, CA, USA
LC3	1:250	Novus Biologicals, Littleton, CO, USA
MAP2	1:2,500	Millipore, Billerica, MA, USA
MYC	1:1,000	Cell Signaling Technology, Danvers, MA, USA

3.4.2 Neurite length

Forty-eight hours after plating on Nunc Labtek 1.0 borosilicate glass 4-well chamber slides, SH-SY5Y cells were transfected. Seventy-two hours after transfections cells were fixed and stained. Neurite length was quantified by GFP fluorescence or rhodamine-phalloidin staining using ImageJ.

3.4.3 Primary dendrite analysis

Seven days after plating on Labtek 1.0 borosilicate glass 4-well chamber slides, mouse primary cortical neurons were transfected. Neurons were fixed and stained seven days post-transfection. Dendrites were manually traced in Adobe Photoshop CS5. The number of dendrites directly branching off the soma was then manually counted.

3.4.4 Sholl analysis

Seven days after plating on Labtek 1.0 borosilicate glass 4-well chamber slides, mouse primary cortical neurons were transfected. Neurons were fixed and stained seven days post-transfection. Dendrites were manually traced in Adobe Photoshop CS5. Skeletons were then extracted and subjected to Sholl analysis using the ImageJ ShollAnalysis plugin [201]. Analysis parameters include a starting radius of 20 μm , ending radius of 100 μm , and step size of 10 μm . A schematic representation of the analysis is depicted in Figure 7.

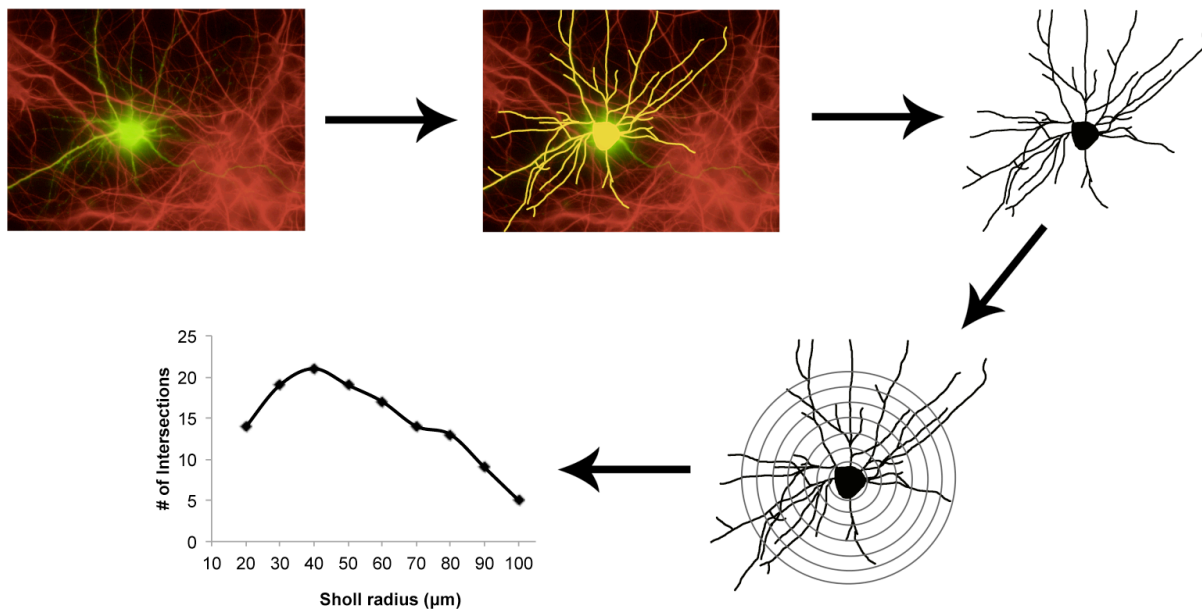


Figure 7: Neuronal morphology analysis.

3.4.5 Dendritic spine analysis

Seven days after plating on Labtek 1.0 borosilicate glass 4-well chamber slides, mouse primary cortical neurons were transfected with IRES-GFP or PINK1-IRES-GFP. Neurons were fixed and

stained seven days post-transfection. Neurons were imaged on a Nikon A1 Spectral confocal microscope. The number and morphology of dendritic spines in a 50 μm segment of secondary dendrite were manually analyzed and quantified. Filopodia were defined as long, thin protrusions without a discernible spine head. All other protrusions were considered spines.

3.4.6 Autophagosome number

SH-SY5Y cells were fixed 72 hours after transfection, and stained for HA-LC3 or endogenous LC3. LC3 positive puncta per cell with a fluorescent intensity equal or greater to 1.5 times the standard deviation of the cytosolic mean intensity were quantified

3.5 STATISTICAL ANALYSES

Statistical analyses were performed using GraphPad Prism 6. The unpaired Student's t-test was used to compare means between two groups. One-way ANOVA was employed when necessary to measure the effect of one independent variable between more than two groups, and two-way ANOVA was utilized to compare differences between groups with two or more independent variables. Bonferroni's correction for multiple comparisons was used when more than two groups were being analyzed. P-values of ≤ 0.05 were considered statistically significant.

4.0 RESULTS

4.1 PINK1 PROMOTES NEURONAL DIFFERENTIATION

To date, studies of PINK1 function have largely focused on its role in maintaining mitochondrial homeostasis, despite a dual localization within cytosol. Interestingly, mitochondrial localization is not required for PINK1 to protect against neuronal cell death induced by complex I inhibition [7] and oxidative stress [117] suggesting that the cytosolic activities of PINK1 are important for neuronal health. To investigate the effect of PINK1 activity on neuronal morphology, WT- and a kinase-deficient mutant (K219M)-PINK1 were transfected into undifferentiated SH-SY5Y cells. Corroborating an earlier report [110], WT- but not K219M-PINK1-GFP, promotes neurite extension (Fig. 8A-B). Dendritic arbors are highly complex and dynamic structures that receive input from other neurons. Stabilization and maintenance of appropriate connections between neurons is essential for their highly specialized functions. Simplification of dendritic arbors has been observed in a wide-variety of neurological disorders [202] including PD [36, 203]. Consistent with a pro-differentiation function, PINK1 overexpression promotes dendrite complexity in mouse cortical neurons, as determined by Sholl analysis (Fig. 8C-D).

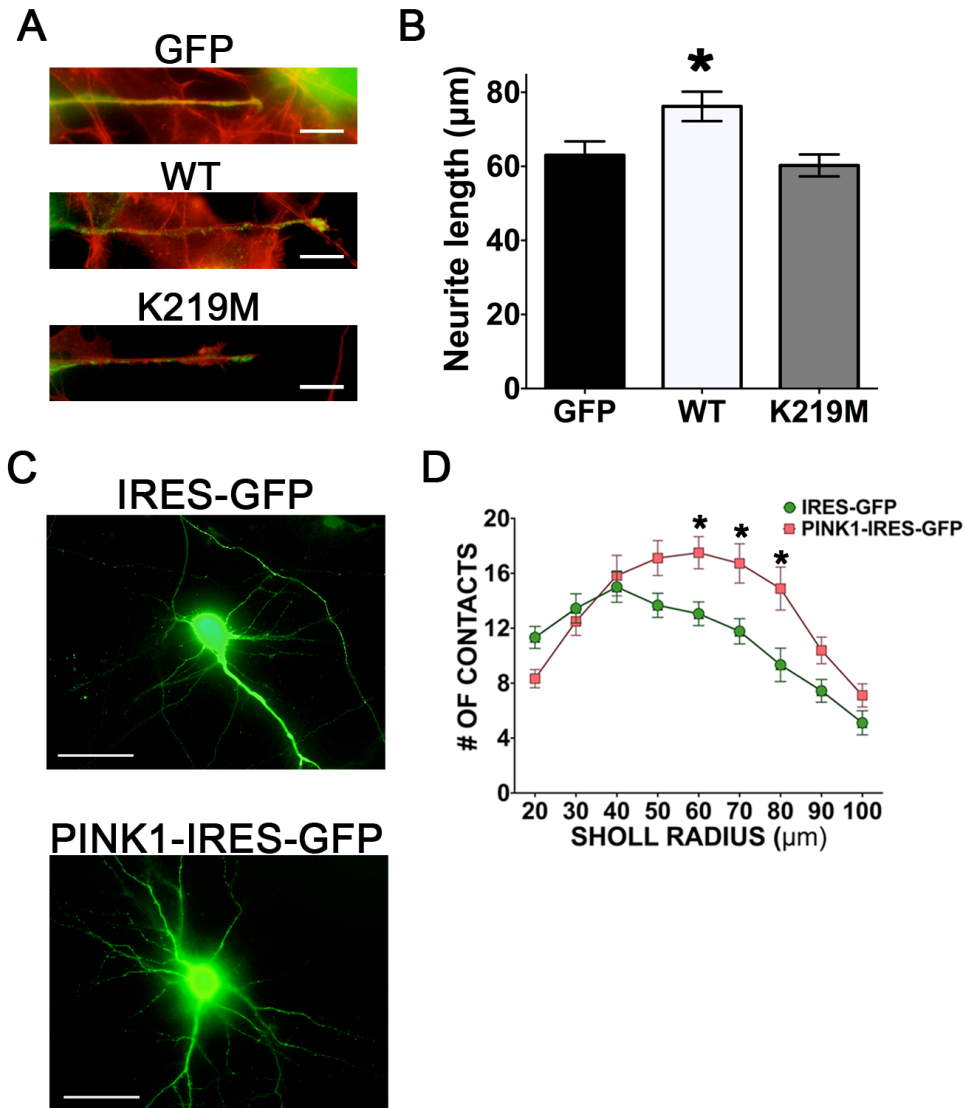


Figure 8: PINK1 promotes neurite extension and dendritic complexity. (A) Representative images of SH-SY5Y cells expressing GFP, WT-, or kinase-deficient (K219M)-PINK1-GFP. Scale bar=10 μm . (B) Quantification of neurite length in SH-SY5Y cells (Mean \pm SEM; 30-44 cells/group compiled from two independent experiments; *P-value<0.05 vs. GFP). (C) Representative images of mouse cortical neurons expressing IRES-GFP or PINK1-IRES-GFP. Scale bar=50 μm . (D) Sholl analyses of cortical neuron dendritic arbors (Mean \pm SEM; 9-10 neurons/group compiled from two independent experiments; *P-value<0.01 vs. IRES-GFP).

4.2 PINK1 INTERACTS WITH VCP

4.2.1 Mass spectrometric identification of PINK1-VCP interaction

An unbiased proteomic approach was utilized to identify potential proteins with which PINK1 interacts to exert these effects on neuronal differentiation. GFP immunoprecipitations (IPs) were performed on lysates from HEK293 cells overexpressing GFP or PINK1-GFP, and IP products were subjected for mass spectrometric analysis. Unsurprisingly, PINK1 was identified as the most abundant protein in the PINK1-GFP IP sample with a sequence coverage of 63.6215% and Log_2 ratio of spectral counts (PINK1-GFP:GFP) of 9.699 (Table 3, Fig. 9A). VCP (sequence coverage 24.194%, Fig. 9B) was among the most enriched proteins co-IPed by PINK1-GFP, with a Log_2 ratio comparable to that of two chaperones, CDC37 and HSP90A, known to bind PINK1 and prevents its degradation (Table 3, [69]). We elected to pursue VCP as a candidate PINK1-interacting protein because, like PINK1, VCP regulates neuronal morphology and autophagy, as well as being linked to several neurodegenerative diseases.

Table 3: PINK1 interacting proteins identified by mass spectrometry.

Protein Name	Log_2 ratio (PINK1-GFP:GFP)	Sequence Coverage (%)
PINK1	9.699	63.621
CDC37	6.570	42.328
VCP	6.476	24.194
HSP90A	2.344	50.410

A

MAVRQALGRGLQLGRALLRFTGKPGRAYGLGRPGPAAGCVRGERPGWAAGPGAEPRRVGLGLPNRLRFFRQSV
 AGLAARLQRQFVVRWGCAGPCGRAVFLAFGLGLGLIEEQAESRRAVSACQEIQAIFTKSKPGPDPLDTRRL
 QGFRLEEYLIGOSIGKGCSSAAVYEATMPTPONLEVTKSTGLLPGRGPGTSAPGEGQERAPGAPAFPLAIKMMWN
 ISAGSSSEAILNTMSQELVPASRVALAGEYGAVTYRKSKRGPQLLAPHNPNIIRVLRRAFTSSVPLLPALVDYDP
 VLPSRLHPEGLGHGRTFLVMKNYPCTLRQYLCVNTSPRLAAMMLLQLEGVLDHLVQOGIAHRDLKSDNILVE
 LDPDGCPLVLIADFGCLADESIGLQLPFSWYVDRGGNGCLMAPEVSTARPGPRAVIDYSKADAWAVGAIAYE
 IFGLVNPFFYGQKAHLESRSYQEAQLPALPESVPPDVRQLVRALLQREASKRPSARVAANVLHLSLWGEHILAL
 KNKLDKMGVWLLQOSAATLLANRLTEKCCVETKMKMLFLANLECETLCOAALLCSWRAAL

B

MASGADSKGDDLSTAILKQKNRPNRLIVDEAINEDNSVVSLSQPKMDELQLFRGDTVLLKGGKRRREAVCIVLSD
 DTCSEKIRMNRVVRNLRVRLGDVSIQPCPDVKYGKRIHVLPIDDTVEGITGNLFEVYLKPYFLEAYRPIRK
 GDIFLVRGGMRAVEFKVVETDPSYCI VAPDTVIHCEGEP I KREDEEESLNEVGYYDDIGGCRKQLAQIKEMVEL
 PLRHPALFKAIGVKPPRGILLYGPPGTGKTLIARAVANETGAFFFLINGPEIMSKLAGESESNLRKAFFEEAEKN
 APAIIFIDELDAIAPKREKTHGEVERRIVSOLLTMDGLQRAHVIVMAATNRPN SIDPLRRFGRFDREVDIGI
 PDATGRLEILQIHTKNMKLADDVDLEQVANETHGHVGADLAALCSEAALQAIRKKMDLIDLEDETI DAEVMNSL
 AVTMDDFRWALSQSNPSALRET VVEVPQVTWEDIGGLEDVKRELQELVQYPVEHPDKFLKFGMTPSKGVLFYGP
 PGCGKTLAKAIAANEQANFISIKPELLTMWFGESEANVREIFDKARQAAPCVLFFDELDSIAKARGGNI GDGG
 GAADRVINQILTEMDGMSTKKNVFIIGATNRPIIDPAILRPGRLDQLIYIPLPDEKSRVAILKANLRKSPVAK
 DVDLEFLAKMTNGFSGADLTEICQACKLAIRESEIEIRRERERQTNPSAMEVEEDDPVEIRRDHFEEAMRF
 ARRSVSDNDIRKYEMFAQTLQQRGFGSFRFP SGNQGGAGPSQSGGGTGGSVYTEDNDDDLYG

Figure 9: Sequence coverage of PINK1 and VCP in PINK1-GFP IP products. (A) PINK1 peptides identified by mass spectrometry (sequence coverage=63.6215) in PINK1-GFP IP products highlighted in green (B) VCP peptides detected in PINK1-GFP IP products highlighted in green (sequence coverage=24.194%).

4.2.2 Immunoblot validation of PINK1-VCP interaction

To confirm that PINK1 interacts with VCP, GFP IP followed by immunoblotting was performed on HEK293 cell lysates (Fig. 10B). Further, in reciprocal IPs performed on HEK293 lysates, VCP-GFP pulled down exogenous FL- and ΔN-PINK1-3xFLAG (Fig. 10C). To determine whether PINK1 interacts with VCP in neuronal cells, endogenous VCP was IPed in vector (M14) and PINK1-3xFLAG overexpressing (#24) SH-SY5Y stable cell lines. Similar to the results in HEK293 cells, endogenous VCP pulled down PINK1 in a PINK1-3xFLAG overexpressing cell line. These immunoblot analyses suggest that the PINK1-VCP interaction is tag-independent and the proteins associate both in neuronal and non-neuronal cells.

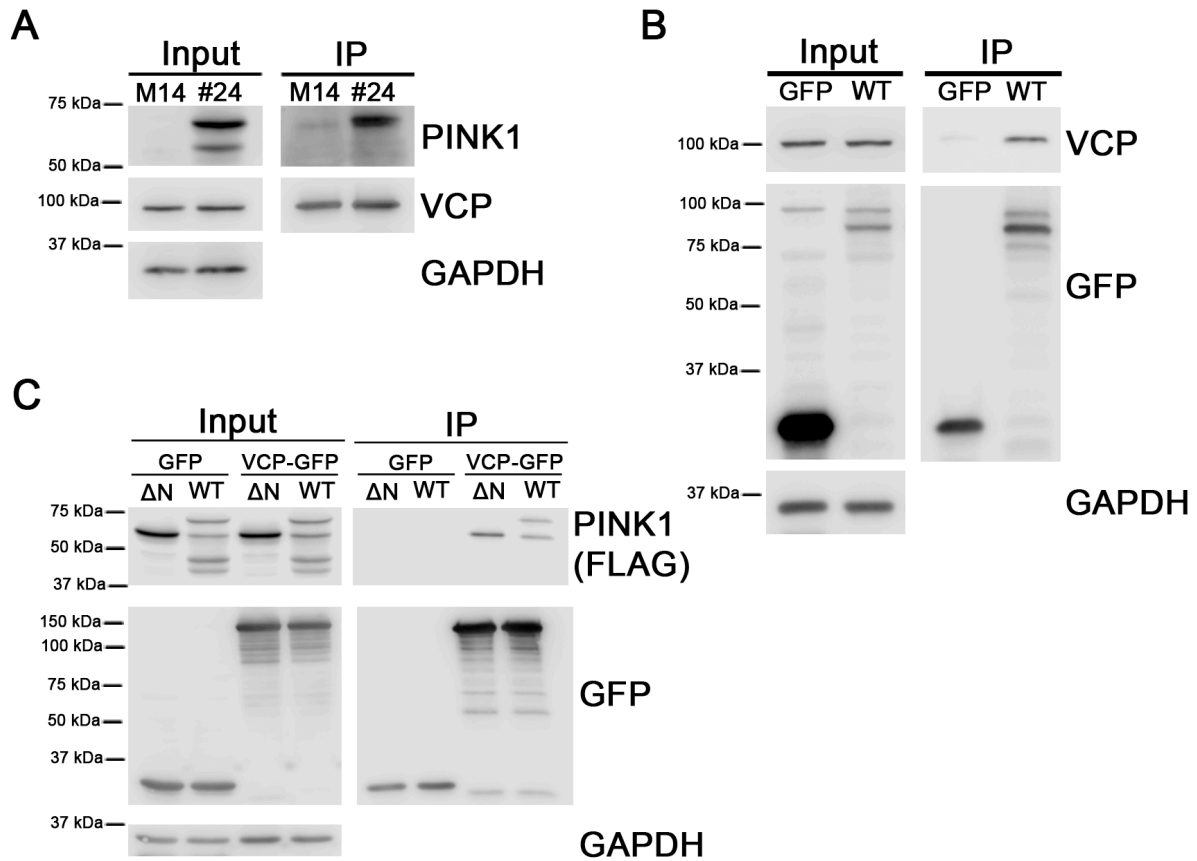


Figure 10: Immunoblot validation of PINK1-VCP interaction. (A) Immunoblot representation of PINK1-3xFLAG pulled down by endogenous VCP immunoprecipitated from vector (M14) and PINK1-3xFLAG overexpressing (#24) SH-SY5Y cell lines. Immunoblot is representative of three independent experiments. (B) Immunoblot of GFP immunoprecipitation products of HEK-293 cells expressing GFP or WT-PINK1-GFP. Immunoblot is representative of 5 independent experiments. (C) Immunoblot of GFP immunoprecipitation products from HEK-293 cells co-expressing GFP or VCP-GFP and Δ N-PINK1-FLAG or WT-PINK1-FLAG. Immunoblot is representative of three independent experiments.

4.2.3 Mitochondrial localization is not required for PINK1-VCP binding

As described in the introduction, mitochondrial localization of PINK1 is required for many of its regulatory effects on mitochondrial homeostasis. Additionally, VCP associates with mitochondria under certain conditions [145, 147] and promotes mitochondrial homeostasis [142, 143]. To determine whether mitochondrial localization is required for its interaction with VCP, PINK1 constructs lacking a mitochondrial targeting sequence (Δ N-PINK1-GFP) or targeted to the outer mitochondrial membrane (OMM-PINK1-GFP) were employed. HEK293 cells expressing these lysates were subjected to GFP IPs followed by immunoblotting. Despite approximately equivalent expression in the input, Δ N-PINK1-GFP pulled down approximately four times more VCP than OMM-PINK1-GFP (Fig 11A-B). To determine whether mitochondrial injury promotes the association of VCP with PINK1 targeted to the outer mitochondrial membrane, HEK293 cells were treated with 10 μ M of the protonophore FCCP for two hours. Dissipation of mitochondrial membrane potential did not increase the amount of VCP pulled down by OMM-PINK1-GFP (Fig. 11C). These data demonstrate that mitochondrial localization is not required for PINK1-VCP binding, suggesting that the cytosolic pool of PINK1 contributes to the functional consequence of the interaction.

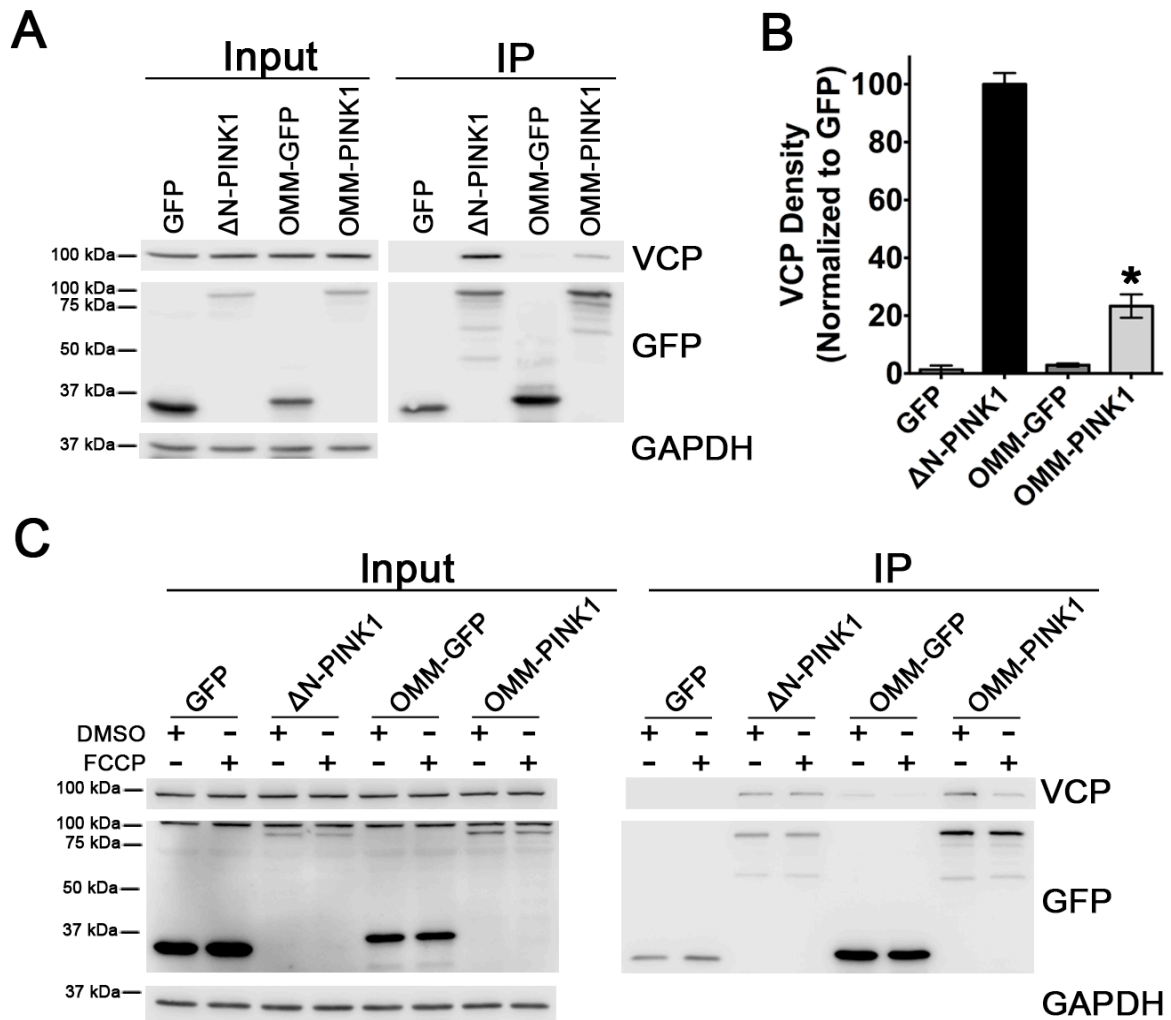


Figure 11: Mitochondrial localization is not required for PINK1-VCP interaction. (A) Representative immunoblot of GFP IP products from HEK293 cells expressing GFP, Δ N-PINK1-GFP, OMM-GFP, and OMM-PINK1-GFP. (B) Densitometric analysis of co-IPed VCP normalized to density of GFP. Data are expressed as mean \pm SEM from three independent experiments (*P-value<0.0001). (C) Representative immunoblot of GFP IP products from HEK293 cells expressing GFP, Δ N-PINK1-GFP, OMM-GFP, and OMM-PINK1-GFP treated with DMSO or 10 μ M FCCP for two hours. Immunoblot is representative of two independent experiments.

4.2.4 PINK1 does not regulate post-translational modification of VCP

PINK1 kinase activity is required for its ability to protect against cell death [7, 204] and promote neuronal differentiation (Fig 8A-B; [110]). To determine whether VCP is a direct or indirect target of PINK1 kinase activity, lysates from PINK1 overexpressing cells were subjected to analysis by 2-D SDS-PAGE. VCP isoelectric focusing was not significantly altered in non-neuronal (HEK293) (Fig. 12A) or neuronal (SH-SY5Y) (Fig. 12B) cells overexpressing PINK1. This result suggests that VCP is not a PINK1 substrate.

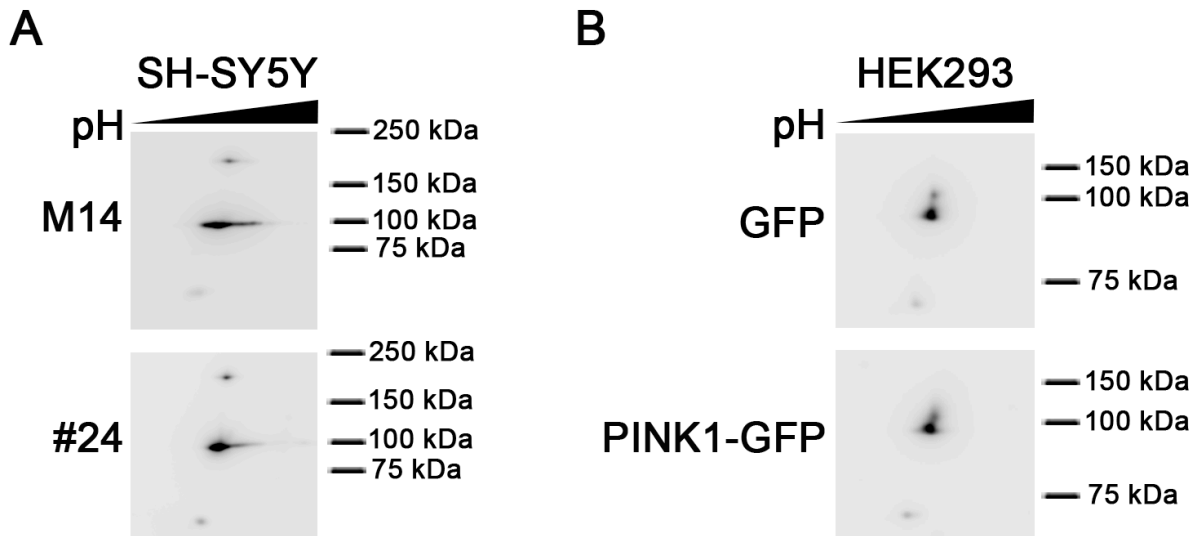


Figure 12: PINK1 overexpression does not alter isoelectric focusing of VCP. (A) 2-D immunoblots of vector (M14) and PINK1-3xFLAG overexpressing (#24) SH-SY5Y cell lines probed for VCP. Immunoblots are representative of three independent experiments. (B) 2-D Immunoblots of HEK293 cells expressing GFP or WT-PINK1-GFP probed for VCP. Immunoblots are representative of two independent experiments.

4.3 VCP ACTS DOWNSTREAM OF PINK1 TO PROMOTE NEURITE EXTENSION AND DENDRITIC COMPLEXITY

4.3.1 VCP overexpression protects against PINK1 KD induced neurite retraction

To determine whether VCP and PINK1 regulate neuronal morphogenesis through a shared mechanism, the ability of VCP overexpression to protect against PINK1 knockdown was assessed. Transient knockdown of PINK1 caused an approximately 10 μm reduction of neurite length in undifferentiated SH-SY5Y cells. This neurite shortening is reversed by VCP overexpression (Fig. 13A-B). Though the exact mechanism is elusive, PINK1 and PKA signaling converge to regulate mitochondrial calcium extrusion and promote neurite extension through convergent pathways [87, 110]. To determine whether inactivation of cAMP signaling pathways was required for the rescue by VCP overexpression, neurite length was measured in PINK1 deficient SH-SY5Y cells treated with the 250 nM of the PKA inhibitor H89 for 14 hours. PKA inhibition impeded the capacity of VCP to restore neurite length in PINK1 deficient cells (Fig. 13C).

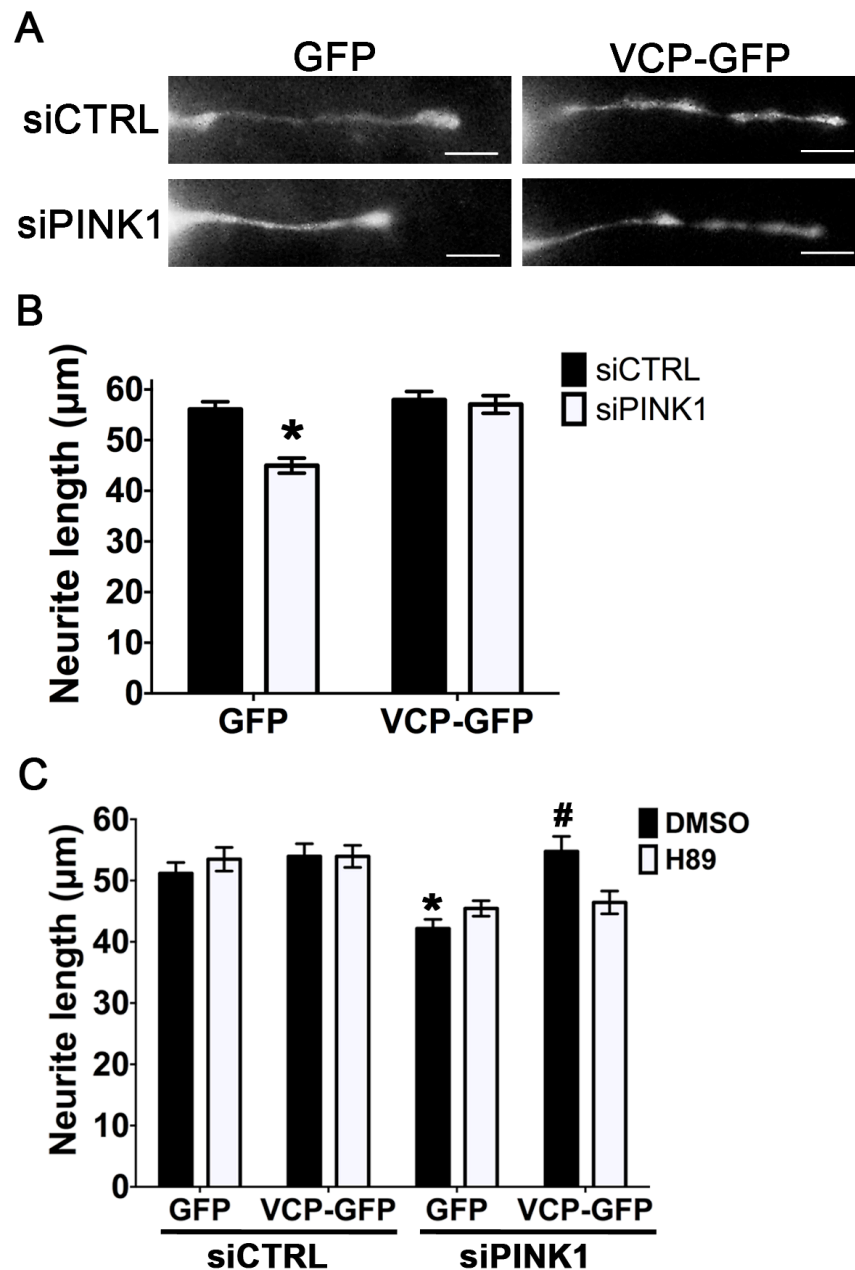


Figure 13: VCP overexpression prevents neurite shortening induced by PINK1 knockdown. (A) Representative images of SH-SY5Y cells transfected with scrambled or PINK1 siRNA and GFP or VCP-GFP. Scale bars=10µm. (B) Neurite length quantification of SH-SY5Y cells in (A) (Mean±SEM; 196-222 cells/group compiled from 4 independent experiments, *P-value<0.0001 vs. siCTRL + GFP). (C) Neurite length of SH-SY5Y cells transfected with scrambled or PINK1 siRNA and GFP or VCP-GFP and treated with DMSO or 250 nM H89 for 14 hours (Mean±SEM; 87-134 cells/group compiled from two independent experiments, *P-value<0.0001 vs. DMSO-treated siCTRL+GFP; #P-value<0.001 vs. H89-treated siPINK1+GFP).

4.3.2 PINK1 requires VCP expression to promote dendrite complexity

The effect of VCP knockdown on the ability of PINK1 to promote dendritic complexity was also examined. Expression of a microRNA construct that targets mouse VCP reduced expression of exogenous mouse VCP-MYC expressed in HEK293 cells (Fig. 14A) as assessed by immunoblot, and endogenous VCP in mouse primary cortical neurons as assessed by immunofluorescence (Fig. 14B). Expression of miRVCP-GFP does not seem to cause significant cell death in transfected neurons by qualitative assessment, or have a basal effect on dendritic arbors in mouse cortical neurons, but inhibits the increased dendritic arborization induced by overexpression of PINK1 (Fig. 14C-E).

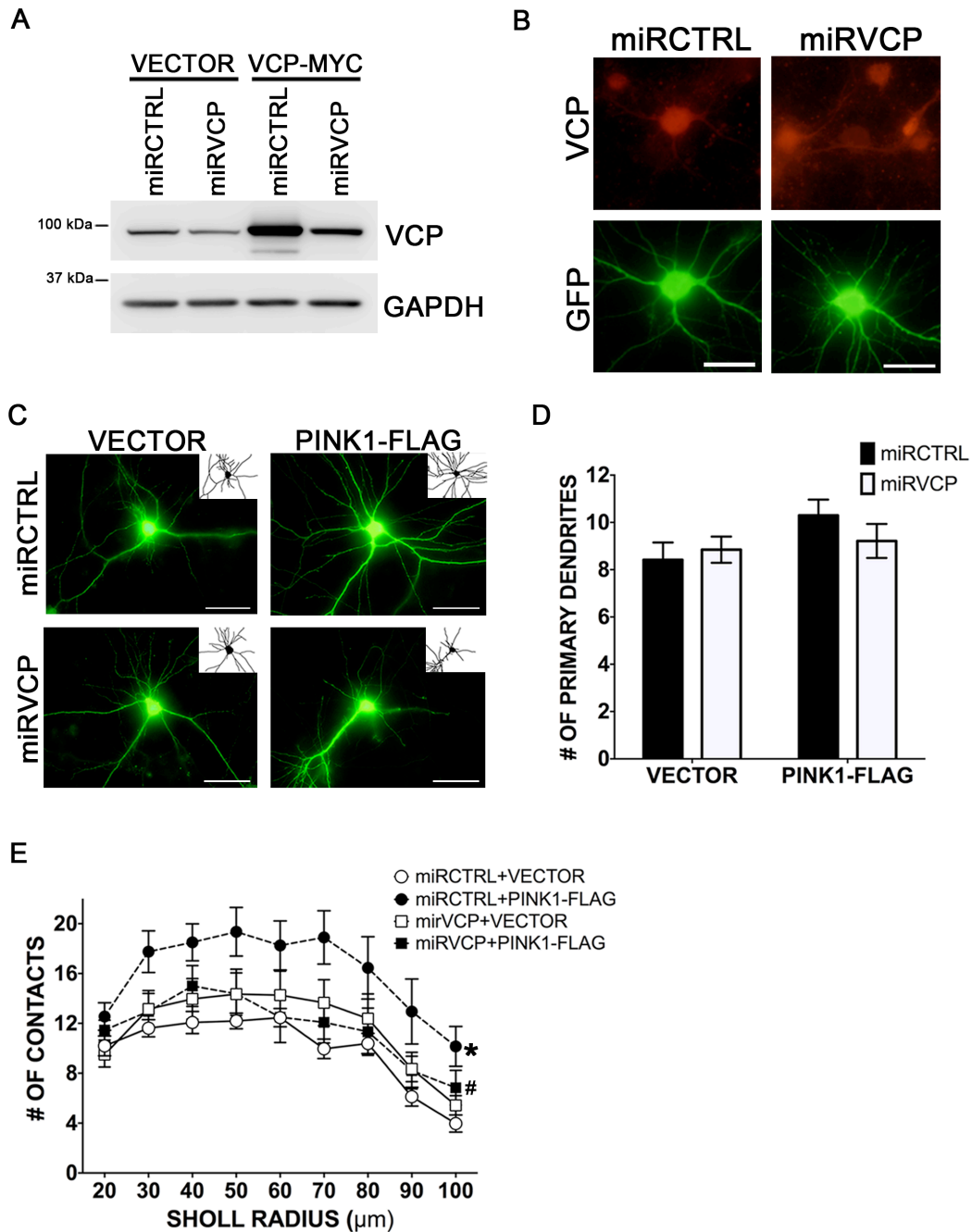


Figure 14: PINK1 requires VCP to promote dendritic complexity. Validation of VCP knockdown in HEK293 cells (A) co-expressing miRCTRL-GFP or miRVCP-GFP and vector or FL-VCP (mouse)-MYC and mouse primary cortical neurons expressing miRCTRL-GFP or miRVCP-GFP (B) Scale bars=25μm. (C) Representative images and dendrite tracings (inset) of cortical mouse neurons transfected with miRCTRL-GFP or miRVCP-GFP and vector or PINK1-FLAG. Scale bars=50 μm. (D) Quantification of primary dendrites and (E) Sholl analyses of dendritic arbors performed on neurons from (C) (mean±SEM; 10-13 neurons/group compiled from three independent experiments; *P-value<0.001 vs. miRCTRL-GFP + vector, #P-value<0.001 vs. miRVCP + PINK1-FLAG.

4.3.3 PINK1 interacts with the D1 domain of VCP

To identify the region of VCP that binds to PINK1, a series of MYC-tagged VCP domain constructs (Fig. 15A) were expressed in HEK293 cells in tandem with PINK1-3xFLAG. The N-terminal co-factor binding domain and D2 ATPase domain were insufficient for VCP-PINK1 binding, but all constructs containing the D1 domain were co-IPed by PINK1-3xFLAG (Fig. 15B). Interestingly, far less monomeric D1 is pulled down by PINK1 than its dimer or the construct containing both the N and D1 domains. This finding emphasizes the importance of the quaternary structure of VCP for its association with PINK1.

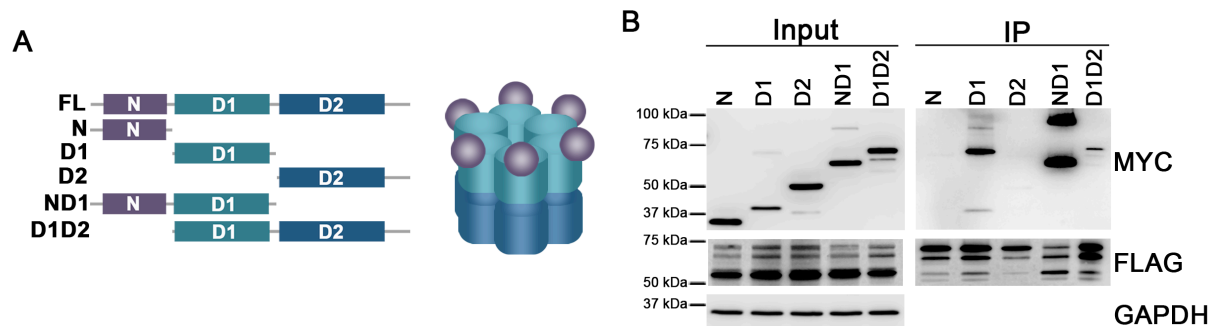


Figure 15: Interaction of VCP with PINK1 requires the D1 domain. (A) Schematic representation of VCP truncation constructs used and the 3-D structure of VCP. (B) Immunoblot of FLAG immunoprecipitation products from HEK293 cells expressing indicated MYC-tagged VCP domain constructs and PINK1-3xFLAG. Immunoblot is representative of four independent experiments.

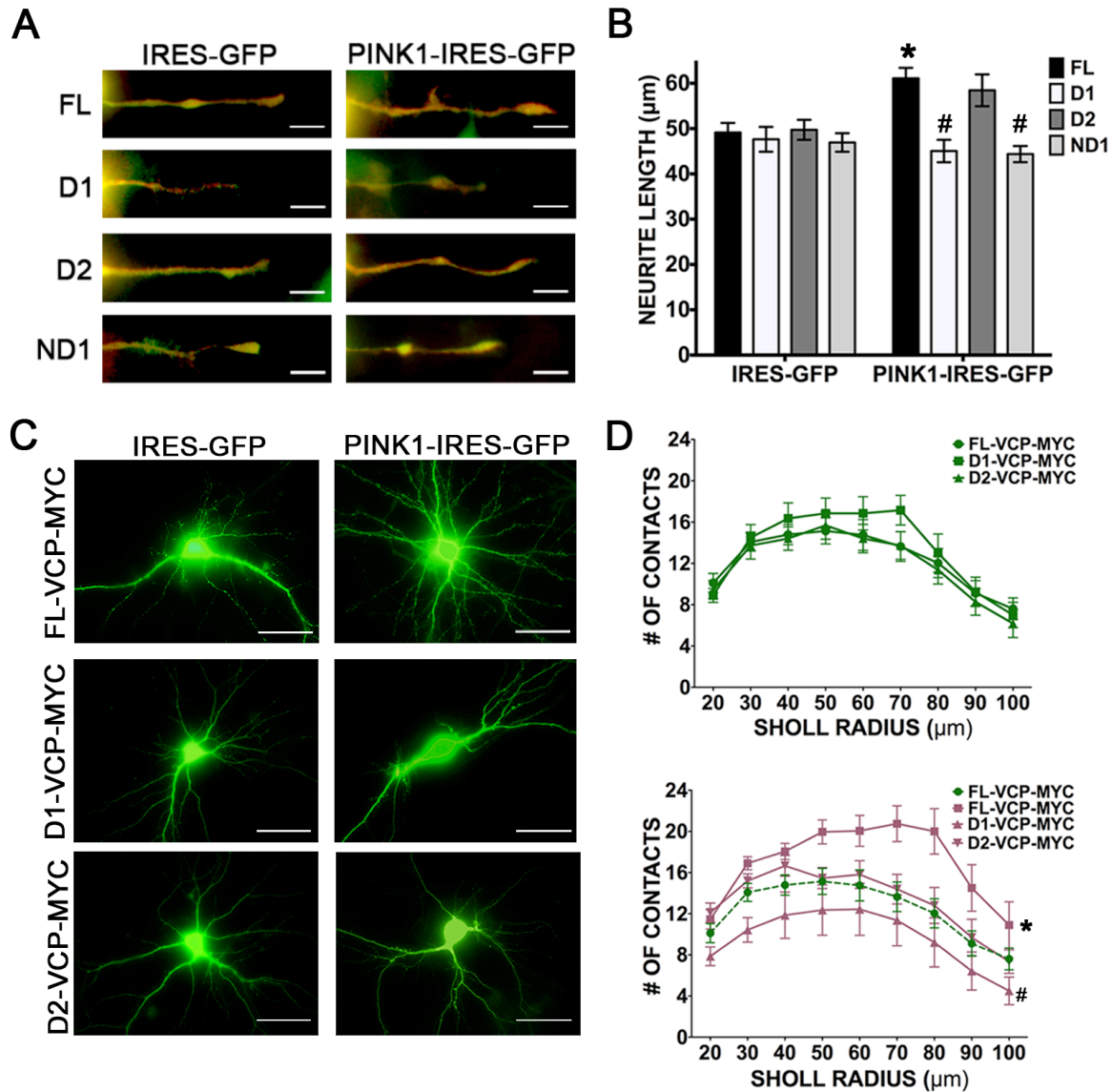


Figure 16: Overexpression of PINK1-binding domain of VCP blocks the effect of PINK1 overexpression on neurites. (A) Representative images of SH-SY5Y cells co-expressing IRES-GFP or PINK1-IRES-GFP and indicated MYC-tagged VCP domain constructs. Scale bar=10 μ m. (B) Neurite length quantification of cells in (A). Data are represented as mean \pm SEM (58-72 cells/group compiled from three independent experiments). (C) Representative images of cortical neurons co-transfected with IRES-GFP or PINK1-IRES-GFP and indicated MYC-tagged domains of VCP. Scale bar=50 μ m. (D) Sholl analyses of dendritic arbors from neurons in (C). Green lines represent neurons co-expressing IRES-GFP and pink lines represent neurons co-expressing PINK1-IRES-GFP (Mean \pm SEM; 10-14 neurons/group from three independent experiments; *P-value<0.0001 vs. IRES-GFP+FL-VCP-MYC; #P-value<0.01 vs. IRES-GFP+FL-VCP-MYC).

The importance of VCP function in PINK1 induced neurite extension and dendrite arborization was further confirmed by expressing these domains in neuronal cells. Overexpression of PINK1-binding domains (D1 and ND1) inhibited PINK1-induced neurite outgrowth in SH-SY5Y cells (Fig. 16A-B). Additionally, PINK1 does not promote dendrite complexity in cortical neurons when co-expressed with the D1 domain of VCP (Fig. 16C-D). While expression of the D1-domain did not have a basal effect on dendrite morphology, its co-expression with PINK1 resulted in further simplification of the dendritic arbor. Taken together, these data identify VCP as a necessary downstream mediator of PINK1 induced neurite outgrowth.

4.3.4 PINK1 requires NF1 to promote neurite outgrowth and dendrite complexity

VCP interacts with NF1 to promote dendritic spinogenesis [152] and NF1 induces dendritic filopodia formation and neurite outgrowth through PKA-dependent mechanisms [170]. To determine whether NF1 was involved in PINK1-induced neurite outgrowth, VCP binding to NF1 was assessed in PINK1 overexpressing neuronal cells. Comparable amounts of VCP were co-IPed by endogenous NF1 IP in vector (M14) and PINK1-3xFLAG overexpressing (#24) SH-SY5Y cell lines as assessed by immunoblot (Fig. 17A). The D1 domain of VCP mediates its association with both NF1 [152] and PINK1 (Fig. 15B). Despite this, PINK1 overexpression does not outcompete NF1 for VCP binding, suggesting that PINK1, VCP, and NF1 may form a functional complex.

To explore this possibility, neurite length and dendrite complexity were analyzed in NF1 deficient neuronal cells. As with VCP knockdown (Fig. 14B,D), NF1 deficiency alone did not

significantly reduce neurite length in SH-SY5Y cells (Fig. 17C,E), but was sufficient to prevent PINK1 induced neurite outgrowth and dendritic arborization (Fig 17C-F). Interestingly, PINK1 overexpression in NF1 deficient neurons caused simplification of the dendritic arbor compared to control neurons (siCTRL+IRES-GFP). This result mirrors the effect of simultaneous expression of PINK1 and the D1 domain of VCP (Fig. 16C-D). Cumulatively, these data indicate that PINK1 regulates neuronal morphology through a mechanism requiring VCP and NF1.

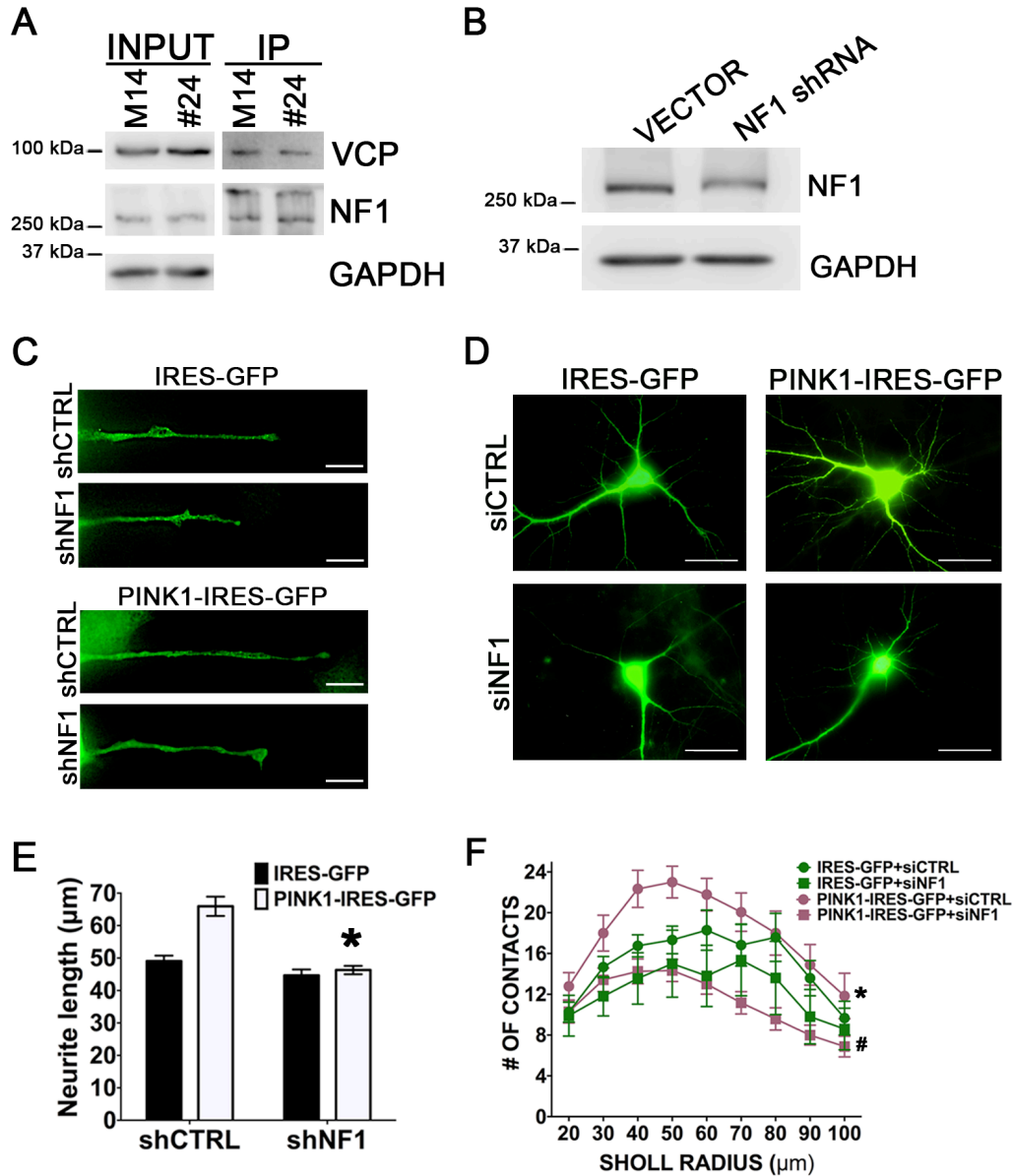


Figure 17: PINK1 requires NF1 expression to promote dendritic complexity. (A) Immunoblot of endogenous NF1 immunoprecipitation products from stable vector (M14) and PINK1-3xFLAG (#24) SH-SY5Y cell lines. Immunoblot is representative of two independent experiments. (B) Immunoblot validation of NF1 knockdown in HEK293 cells. Immunoblot represents one experiment. (C) Representative images of SH-SY5Y cells co-transfected with scrambled or NF1 shRNA and IRES-GFP or PINK1-IRES-GFP. Scale bar=10 µm. (E) Neurite length quantification of cells from (B). Data are represented as mean±SEM (86-98 cells/group compiled from three independent experiments; *P-value<0.001 vs. IRES-GFP+shCTRL). (D) Representative images of primary cortical neurons co-transfected with scrambled or NF1 siRNA and IRES-GFP or PINK1-IRES-GFP. Scale bar=50 µm. (F) Sholl analyses of dendritic arbors from neurons in (D). Data are represented as mean±SEM (9-12 neurons/group; *P-value<0.01 vs. IRES-GFP+siCTRL; #P-value<0.0001 vs. PINK1-IRES-GFP+siCTRL)

4.3.5 VCP binding is impaired in two PD-associated PINK1 mutants

A panel of PD-associated PINK1-GFP mutants generated by site-directed mutagenesis of the parental plasmid was used to evaluate the effect of these mutations on VCP-binding (Fig. 18A). HEK293 cells were transfected with these constructs, and resulting lysates were subjected to GFP immunoprecipitation. As assessed by immunoblot, G309D- and G409V-PINK1-GFP pulled down significantly less VCP than WT-PINK1-GFP (Fig. 18B-C). VCP pull-down was normalized to the band that migrates at the predicted molecular weight of full-length PINK1-GFP. To determine whether the ability of these PD-associated PINK1 constructs to promote neurite extension was impaired by deficient VCP binding, neurite length was measured in SH-SY5Y cells expressing G309D- and G409V-PINK1-GFP. These two PD-associated PINK1 mutants failed to promote neurite extension, but did not cause neurite retraction (Fig. 18D-E).

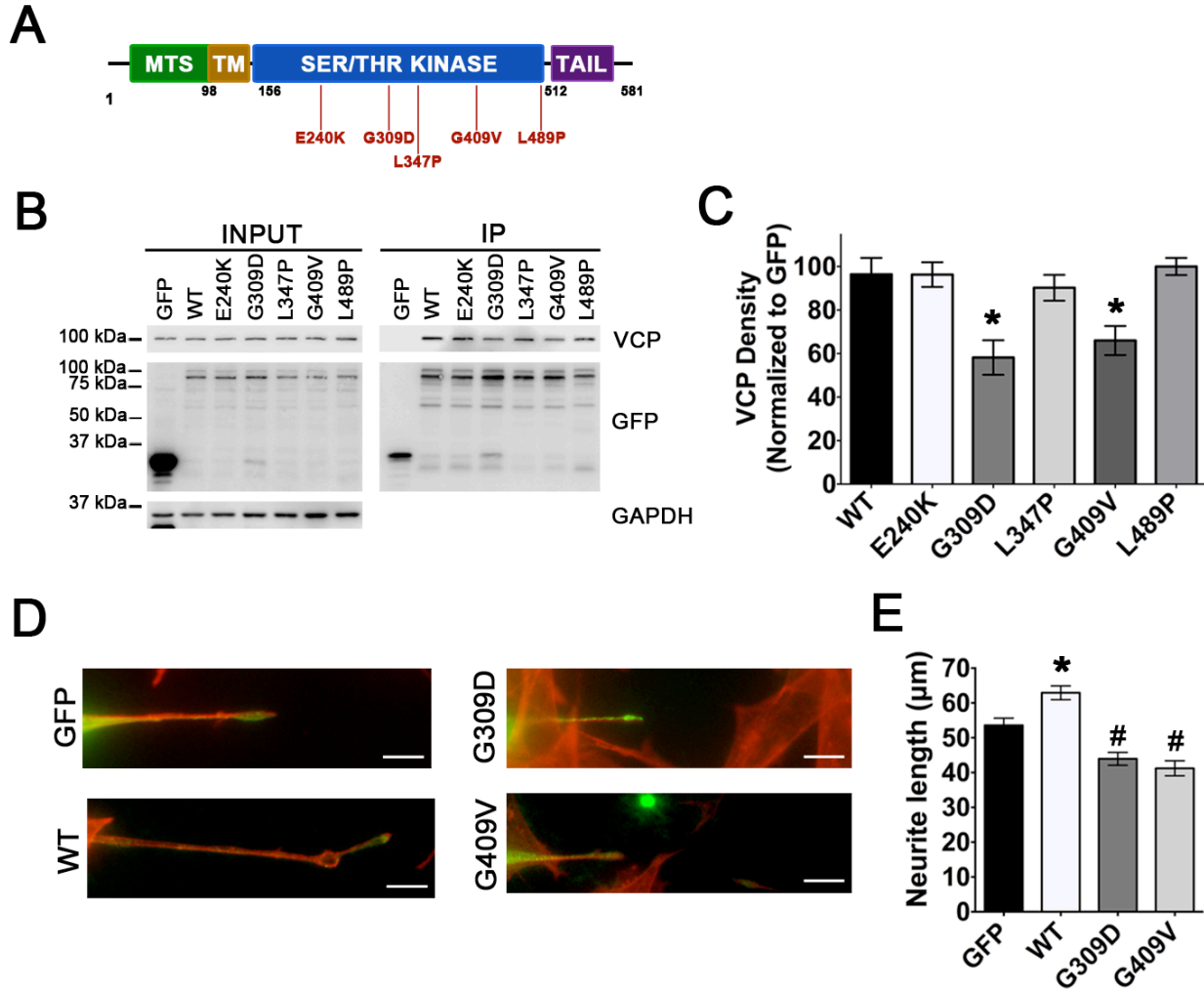


Figure 18: G309D- and G409V-PINK1-GFP co-immunoprecipitate less VCP and fail to promote neurite extension. (A) Schematic representation of PINK1 domains including PD-associated mutants used. (B) Immunoblot of GFP immunoprecipitation products from HEK293 cells transfected with GFP, WT-, or PD-associated PINK1-GFP mutants. (C) Densitometric analysis of VCP co-immunoprecipitated with PINK1-GFP normalized to GFP density. Data are represented as mean±SEM from four independent experiments (*P-value<0.05 vs. WT-PINK1-GFP). (D) Representative images of SH-SY5Y cells transfected with GFP, WT-, G309D-, or G409V-PINK1-GFP and stained with rhodamine-phalloidin. Scale bar=10 µm. (E) Quantification of neurite lengths from cells in (D). Data are represented as mean±SEM (78-100 cells/group compiled from four independent experiments; *P-value<0.01 vs. GFP, #P-value<0.0001 vs. WT-PINK1-GFP).

4.4 PINK1 INTERACTS WITH CRMP2

NF1 associates with CRMP2 to regulate neurite length [172]. Interestingly, a quantitative proteomics study recently discovered reduced expression of several proteins involved in neuronal morphogenesis and synaptic plasticity, including CRMP2, in the brains of PINK1 KO mice [205]. To determine whether CRMP2 is a component of the PINK1-VCP signaling hub, GFP IP products from HEK293 cells expressing PINK1-GFP were probed for CRMP2. CRMP2 was co-immunoprecipitated by PINK1 (Fig. 19A). Additionally, VCP-GFP co-IPs CRMP2, but the amount pulled down was dramatically increased upon co-expression with PINK1-3xFLAG (Fig. 19B). Further, co-expression of MYC-VCP had little effect on the amount of CRMP2 pulled down by PINK1-GFP (Fig. 19C), suggesting that this association is predominantly mediated through an interaction with PINK1.

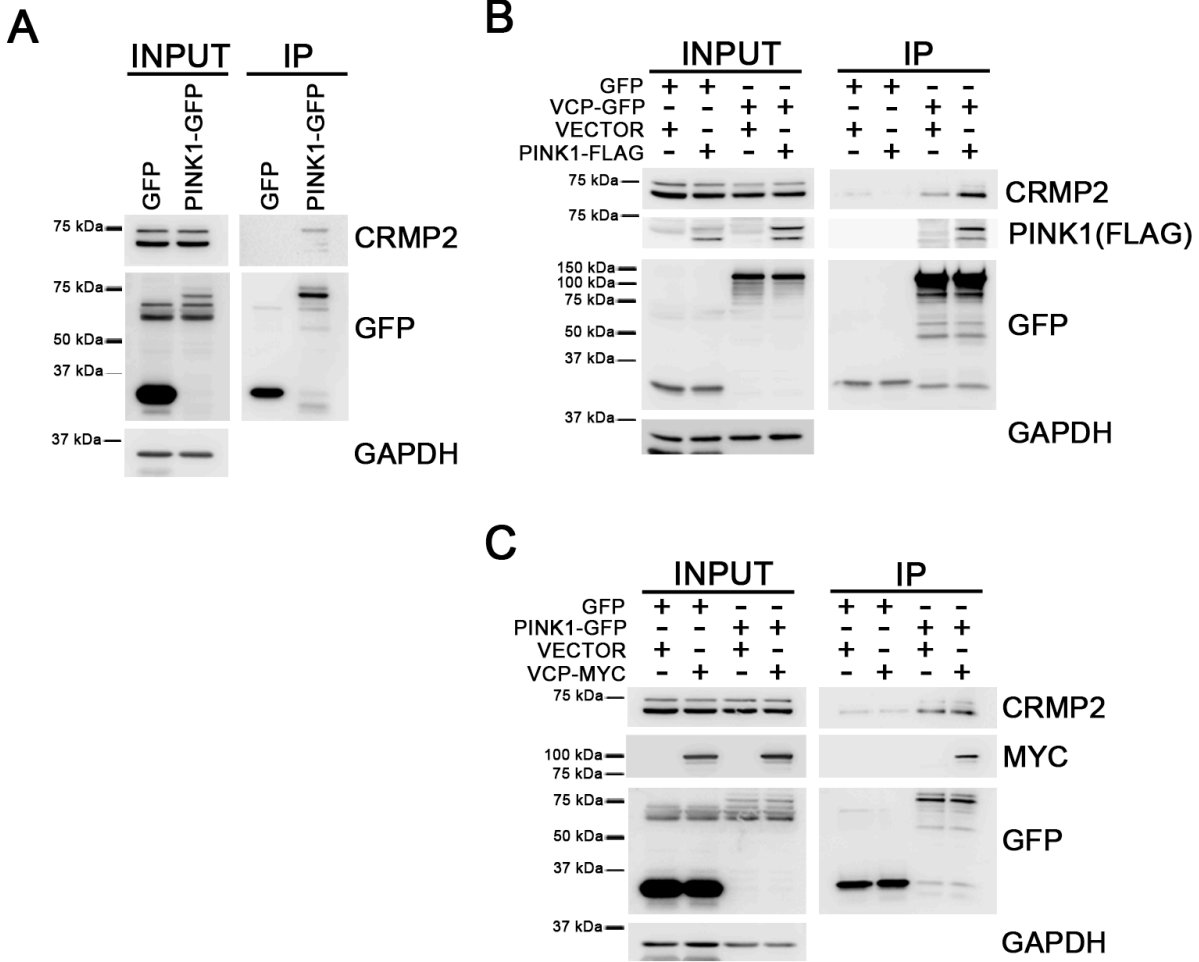


Figure 19: PINK1 interacts with CRMP2. (A) Representative immunoblot of GFP immunoprecipitation products from HEK293 cells expressing GFP or PINK1-GFP. Immunoblot represents three independent experiments. (B) Immunoblot of GFP immunoprecipitation products from HEK293 cells co-transfected with GFP or VCP-GFP and vector or PINK1-FLAG. Immunoblot represents one experiment. (C) Immunoblot of GFP products from HEK293 cells co-transfected with GFP or PINK1-GFP and vector or VCP-MYC. Immunoblot represents one experiment.

4.4.1 PINK1 regulates CRMP2 phosphorylation

NF1 regulates phosphorylation of CRMP2 [172]. To determine whether PINK1 also contributes to this regulation in neuronal cells, whole cell lysates from vector (M14) and PINK1-3xFLAG overexpressing (#24) SH-SY5Y cell lines were subjected to analysis by 2-D SDS-PAGE and probed for CRMP2. The intensity of multiple spots was dramatically increased in PINK1 overexpressing cell lines (Fig. 20A). These shifts in intensity are consistent with alterations in CRMP2 phosphorylation status. To further examine this possibility, levels of CRMP2 phosphorylated at Ser522, a phosphorylation site known to promote appropriate dendritic field organization [196] and dendritic spine development [195] were examined in PINK1 overexpressing SH-SY5Y cells. Phosphorylation of CRMP2 at Ser522 was increased by approximately 50% in PINK1 overexpressing cells (Fig. 20B-C).

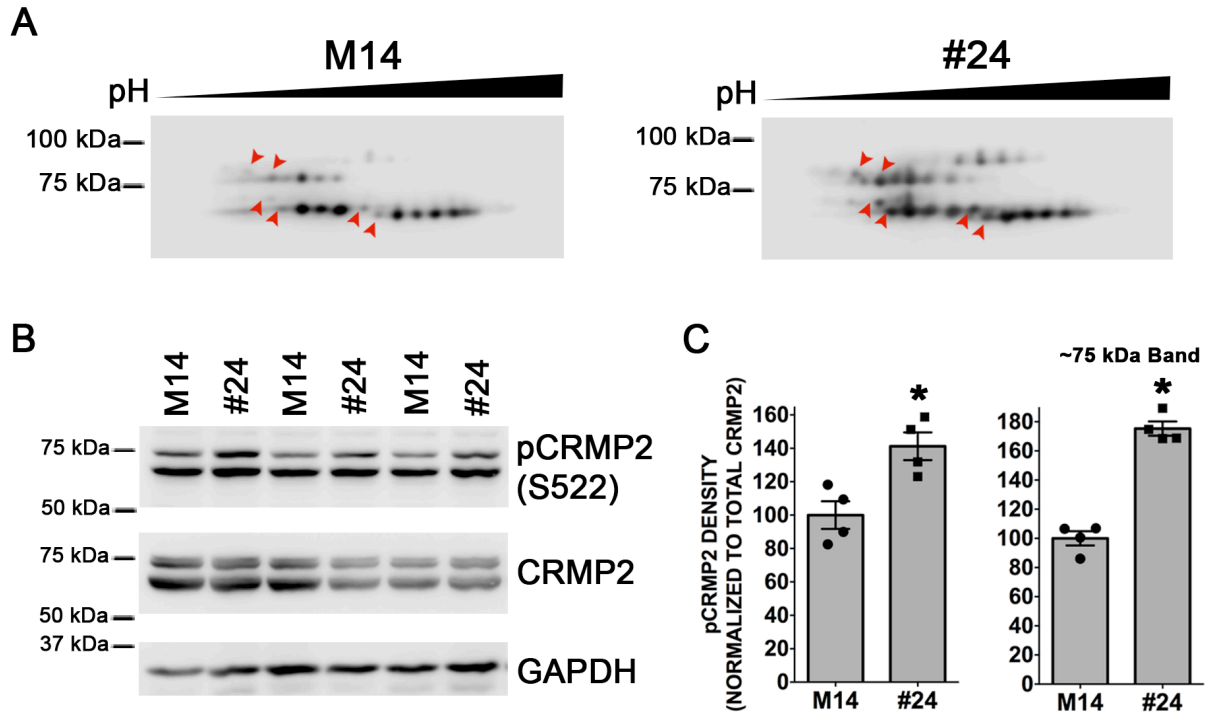


Figure 20: PINK1 overexpression promotes phosphorylation of CRMP2 at Ser522. (A) 2-D immunoblots of vector (M14) and PINK1-3xFLAG (#24) overexpressing SH-SY5Y cells probed for CRMP2. Immunoblot represents three independent experiments. (B) Representative immunoblot of M14 and #24 lysates probed for pCRMP2 (Ser522) and total CRMP2. (C) Densitometric analysis of pCRMP2 normalized to total CRMP2 in M14 and #24 cells. Data are represented as mean \pm SEM of four independent experiments (*P-value \leq 0.01 vs. M14)

The effect of PINK1 knockout on CRMP2 expression and phosphorylation were also examined. Lysates from the ventral midbrain of 6-month-old wild type and PINK1 KO mice were subjected to 2-D SDS-PAGE and probed for CRMP2. There was a striking shift of CRMP2 spot intensity in PINK1 KO mice (Fig. 21A), consistent with alterations in CRMP2 phosphorylation species. To confirm this finding, phospho-CRMP2 (Ser522) levels were assayed in the ventral midbrain of 6-month-old (Fig. 21B-C) and 12-month-old (Fig. 21D-E) wild type and PINK1 KO mice. Phosphorylation of CRMP2 was reduced by ~20% in the ventral midbrain of these animals. Taken together, these data identify PINK1 as regulator of CRMP2 phosphorylation in both in vitro and in vivo model systems.

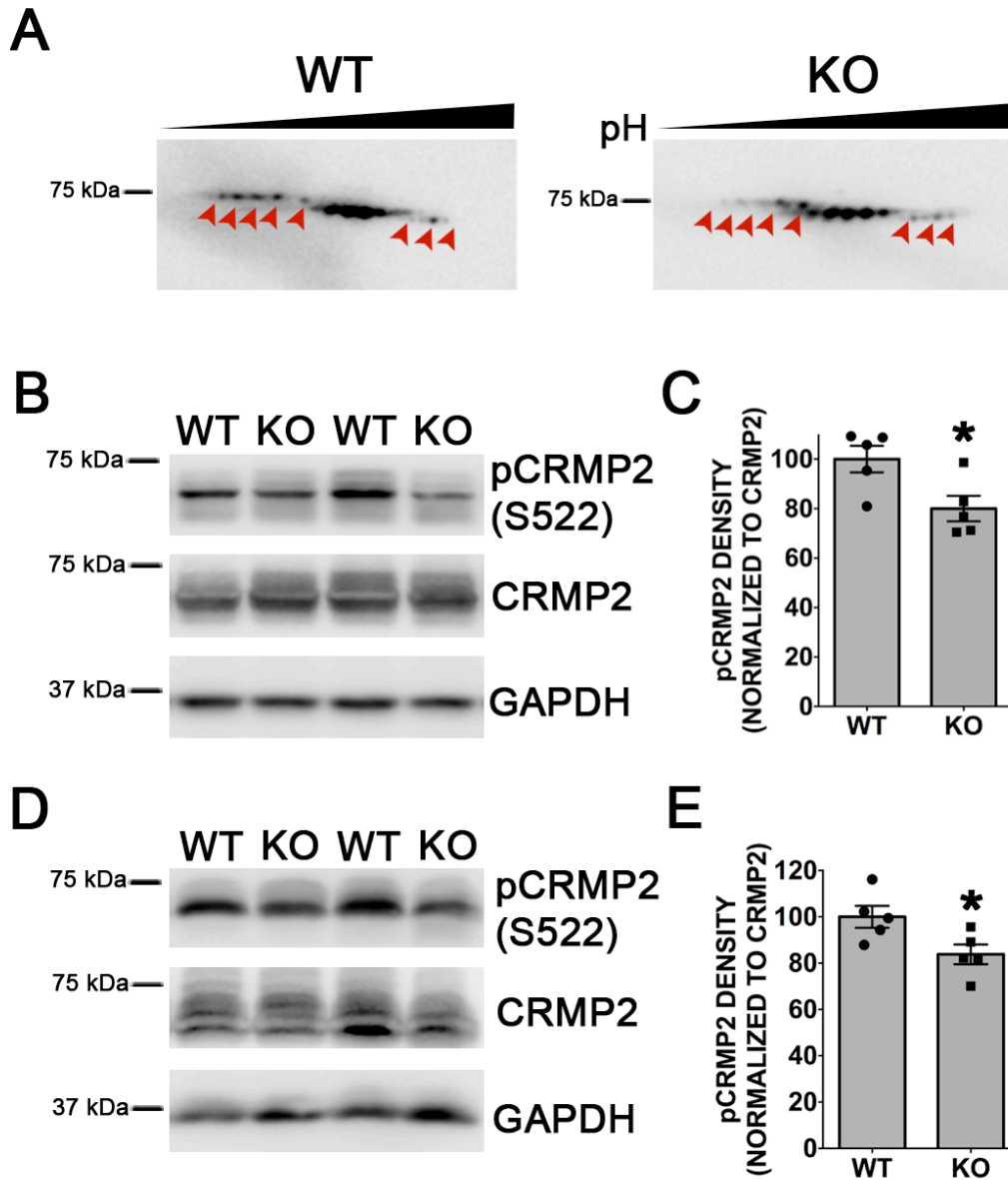


Figure 21: Phosphorylation of CRMP2 at Ser522 is reduced in PINK1 KO mice. (A) 2-D immunoblots of ventral midbrain lysates from six-month-old WT and PINK1 KO probed for CRMP2. Immunoblots are representative of three animals from each cohort. (B) Representative immunoblot of ventral midbrain lysates from six-month-old WT and PINK1 KO mice probed for pCRMP2 (Ser522) and total CRMP2. (C) Densitometric analysis of pCRMP2 (Ser522) levels normalized to total CRMP2. Data are represented as mean \pm SEM of five animals for each cohort (*P-value=0.0279 vs. WT). (D) Representative immunoblot of ventral midbrain lysates from 12-month-old WT and PINK1 KO mice probed for pCRMP2 (Ser522) to total CRMP2. (D) Densitometric analysis of pCRMP2 (Ser522) levels normalized to total CRMP2. Data are represented as mean \pm SEM of five animals from each cohort (*P-value=0.0342 vs. WT)

4.4.2 PINK1 does not affect CRMP2-Tubulin binding

Binding tubulin at the plus end to stabilize microtubules, is the canonical function of CRMP2 known to regulate neuronal morphology [174]. Hyperphosphorylation of CRMP2 promotes its dissociation from tubulin heterodimers, resulting in neurite retraction. To determine whether PINK1 affect the ability of CRMP2 to bind tubulin, endogenous CRMP2 was IPed from vector (M14) and PINK1 overexpressing (#24) SH-SY5Y cell lines. There was not an observable difference in the amount of tubulin pulled down by CRMP2 between these cell lines (Fig. 22). This finding suggests the mechanism by which PINK1-VCP promotes neuronal differentiation does not alter CRMP2-tubulin binding.

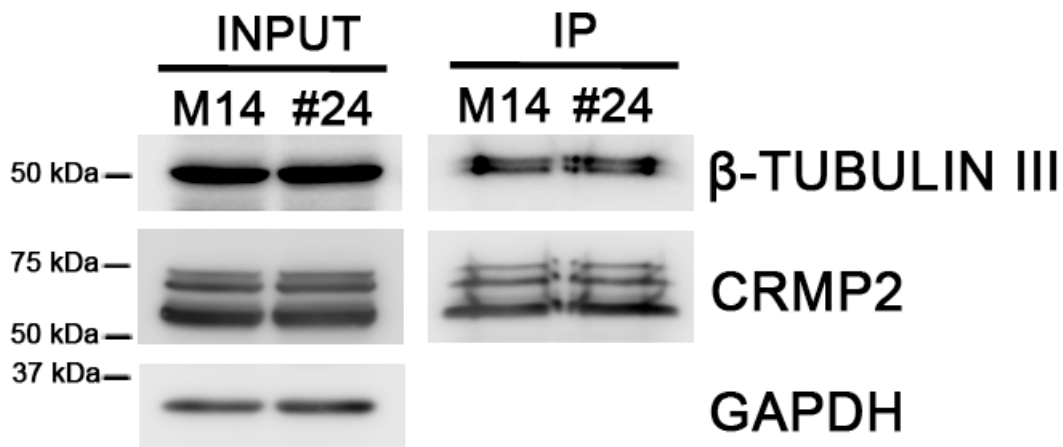


Figure 22: PINK1 does not alter CRMP2 binding to tubulin. Immunoblot of endogenous CRMP2 immunoprecipitation products from vector (M14) and PINK1-3xFLAG overexpressing SH-SY5Y cell lines probed for β -tubulin III and CRMP2. Data represents one experiment.

4.5 PINK1 REGULATES SYNAPSES

VCP [155], NF1 [152, 170], and phosphorylation of CRMP2 at Ser522 [195] all contribute to the regulation of dendritic spinogenesis. To determine if PINK1 also contributes to formation and maintenance of synapses, ventral midbrain lysates from PINK1 KO and wild type mice were analyzed by immunoblot. Expression of pre-synaptic (VGLUT1, SYN1) and post-synaptic (PSD95) markers was unaltered in PINK1 KO mice at three months (Fig. 23A,D-F). Further, loss of PINK1 did not affect protein levels of VCP or NF1 (Fig. 22A-C), and there was no correlation between NF1 expression and synaptic marker expression (Fig. 23G-I). By six months, expression of all probed synaptic markers was significantly lower in PINK1 KO mice (Fig. 24A, D-F) concomitant with a reduction in NF1 expression (Fig. 24A, C). Interestingly, NF1 expression is strongly correlated with expression of all probed synaptic markers at this age (Fig. 24A, G-I). These data suggest that loss of PINK1 function causes an age-dependent loss of synapses in the ventral midbrain of mice.

To more directly assess the effect of PINK1 expression on dendritic spinogenesis, spine density and morphology were analyzed in mouse cortical neurons were transfected with PINK1-IRES-GFP. Seven days after transfection (DIV 14), there was not a significant difference in total number of protrusions/50 μm (Fig. 25A-B). However, at this time point, PINK1 overexpression caused a reduction in the number of dendritic filopodia with a concurrent increase in the number of spines (Fig 25A-B). Cumulatively, these results suggest that PINK1 contributes to the regulation of dendritic spine formation and/or synaptic maintenance.

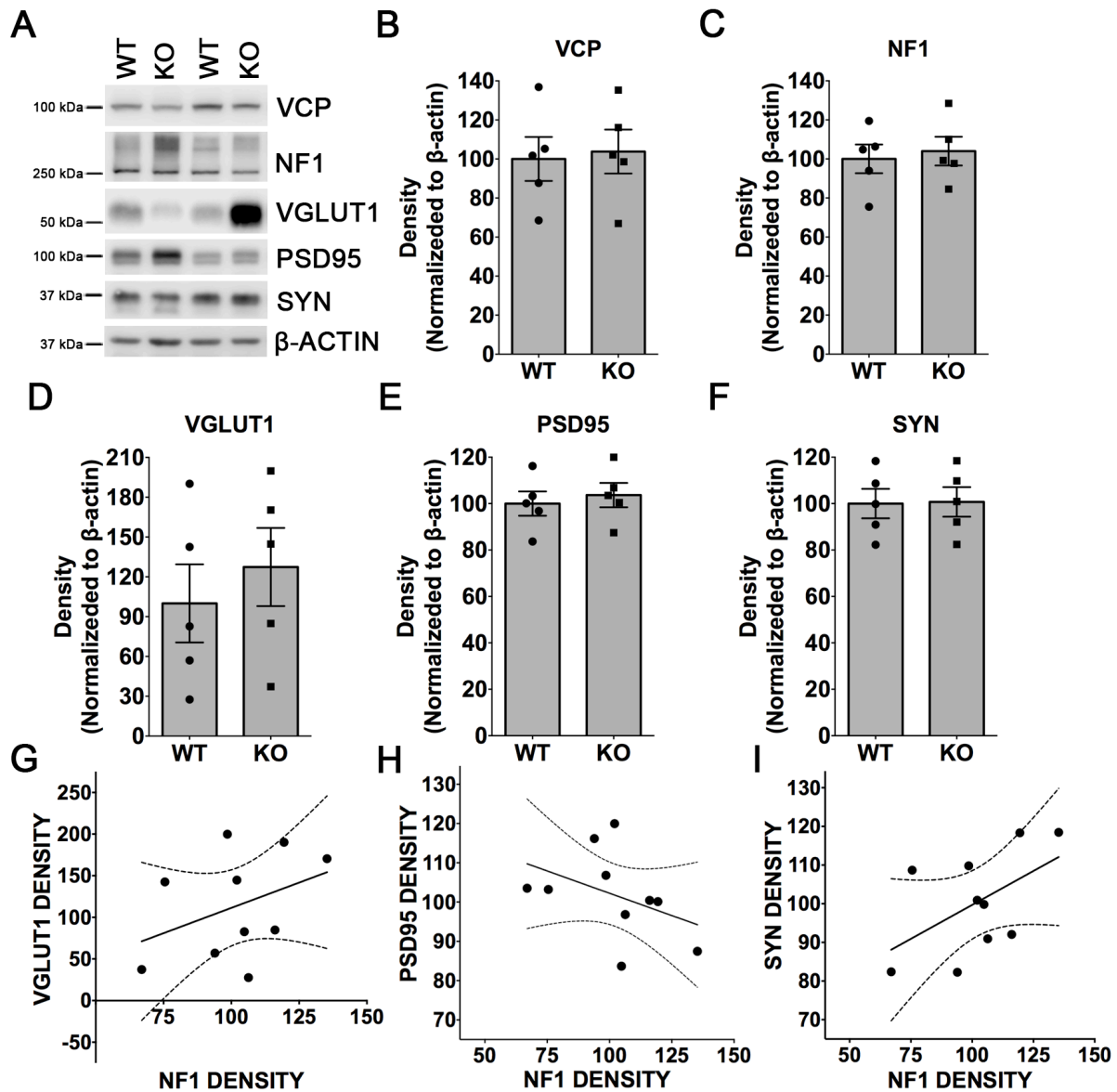


Figure 23: Expression of synaptic markers is unaltered at 3 months in PINK1 KO mice. (A) Representative immunoblot of ventral midbrain lysates from 3-month-old WT and PINK1 KO mice. Densitometric analysis of VCP (B), NF1 (C), VGLUT1 (D), PSD95 (E), and synaptophysin (SYN) (F) normalized to β -actin. Data are represented as mean \pm SEM of five mice from each cohort. Regression analyses of NF1 expression vs. VGLUT1 (G), PSD95 (H) and SYN (I) expression. NF1 expression did not correlate with expression of any of the synaptic markers at this time point with R^2 values of 0.1474, P-value=0.2734 (G), 0.1664, P-value=0.2419 (H), and 0.2778, P-value=0.1175 (I).

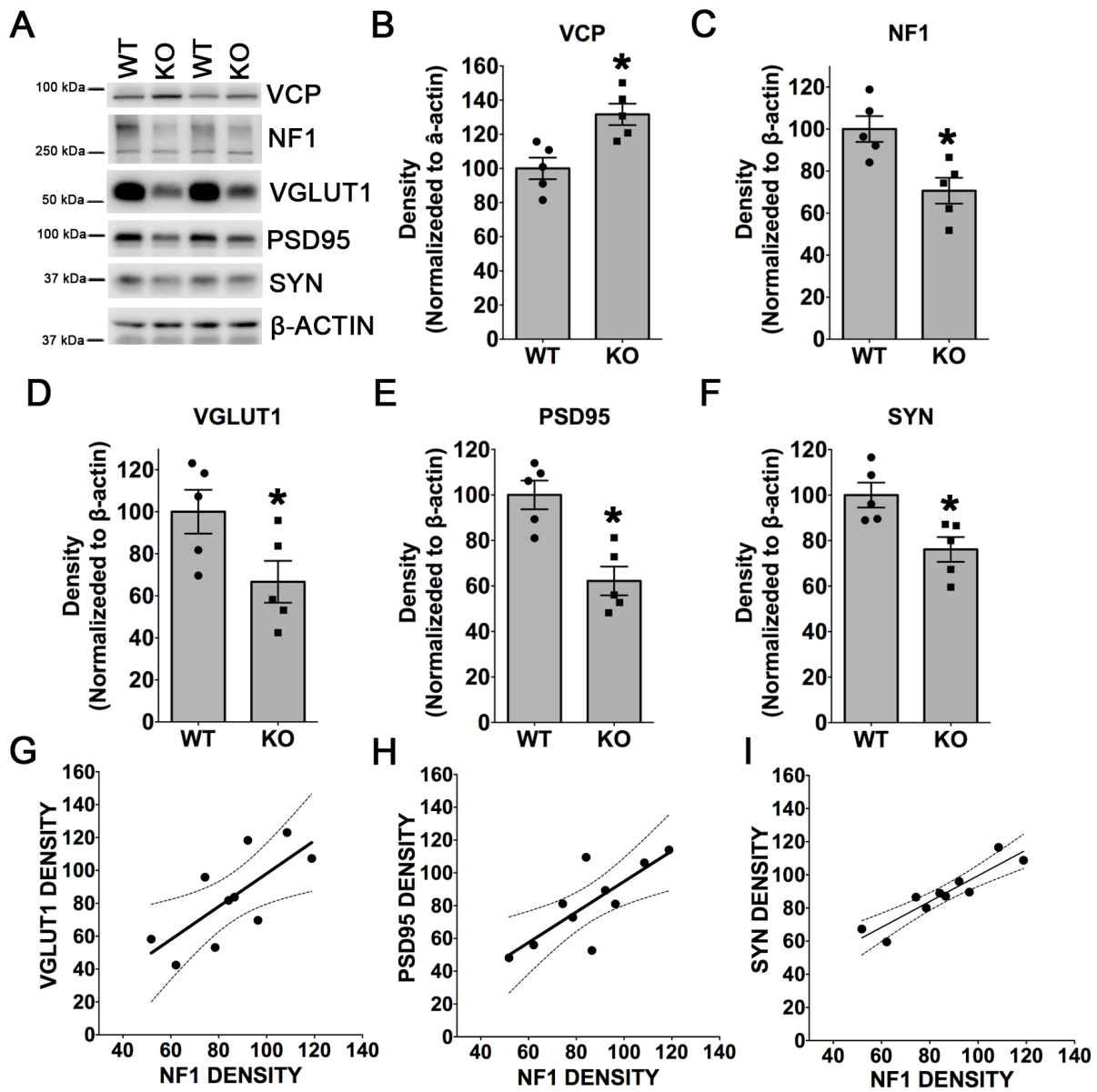


Figure 24: Expression of synaptic markers is decreased at 6 months in PINK1 KO mice. (A) Representative immunoblot of ventral midbrain lysates from 6-month-old WT and PINK1 KO mice. Densitometric analysis of VCP (B), NF1 (C), VGLUT1 (D), PSD95 (E), and synaptophysin (SYN) (F) normalized to β -actin. Data are represented as mean \pm SEM of five mice from each cohort (*P-value<0.05 vs. WT). Regression analyses of NF1 expression vs. VGLUT1 (G), PSD95 (H) and SYN (I) expression. NF1 expression was positively correlated with expression of all of the synaptic markers at this time point with R^2 values of 0.5305, P-value=0.0169 (G), 0.6138, P-value=0.0073 (H), and 0.8481, P-value=0.0002 (I).

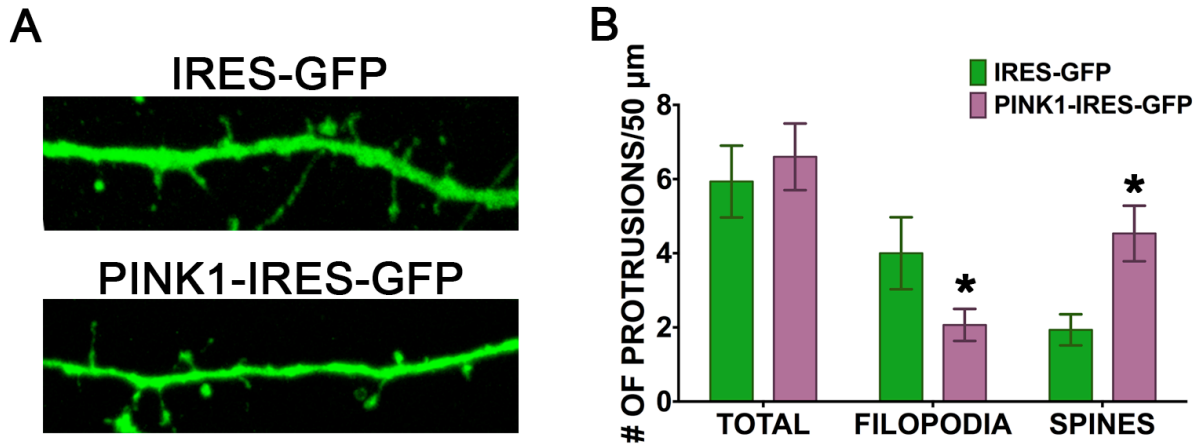


Figure 25: PINK1 promotes dendritic spinogenesis. (A) Representative images of dendritic spines in mouse cortical neurons expressing IRES-GFP or PINK1-IRES-GFP. (B) Quantification of filopodia and spine density in neurons from (A). Data are represented as mean±SEM (n=8-9 neurons/group collected from three independent experiments, *P-value<0.05).

4.6 PINK1 AND VCP CO-REGULATE AUTOPHAGY

4.6.1 PINK1 expression modulates sensitivity to autophagy induced by chemical inhibition of VCP

PINK1 knockdown promotes autophagosome accumulation [117, 118]. Similarly, VCP inactivation by chemical inhibition [206] or expression of ATPase deficient mutants [133, 207] results in the accrual of autophagosomes. Overexpression of PINK1 also protects against autophagic stress in cells treated with 6-OHDA [198]. In order to determine whether PINK1 modulates autophagy induced by VCP-inhibition, LC3 lipidation was monitored in PINK1 overexpressing cells treated with the VCP inhibitor DBeQ. LC3-II levels were significantly reduced in both non-neuronal HEK293 (Fig. 26A-B), and neuronal SH-SY5Y (Fig. 26C-D) cells

overexpressing PINK1. Additionally, transient knockdown of PINK1 sensitized SH-SY5Y cells to autophagosome accumulation following treatment with DBeQ (Fig. 26E-F).

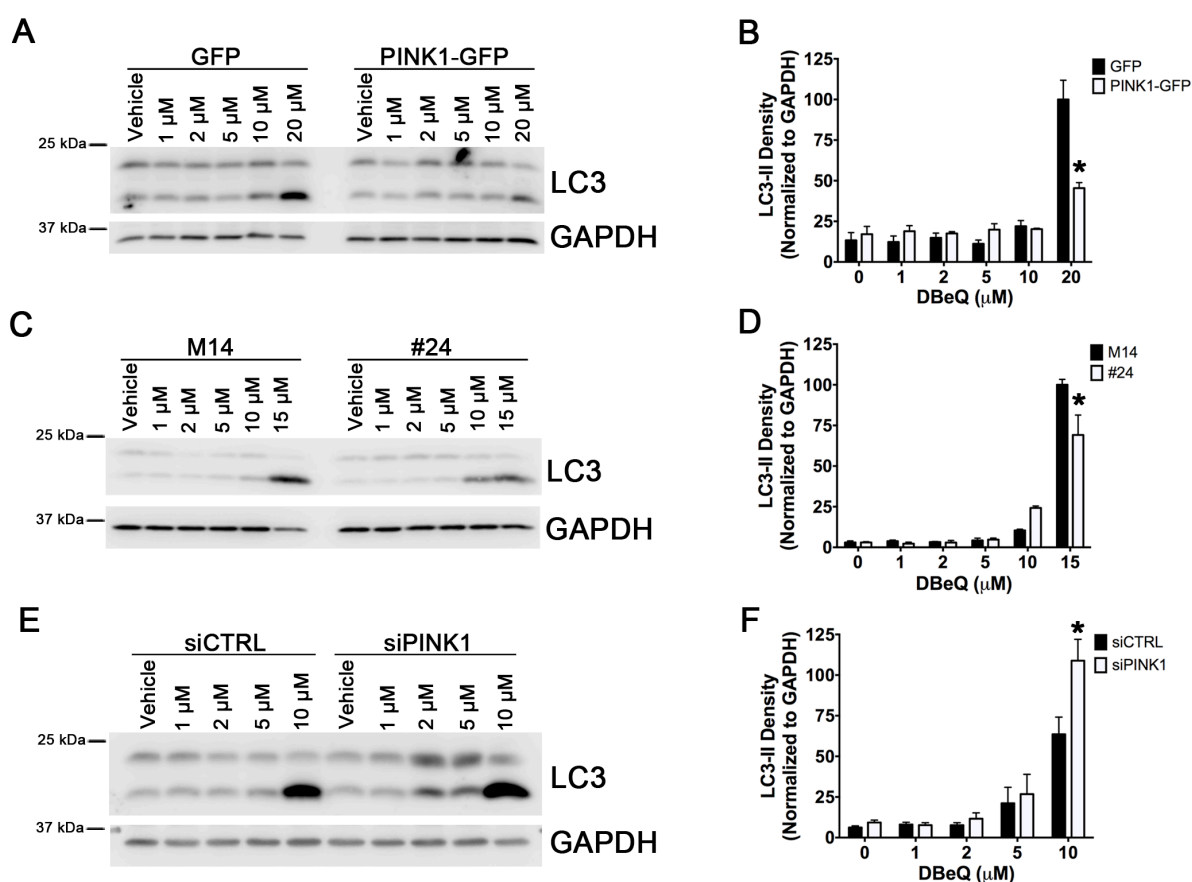


Figure 26: PINK1 modulates sensitivity to VCP inhibition. (A) Representative immunoblot of lysates from HEK293 cells transfected with GFP or PINK1-GFP and treated with indicated doses of the VCP inhibitor DBeQ for four hours. (B) Densitometric analysis of LC3-II normalized to GAPDH. Data are represented as mean \pm SEM compiled from four independent experiments (*P-value<0.0001 vs. GFP+20 μ M DBeQ). (C) Representative immunoblot of lysates from vector (M14) and PINK1-3xFLAG (#24) SH-SY5Y cell lines treated with indicated doses of DBeQ for four hours. (D) Densitometric analysis of LC3-II normalized to GAPDH. Data are represented as mean \pm SEM compiled from three independent experiments (*P-value<0.001 vs. M14+15 μ M DBeQ). (E) Representative immunoblot of lysates from SH-SY5Y cells transfected with scrambled or PINK1 siRNA and treated with indicated doses of DBeQ for four hours. (F) Densitometric analysis of LC3-II normalized to GAPDH. Data are represented as mean \pm SEM compiled from four independent experiments (*P-value<0.001 vs. siCTRL+10 μ M DBeQ).

4.6.2 VCP protects against autophagosome accumulation induced by PINK1 knockdown

To determine whether VCP overexpression was sufficient to prevent autophagosome accumulation in PINK1 deficient cells, LC3 puncta were quantified in SH-SY5Y cells. Transient knockdown of PINK1 caused accumulation of autophagosomes (Fig. 26A-B), consistent with an earlier observation in stable PINK1 knockdown cell lines [117]. Accumulation of LC3 puncta was reversed by co-transfection with VCP-GFP (Fig. 27A-B), suggesting that VCP is unlikely to act upstream of PINK1 autophagy regulation as well as neuronal morphogenesis.

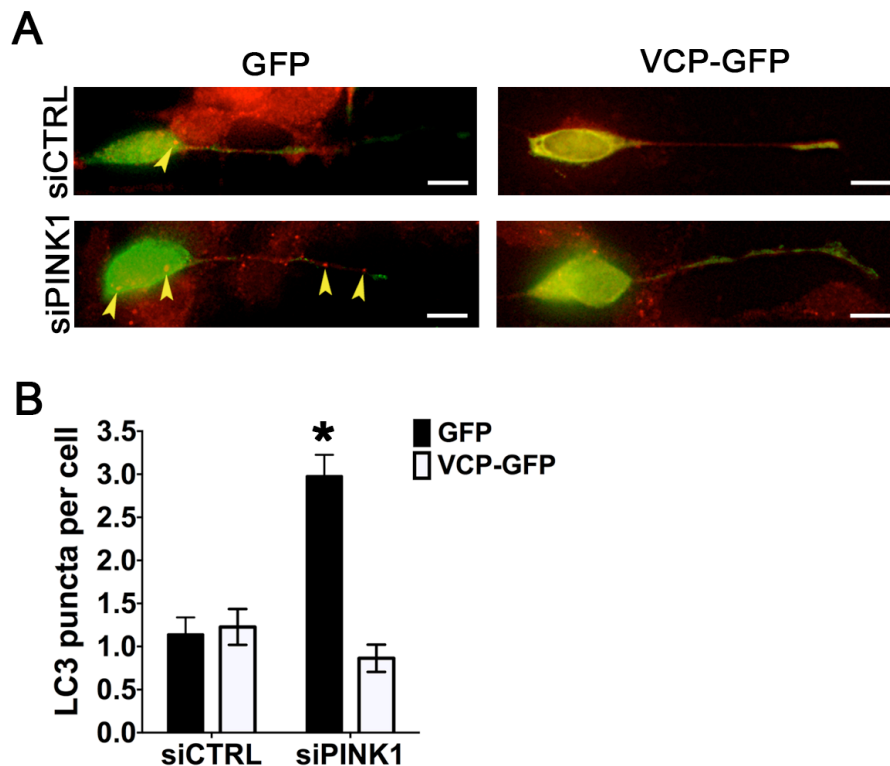


Figure 27: VCP overexpression protects against autophagy induced by PINK1 knockdown. (A) Representative images of SH-SY5Y cells co-transfected with scrambled or PINK1 siRNA and GFP or VCP-GFP and immunostained for endogenous LC3. Scale bar=10 μ m. (B) Quantification of autophagosomes in SH-SY5Y cells co-transfected with scrambled or PINK1 siRNA and GFP or VCP-GFP (Mean \pm SEM; 43-44 cells/group compiled from three independent experiments; *P-value<0.0001 vs. siCTRL+GFP).

4.6.3 Role of autophagy in PINK1-induced neurite extension

Autophagy induced neurite retraction has been observed in genetic and toxin models of PD [199, 208]. To examine whether autophagy suppression contributes to PINK1 induced neurite outgrowth, the essential autophagy protein ATG7 was transiently knocked down in PINK1 overexpressing cells. ATG7 knockdown did not further promote neurite extension in undifferentiated SH-SY5Y cells overexpressing PINK1 (Fig. 28A-B). Neurite length was sufficiently increased by ATG7 silencing in SH-SY5Y cells expressing GFP, to make the comparison with PINK1-GFP statistically insignificant. This finding suggests that suppression of autophagosome accumulation contributes, but is not the sole mechanism through which PINK1 promotes neurite outgrowth.

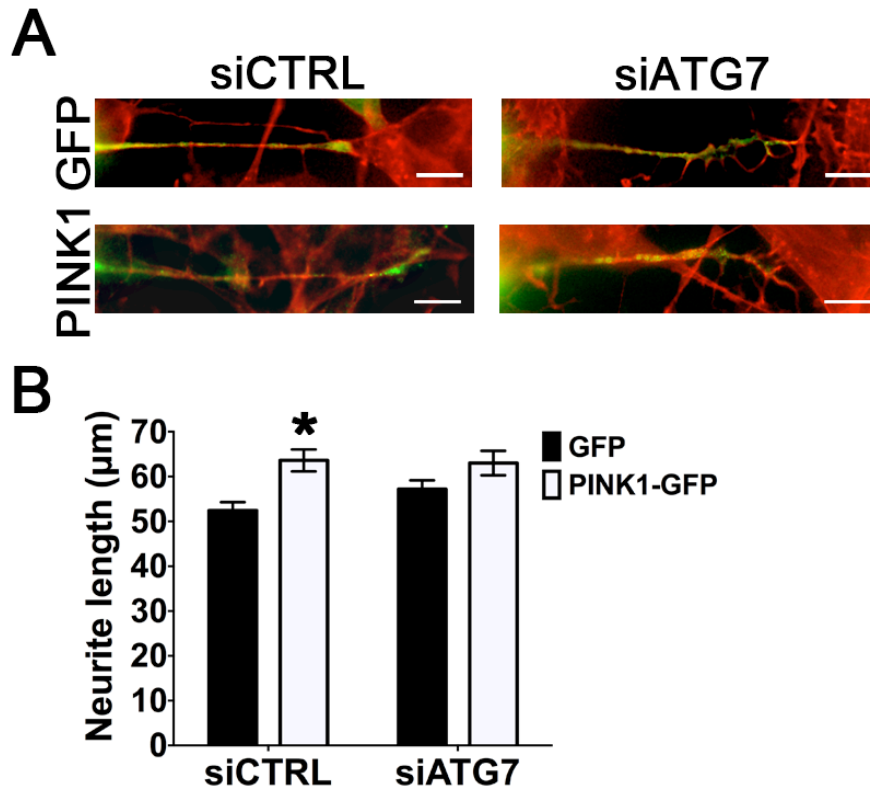


Figure 28: ATG7 knockdown abrogates neurite length differences between SH-SY5Ys expressing GFP and PINK1-GFP. (A) Representative images of SH-SY5Y cells co-transfected with scrambled or ATG7 siRNA and GFP or PINK1-GFP and stained with rhodamine-phalloidin. Scale bar=10 μ m. (B) Quantification of neurite length in SH-SY5Y cells co-transfected with scrambled or ATG7 siRNA and GFP or PINK1-GFP (Mean \pm SEM; 90-102 cells/group compiled from four independent experiments; *P-value<0.01 vs. siCTRL+GFP).

4.6.4 PKA phosphorylation of LC3 in PINK1 overexpressing cells

LC3 phosphorylation by PKA at Ser12 suppresses autophagy, and protects against neurite shortening in genetic and toxin models of PD [199]. Given that PKA signaling is implicated in PINK1-VCP induced neurite outgrowth (Fig. 12C), regulation of this phosphorylation site was examined in PINK1 overexpressing SH-SY5Y cells. PINK1-3xFLAG overexpression (#24 cell

line) caused an unexpected and dramatic reduction in density of the ~20 kDa phospho-LC3 (Ser12) band (Fig 29A-B). Intriguingly, a concomitant increase in density of a high molecular weight (>250 kDa) pLC3-immunoreactive band was also observed in these lysates (Fig. 29A, C). To verify that this high molecular weight band was PKA phosphorylated- LC3, vector (M14) and PINK1-3xFLAG (#24) cells were treated with a PKA inhibitor (H89). Surprisingly, the 20 kDa pLC3 band was largely unaffected by this treatment, but there was a striking reduction in density of the >250 kDa band (Fig. 30).

To examine the functional consequence of this phosphorylated species of LC3 in PINK1 overexpressing cells, LC3 puncta number and neurite length were quantified in SH-SY5Y cells expressing an unphosphorylatable LC3 mutant (S12A-LC3). Consistent with earlier work [199], expression of this mutant doubled the number of LC3-HA puncta per cell, and caused a slight, but non-significant reduction of neurite length in GFP expressing cells (Fig. 29D-E). PINK1 overexpression had no effect on S12A-LC3-HA puncta formation, suggesting that PINK1 acts either upstream of PKA or in a parallel pathway to regulate autophagy. This autophagy induction abolished the ability of PINK1 to promote neurite extension (Fig. 29F).

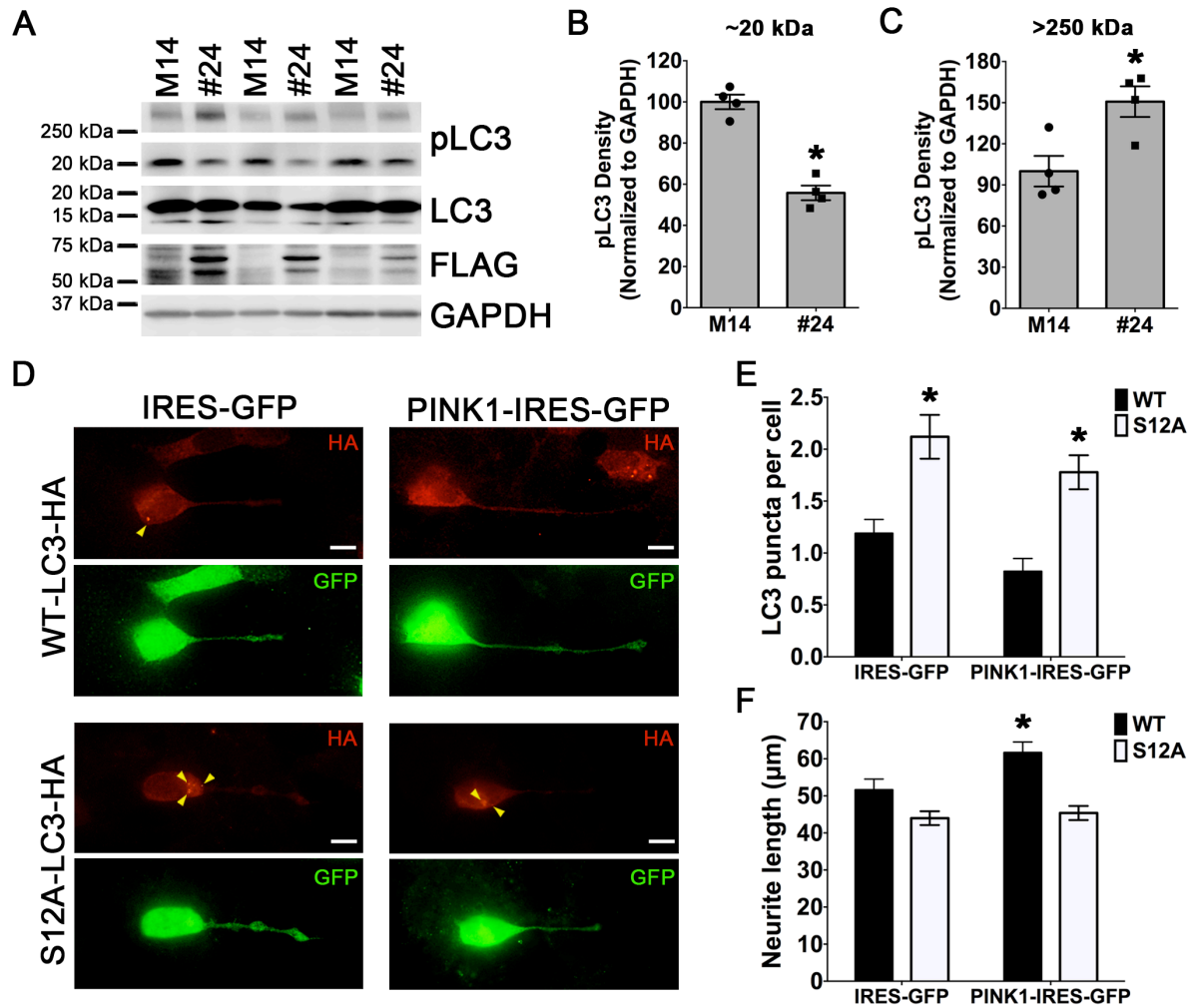


Figure 29: LC3 phosphorylation at Ser12 in PINK1 overexpressing cells. (A) Representative immunoblot of vector (M14) and PINK1-3xFLAG (#24) overexpressing stable SH-SY5Y cell lines lysates probed for pLC3 (Ser12) and total LC3. (B) Densitometric analyses of the ~25 kDa (B) and >250 kDa (C) bands recognized by the pLC3 antibody normalized to GAPDH. Data are represented as mean \pm SEM of four independent experiments. (D) Representative images of SH-SY5Y cells co-transfected with IRES-GFP or PINK1-IRES-GFP and WT- or S12A-LC3-HA. Scale bar=10 μm . Quantification of WT- or S12A-LC3-HA puncta (E) and neurite length (F) of SH-SY5Y cells from (D). Data are represented as mean \pm SEM (n=63-81 cells/group; *P-value<0.05 vs. IRES-GFP+WT=LC3-HA).

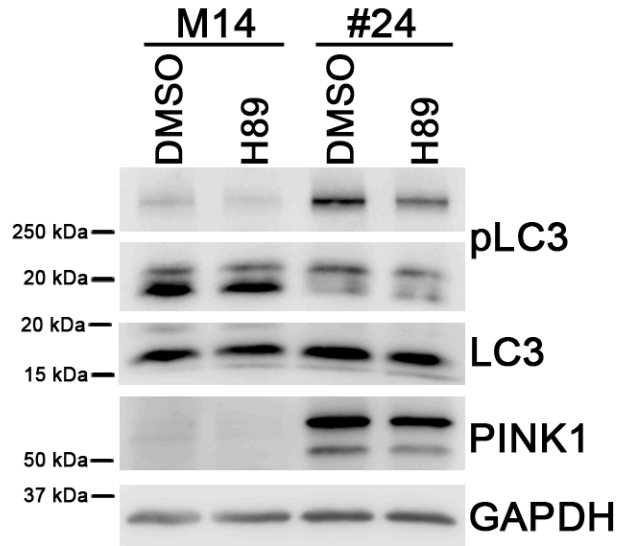


Figure 30: PKA inhibition prevents accumulation of high molecular weight phospho-LC3. Immunoblot of lysates from vector (M14) or PINK1-3xFLAG (#24) stable cell lines were treated with DMSO or 250 nM H89 for 14 hours. Immunoblot was probed for pLC3 and total LC3 and represents one experiment.

4.6.5 PINK1 overexpression promotes accumulation of high molecular weight ubiquitinated proteins

PINK1 is the first identified ubiquitin kinase [4, 100, 101]. Since phosphorylation of ubiquitin by mitochondrially localized PINK1 promotes mitophagy, and Δ N-PINK1 has increased kinase activity [60], the effect of overexpressing cytosolic PINK1 on ubiquitin was investigated. Whole cell lysates from HEK293 cells expressing cytosolic PINK1 and PINK1 targeted to the outer mitochondrial membrane were subjected to SDS-PAGE and immunoblotted for ubiquitin. Cytosolic, but not OMM-PINK1 caused a marked accumulation of very high molecular weight ubiquitinated products (Fig. 31A). This accumulation is also observed in HEK293 cells expressing the two PD-associated PINK1 mutants with impaired VCP binding (Fig. 31C). Levels of free ubiquitin are unaffected by overexpression of PINK (Fig. 31C), suggesting that this

accumulation arises from suppressed degradation of ubiquitination products or promotion of ubiquitin conjugation. Overexpression of PINK1 alone did not cause accumulation of these ubiquitination products in a neuronal cell line (Fig. 31B), but buildup of these products is more pronounced in PINK1 overexpressing cells following treatment with the VCP inhibitor DBeQ. Interestingly, this accrual caused by VCP inhibition was accompanied by cleavage of PARP-1. This result indicates the PINK1 overexpression modulates the mechanism by which VCP inhibition causes toxicity. Accumulation of high molecular weight ubiquitin conjugates was similar between vector and PINK1-3xFLAG overexpressing cells following proteasomal inhibition with MG132 (Fig. 31B). This finding indicates that impaired proteasomal degradation is unlikely to be responsible for the buildup of these ubiquitinated proteins in PINK1 overexpressing cells.

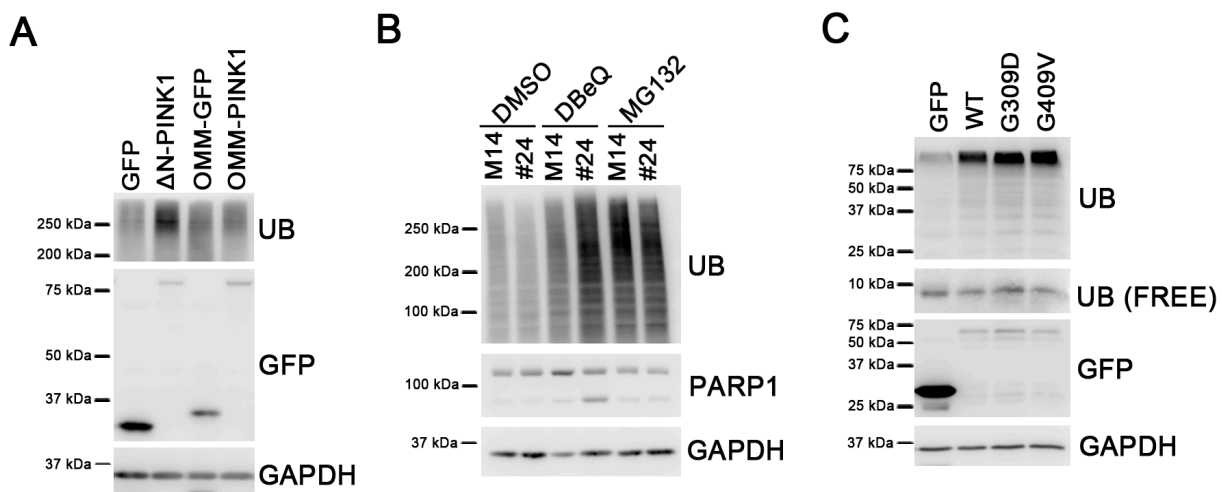


Figure 31: PINK1 overexpression promotes accumulation of poly-ubiquitinated proteins (A) Immunoblot of lysates collected from HEK293 cells transfected with GFP, Δ N-PINK1-GFP, OMM-GFP, or OMM-PINK1-GFP and probed for ubiquitin. Immunoblot represents three independent experiments. (B) Immunoblot of lysates collected from vector (M14) or PINK1-3xFLAG overexpressing (#24) SH-SY5Y cell lines treated with DMSO, 15 μ M DBE-Q, or 10 μ M MG132 for four hours. Immunoblot was probed for ubiquitin and PARP-1. Immunoblot represents four independent experiments. (C) Immunoblot of lysates collected from HEK293 cells transfected with GFP, WT-, G309D-, or G409V-PINK1-GFP and probed for ubiquitin. Immunoblot represents three independent experiments.

5.0 DISCUSSION

The potential biological roles of PINK1, as with any other kinase, vary depending on its subcellular localization and accessibility to downstream signaling partners. A better understanding of the processing and regulation of PINK1 in the presence of functional mitochondria provide important information for spectrum of PINK1-dependent functions that may be disrupted by recessive PD-linked mutations. While much has been learned about the catabolic function of PINK1 in response to mitochondrial depolarization, another emerging body of data suggests that the export of processed PINK1 from healthy mitochondria may function as a signal of energetic competence to promote neuronal trophic responses. Very little is known about the signaling network through which the cytosolic pool of PINK1 relays this message.

As an initial step to redress this discrepancy, this project aimed to identify PINK1 interactors that contribute to its function(s) in cells with healthy mitochondria. In the course of this study, two cytosolic proteins (VCP, CRMP2) were found to co-IP with PINK1. Interestingly, both of these proteins regulate neuronal morphology in cooperation with their shared interaction partner NF1. This work discovered that expression of VCP and NF1 is required for PINK1 to promote dendritic complexity. These studies also found that PINK1 promotes the phosphorylation of CRMP2 at a site known to regulate dendritic field organization [196] and dendritic spine density [195]. Further, data shown here suggests that PINK1 and VCP cooperate

to regulate autophagy. These functional overlaps will be discussed in the context of known VCP, NF1, CRMP2, and PINK1 regulators below.

5.1 PINK1-VCP-NF1-CRMP2 AS A SIGNALING HUB THAT REGULATES NEURONAL MORPHOLOGY

Reduced number of dendritic spines has been observed in the striatum [31-34] and substantia nigra [36] of post-mortem PD brains. This loss of dendritic spines is accompanied by simplification of the dendritic arbor [32-35]. The data presented here suggest that PINK1, VCP, NF1, and CRMP2 act as a signaling hub that promotes dendritic complexity and dendritic spine maintenance (Fig. 32).

NF1 interacts with CRMP2 and prevent its hyper-phosphorylation in neuronal cells [172]. Phosphorylation of CRMP2 at Thr509 and Thr514 by GSK3- β , preceded by a priming phosphorylation at Ser522 by Cdk5, promotes growth cone collapse and axonal retraction [174, 175, 182]. These axonal effects are primarily mediated through disruption of the microtubule stabilizing association of CRMP2 with tubulin. Interestingly, the interaction of NF1 with CRMP2 requires phosphorylation by Cdk5 [173]. These experiments demonstrate that while PINK1 promotes phosphorylation of CRMP2 at Ser522 (Fig. 19), it does not affect the ability of CRMP2 to pull down β -tubulin III (Fig. 21). Further, PINK1 induced neurite outgrowth and dendritic arborization requires expression of NF1 (Fig16B-E). One possible explanation for these findings is that PINK1 and NF1 collaborate to tightly regulate phosphorylation of CRMP2. In this scenario, PINK1 may foster phosphorylation at Ser522 and facilitate NF1-CRMP2 binding

to prevent its subsequent phosphorylation by GSK3- β . VCP, as a shared binding partner of PINK1 and NF1, may participate in this process by bringing PINK1 and NF1 into close proximity. CRMP2-NF1 binding and the effect of NF1 and VCP deficiency on CRMP2 phosphorylation in PINK1 overexpressing cells will need to be assayed to test this hypothesis. Future experiments employing in vivo cross-linking followed by IP, or Blue native PAGE could be used to investigate whether PINK1, VCP, NF1, and CRMP2 form a complex.

Previous work has established a link between PINK1 signaling and kinases and phosphatases known to regulate CRMP2 phosphorylation. Tau is a microtubule-associated protein that promotes microtubule assembly and stability. Like CRMP2, phosphorylation of tau by Cdk5 and GSK3- β decreases its affinity for microtubules. Overexpression of PD-associated G309D-PINK1 mutant, but not WT-PINK1, promotes tau hyperphosphorylation [209]. Failure to deactivate GSK3- β is primarily responsible for the accrual of highly phosphorylated tau in this context. PINK1 deficiency also inhibits serine/threonine phosphatase protein phosphatase 2A (PP2A) activity [118], another regulator of both tau [210, 211] and CRMP2 phosphorylation [175, 212-214]. Relative to other phosphorylation sites on CRMP2, Ser522 is impervious to PP2A-mediated dephosphorylation [212]. Further, VCP interacts with PP2A and promotes its phosphatase activity under certain conditions [215]. These studies suggest that PINK1-VCP may inhibit CRMP2 phosphorylation at Thr509 and Thr514 by modulating the activity of GSK3- β and PP2A.

PKA signaling amplifies neurite outgrowth induced by PINK1 [110]. This suggests that PINK1 and PKA signaling pathways may converge to co-regulate neurite extension, though the mechanism by which PINK1 fosters PKA activation has not yet been described. This study determined that VCP overexpression does not prevent neurite shortening induced by PINK1

deficiency in the presence of a PKA inhibitor (Fig. 13C). Interestingly, reduced production of cAMP correlates with neurite shortening in CNS neurons of haploinsufficient NF1 mice [169]. Further, restoration of PKA activity prevents neurite shortening in neurons isolated from these mice. Therefore, it is conceivable that PINK1-VCP promotes PKA activation through stimulation of NF1-dependent cAMP production.

5.2 REGULATION OF SYNAPSES BY PINK1

Altered morphology and reduced number of dendritic spines from the substantia nigra [36] and striatum [216] in PD patients was reported over two decades ago. Synaptic pathologies have since been reported in multiple animal models of PD [217-219], though the mechanism underlying these defects remains poorly understood. This work has demonstrated that loss of PINK1 expression causes an age-dependent reduction in synaptic marker expression in the ventral midbrain of PINK1 KO mice (Fig. 22-23). Additionally, overexpression of PINK1 promotes maturation of dendritic spines (Fig. 24). These observations suggest that PINK1 regulates synapse maturation and/or preservation. This is consistent with the previously reported finding that loss of PINK1 expression results defects in long-term potentiation (LTP) [113].

As described in the introduction, loss of dendritic spines from striatal neurons is a well-established pathological feature of PD [31, 35, 216]. This striatal dendritic spine loss positively correlates with the reduction in number of dopaminergic projections from the SNc [35], but findings in animal models of PD suggest that glutamatergic inputs from the cortex also contribute to this pathology [220, 221]. In this project, we did not observe a significant decrease

in synaptic marker expression in the striatum of PINK1 KO mice at 3, 6, or 12 months (Data not shown). One potential explanation for this finding is that dopamine depletion from the striatum is not severe enough at these ages to destabilize dendritic spines. In fact, basal levels of striatal dopamine are unaltered in young PINK1 KO mice [112, 113], lending support to this hypothesis. Additionally, it is possible that alterations in both nigral and cortical input are necessary to induce loss of dendritic spines in the striatum, and the PINK1 KO mice used in these studies do not recapitulate this dysfunction at the ages evaluated in this study (or ever).

During the course of this work, two proteins known to regulate dendritic spine density were identified as PINK1 interactors (Table 3, Fig. 9-10, 18). VCP physically associates with NF1 to promote spinogenesis [152]. Interestingly, the expression of synaptic markers was highly correlated with expression of NF1 in the ventral midbrain of six-month-old mice (Fig. 23G-I). NF1 regulates dendritic filopodia formation through a PKA-dependent mechanism [170]. Further, PKA potentiates calcium influx through NMDAR, a crucial regulator of LTP potentiation [222]. CRMP2, the other PINK1 interacting protein identified in this study (Fig. 18), interacts with a subunit of the NMDAR (NR2B) [223]. Dissociation of the interaction between CRMP2 and NR2B reduces NR2B surface expression and NMDAR current. NR2B function is essential for normal synaptogenesis and spine maturation [224]. Therefore, if loss of PINK1 disrupts the interaction between CRMP2 and NR2B, deficient NMDAR activation may impair synaptic maintenance in PINK1 KO mice. CRMP2 also associates with a N-type voltage gated calcium channel CaV2.2 [191]. Phosphorylation of CRMP2 at Ser522 enhances this interaction [194], resulting in increased calcium entry through the channel [194, 225]. This study found that PINK1 regulates phosphorylation of CRMP2 at Ser522 (Fig. 19-20). Calcium entry through CaV2.2 at the axon terminal promotes neurotransmitter release [193]. It is conceivable that

diminished calcium entry through this channel, due to impaired binding with CRMP2, may underlie the evoked catecholamine release deficit in PINK1 KO and +/- mice [113, 114]. Further, somatodendritic localization of these channels coincides with maturation of dendritic spines [226]. Study of the role of CRMP2 binding partners in the PINK1 pathway described here is an exciting new direction for this project that will be further discussed in section 6.1.

Although the mitochondrial functions of PINK1 were not investigated here, another possible interpretation of this data is that mitochondrial dyshomeostasis underlies the synaptic pathology in PINK1 KO mice. Synaptic transmission is the largest consumer of ATP in the brain [227], and neurons are heavily reliant on mitochondrial respiration to produce energy. Loss of PINK1 impairs mitochondrial respiration in the cortex of aged mice [228]. The resulting depletion in ATP may limit the ability of PINK1 KO neurons to support the high energetic demands of the synapse. In addition to energy production, mitochondria also are crucial regulators of neuronal calcium buffering. Transient elevations in synaptic calcium are required for maturation and maintenance of synapses, but prolonged increases in cytosolic calcium levels can lead to excitotoxic injury. Excitotoxic stimuli induces excessive mitochondrial calcium influx, leading to dissipation of mitochondrial membrane potential, perturbed mitochondrial respiration, and increased reactive oxygen species production (reviewed in [229]). PINK1, in cooperation with PKA, regulates extrusion of calcium from the mitochondria via the $\text{Na}^+/\text{Ca}^{2+}$ exchanger to protect against mitochondria calcium overload [87]. As synapse loss is an early event in excitotoxic injury, deregulation of the primary mechanism of mitochondrial calcium efflux may be partially responsible for reduced synaptic marker expression in PINK1 KO mice.

PINK1 deficiency induces accumulation of LC3-positive puncta in neuronal cells (Fig. 26, [117, 118]). Recently, dendritic spine pruning defects were linked to deficient neuronal

autophagy in a mouse model of autism [230]. Similar impairments in synapse elimination were observed in mice lacking expression of the essential autophagy protein Atg7. Therefore, it is conceivable that the reverse is true in PINK1 KO mice, and overactivation of autophagy leads to unnecessary elimination of functional synapses. Further, chemical induction of autophagy depresses evoked dopamine release [231], a phenotype also observed in the striatum of PINK1 KO and +/- mice [113, 114]. Thus, chronic autophagic stress may contribute to the loss of synapses in PINK KO mice.

These three proposed mechanisms are by no means exclusive. It is entirely conceivable that PINK1 finely tunes transient elevations in synaptic calcium by promoting calcium entry through CaV2.2 or NMDAR and calcium extrusion from the mitochondria [87]. Loss of PINK1 would perturb this tightly regulated process leading to depolarization of mitochondria, and eventually, impaired mitochondrial function. Diminished intracellular levels of ATP may then activate AMP-activated protein kinase (AMPK), which is known to promote autophagy induction [232].

5.3 PINK1 AND VCP COOPERATE TO REGULATE AUTOPHAGY

Phosphorylation of LC3 at Ser12 by PKA inhibits its incorporation into autophagosomes [199]. PINK1 overexpressing neuronal cell lines are resistant to accumulation of LC3 puncta induced by treatment with the PD-associated toxin 6-hydroxydopamine [117]. Additionally, PINK1 deficiency promotes LC3 lipidation in dopaminergic neuronal cell lines [117, 118] and the striatum of mice injected with PINK1 shRNA lentivirus [118]. PKA inhibition reverses the

rescue of neurite length in PINK1 deficient cells by overexpression of VCP (Fig. 13C). Given that VCP overexpression also prevents accumulation of autophagosomes induced by PINK1 knockdown (Fig. 26), the contribution of PKA phosphorylated LC3 to the regulation of autophagy by PINK1 was explored. Contrary to expectations, PINK1 overexpression caused a dramatic reduction in density of the ~20 kDa phospho-LC3 (Ser12) band (Fig 29). This decrease was accompanied by increased density of a pLC3 immunoreactive band above 250 kDa. Further, intensity of the phospho-LC3 immunoreactive band above 250 kDa is reduced by treatment with a PKA inhibitor, whereas the ~20 kDa band remains unaffected. This finding may suggest that PINK1 promotes the association of PKA phosphorylated LC3 with an unidentified binding partner. Diffusion dynamics suggest that LC3 does not exist as a freely diffusing monomer in the soluble fraction, and is more likely to be incorporated into macromolecular complexes [233, 234]. It is possible that phosphorylation of LC3 at Ser12 augments its incorporation into one of these complexes, thereby limiting its availability for autophagy induction.

Perhaps the most surprising finding of this project was that overexpression of PINK1 promotes accumulation of high-molecular weight ubiquitination products (Fig. 30A-C). One straightforward explanation for this phenomenon is that PINK1 may modulate free ubiquitin levels. Increased levels of monomeric ubiquitin may facilitate accumulation of high molecular weight ubiquitination products by overcoming the obstacle of substrate availability. At least in HEK293 cells, free ubiquitin levels were unaltered by overexpression of WT- or PD-associated PINK1 mutants (Fig. 30C). Thus, other mechanisms that promote the accumulation of ubiquitin conjugates are more likely.

Another reasonable hypothesis is that PINK1 suppresses proteasomal degradation of poly-ubiquitinated proteins. The majority of cytosolic proteins are targeted for degradation by

the ubiquitin proteasome system (UPS) [235]. Disruption of this degradation pathway results in the accumulation of ubiquitin conjugates. Impaired UPS function has been linked to PD, Alzheimer's disease, Huntington's disease, and amyotrophic lateral sclerosis (reviewed in [236]). However, multiple pieces of evidence indicate that PINK1 is unlikely to inhibit global function of the proteasome. First, inhibition of the proteasome with MG132 does not differentially affect accumulation of ubiquitin conjugates in control and PINK1 overexpressing cells (Fig. 30B). If PINK1 already inhibited proteasomal activity, a more robust buildup of ubiquitin conjugates would be anticipated following treatment with MG132. One possibility is that PINK1 alone is sufficient to completely inhibit proteasome activity, so treatment with MG132 has no additive effect. This is unlikely, as overexpression of PINK1 in neuronal cells does not cause an accumulation of ubiquitin conjugates in untreated cells. It is possible that the MG132 treatment paradigm used here completely inhibits the proteasome, masking any effect of PINK1 overexpression. To substantiate or refute this hypothesis, a MG132 dose curve could be employed to test sensitivity of PINK1 overexpressing cells to ubiquitin accumulation induced by proteasomal inhibition. It is widely accepted that proteasome inhibition promotes activation of autophagy (reviewed in [237]). The general consensus is that autophagy likely acts as a backup mechanism in this context in order to maintain proteostasis while proteasomal degradation is overburdened. Incongruously, overexpression of PINK1 reduces LC3 lipidation following treatment with a VCP inhibitor (Fig. 25A-D). It seems more probable that PINK1 only interferes with the proteasomal degradation of a subset of VCP client proteins. PINK1 pulls down the ND1 domain of VCP with the greatest efficiency, a construct containing the N-domain of VCP, which is the primary site of cofactor binding [126]. Thus, it is possible that PINK1 modulates the association of VCP with some of these cofactors, but further investigation will be required to

determine whether PINK1 overexpression substantially alters the VCP interactome and whether any observed changes may contribute to ubiquitin accumulation.

Alternatively, PINK1 may facilitate cargo loading of autophagosomes. PINK1 phosphorylates ubiquitin (Ser65) at the mitochondrial surface to promote autophagic clearance of mitochondria [4, 100, 101]. Additionally, phosphorylated ubiquitin (Ser65) has been reported to localize to the periphery of Lewy bodies in the brains of PD patients [121]. One potential interpretation of these findings is that ubiquitin phosphorylated by PINK1 acts as a signal for expedited clearance of cargo by selective autophagy. Deficient cargo loading was recently identified in multiple models of Huntington's disease [238]. While formation and clearance of autophagic vacuoles is largely intact, the polyubiquitinated content of autophagosomes was dramatically reduced in cells bearing a polyglutamine expansion in the mouse homolog of the huntingtin gene. It is conceivable that inefficient degradation of substrates through this mechanism may lead to accumulation of autophagosomes, either by delayed loading or compensatory upregulation of autophagy induction.

This proposed role for PINK1 in cargo loading of autophagosomes seems to better fit the data generated during the course of this project. Here we reported that PINK1 overexpression prevented the accumulation of lipidated LC3 induced by VCP inhibition (Fig. 25A-B). VCP inhibition impairs maturation of autophagosomes containing ubiquitinated substrates [133]. If PINK1 fosters sequestration of misfolded proteins and damaged organelles, the positive feedback loop stimulated by inefficient autophagic clearance could be disrupted despite partial blockage of autophagosome maturation. It follows that PINK1 knockdown cells would be more sensitive to autophagosome accumulation induced by VCP inhibition (Fig. 25C) if multiple steps of the process are impaired. Further, overexpression of VCP may compensate for uneconomical

loading of a cargo induced by PINK1 deficiency by expediting autophagosome maturation. Introduction of PINK1 into HEK293 cells, given their high level of exogenous protein expression, may exceed the capacity of the cell for autophagic degradation of targeted cargo. This speculation is consistent with data demonstrating less robust overexpression of PINK1 does not cause accrual of polyubiquitinated products in SH-SY5Y cells (Fig. 30B). In this experimental paradigm, the additional stress of VCP inhibition was required to promote accumulation of high molecular weight ubiquitin conjugates. It is also possible that this discrepancy is a cell-type (neuronal vs. non-neuronal) specific effect rather than a result of increased expression.

The mechanism by which the phosphorylation of ubiquitin by PINK1 promotes recruitment of parkin has not yet been described in the literature. One potential explanation is that phosphorylation at Ser65 stabilizes ubiquitin chains, increasing the likelihood that they will bind to parkin. The ability of multiple deubiquitinating enzymes, including ataxin-3, to hydrolyze polyubiquitin chains phosphorylated at Ser65 is impaired *in vitro* [239]. Glutamine expansions in the gene encoding for ataxin-3 are the genetic cause of Machado–Joseph disease, a spinal-cerebellar ataxia. Like many other neurodegenerative diseases, large proteinaceous inclusions are observed in the brains of Machado-Joseph disease patients [240, 241]. There is an expanding body of evidence that ataxin-3 is both a component of these aggregates, and involved in autophagic clearance of aggregated proteins. Ataxin-3 facilitates delivery of ubiquitinated proteins to aggresomes targeted for autophagic degradation by trimming K63-linked ubiquitin chains [242]. Subsequently, ataxin-3 edited chains promote the association of aggregated proteins with histone deacetylase 6 [243], enabling delivery to aggresomes through dynein mediated trafficking [244]. Interestingly, ataxin-3 is a VCP binding partner, and this association

augments the hydrolytic activity of ataxin-3 [245]. Therefore, inhibition of VCP may enhance the accumulation of high-molecular weight conjugates by disabling ataxin-3 processing of PINK1 phosphorylated ubiquitin chains.

Another perplexing finding reported here is that PINK1 overexpression promotes PARP1 cleavage following treatment with a VCP inhibitor (Fig. 30B). This was particularly surprising given that PINK1 protects against apoptosis induced by oxidative stress [76], proteasomal inhibition [55], mitochondrial depolarization [77], and ETC complex I inhibition [78]. Though an unanticipated result, it is clear that PINK1 overexpression modulates the mechanism through which DBE-Q causes toxicity. Inhibition of VCP results in the accumulation of nuclear Lys48-conjugated ubiquitination products that leads to persistence of double-stranded breaks in DNA [246]. PARP1 plays a pivotal role in detection and repair of damaged DNA, and its activity is modulated in apoptosis, necroptosis, parthanatos, and autophagic cell death (reviewed in [247]). While the PARP1 cleavage observed in PINK1 overexpressing cells is characteristic of apoptotic cell death, increased expression of full-length PARP1 in control cells is more consistent with autophagy activation and necroptosis induced by DNA damage [248, 249]. Cells that depend on aerobic glycolysis for ATP production are more susceptible to necroptosis induced by DNA damage, whereas cells that are able to produce energy through oxidative phosphorylation are relatively resistant to this mode of cell death [250]. PINK1 promotes electron transport chain complex I [82-85, 251], and II [82, 84, 85] linked respiration. Though further study will be required, it is possible that this alteration in response to VCP inhibition may be due to the increased capacity of cells overexpressing PINK1 for mitochondrial respiration, rather than modulation of the primary insult.

5.4 LIMITATIONS TO DATA INTERPRETATION

Several pieces of preliminary data were included in this dissertation that provided rationale for subsequent experiments. In some studies, experiments were also performed with PINK1 constructs with different tags to ensure that results were tag-independent (Fig. 12B), or to validate findings by others that had worked on the project (Fig. 9A-B). Certainly, these experiments and the other preliminary studies included here need to be repeated to meet the rigors of peer-review for publication and would provide meaningful support for hypotheses generated during the course of this project.

Tagged LC3, particularly LC3-GFP, has been shown to aggregate in an autophagy-independent manner [252]. Additionally, lipidated LC3 can be observed in a number of genetically modified cell lines, even though autophagy is almost completely inhibited [253]. For these reasons, though LC3 lipidation and puncta formation are the gold standard for monitoring autophagy regulation, measures that provide additional information about observed impairments and confirmation of LC3 findings should be analyzed. In initial experiments analyzing the effects of VCP inhibition on autophagy in PINK1 overexpressing or knockdown cells, expression level of another autophagic marker (p62) was also probed. The p62 data was not included here because the results were highly variable between experiments, making the findings impossible to interpret. Biochemical experiments employing pharmacologic and/or genetic manipulators of autophagy induction and autophagic flux and electron microscopy studies would improve confidence when drawing conclusions about the data reported here.

6.0 FUTURE DIRECTIONS

6.1 PINK1 AND SYNAPTIC CALCIUM

Phosphorylation of CRMP2 at Ser522 promotes its association with N-type voltage gated calcium channels (CaV2.2) [194]. This association augments CaV2.2 current and neurotransmitter release into the synapse [191, 192, 194]. Deficient evoked catecholamine release and LTP failure that could be rescued by chemically induced dopamine release have been reported for heterozygous PINK1 KO mice [114]. Considered in connection with the findings reported here, CaV2.2 is a promising, potential downstream effector of PINK1 signaling.

Calcium influx in the axon terminal and dendritic spines of PINK1 knockout and overexpressing neurons could be monitored with a genetically encoded calcium indicator (GCaMP) [254], or a cell-permeable, ratiometric calcium binding dye (Fura2-AM). The CaV2.2 inhibitor, ω -conotoxin could be used to evaluate the contribution of N-type voltage gated calcium channels to calcium entry in these neurons. A peptide derived from the CaV2.2 binding domain of CRMP2 fused to an N-terminal myristate group (myr-tat-CBD3) disrupts the interaction between CRMP2 and CaV2.2 [191, 223, 225]. This reagent could be used to more directly assess the role of the CRMP2-CaV2.2 interaction in calcium influx in PINK1 overexpressing or knockdown neurons. The contribution of CaV2.2 mediated calcium entry to

regulation of dendritic spine density and dendrite arborization could also be evaluated in PINK1 overexpressing and knockout neurons exposed to ω -conotoxin or myr-tat-CBD3.

Synaptic maturation coincides with increasing somatodendritic localization of CaV2.2 [226]. Additionally, dissociation of the interaction between CRMP2 and CaV2.2 perturbs intracellular delivery of CaV2.2 to the synaptic membrane [225]. Thus, intracellular distribution of CaV2.2 and its co-localization with CRMP2 could be investigated in PINK1 knockout and overexpressing neurons. Further, the dynamics of somatodendritic CaV2.2 localization and synaptic maturation in PINK1 overexpressing neurons could be monitored to determine how closely they coincide.

CRMP2 also binds to the NR2B subunit of the NMDA receptor, another regulator of calcium entry in dendritic spines [255]. Through regulation of synaptic calcium entry, NR2B plays a key role in LTP [256, 257] and spine maturation [224]. Additionally, calcium influx through the NMDAR is potentiated by PKA signaling [222]. Thus, the contribution of NMDAR activation to dendritic calcium influx, spinogenesis, and arborization could be evaluated in PINK1 overexpressing and knockdown neurons treated with the NMDAR inhibitor memantine and/or the PKA inhibitor H89. Disruption of the CRMP2-NR2B interaction reduces NMDAR surface expression [223]. Therefore, distribution of NMDAR and its co-localization with CRMP2 could also be evaluated in PINK1 overexpressing and knockout neurons.

As mentioned above, disruption of the association between CRMP2 and NR2B or CaV2.2 reduces their surface expression. Though most recognized for its role in extracting proteins from organellar membranes, VCP also targets target mono-ubiquitinated caveolin-1 to multiple vesicular bodies for degradation through endosomal sorting [134, 258]. NR2B [259] and CaV2.2 [260] are also endocytosed and targeted for lysosomal or proteasomal degradation

respectively. Given that CRMP2 regulates endosomal transport [184], it is possible that PINK1-VCP and CRMP2 cooperate to regulate NR2B and CaV2.2 degradation. To test this hypothesis, NR2B and CaV2.2 expression could be assessed in PINK1 overexpressing neuronal cells following transient knockdown or pharmacological inhibition of VCP. Cumulatively, these studies could determine whether synaptic calcium influx, through previously identified CRMP2 interacting proteins, contributes to PINK1-VCP regulation of neuronal morphology and spinogenesis.

6.2 REGULATION OF CRMP2 PHOSPHORYLATION BY PINK1

CRMP2 activity is tightly regulated by post-translation modifications [178]. Based on the findings of this project, PINK1 will be added to the growing list of proteins that regulate CRMP2 phosphorylation. Evidence shown here, when considered in context with the known dendritic functions of phospho-CRMP2 (Ser522), suggests that the effects of PINK1 on spine maturation and neuronal morphology are mediated through CRMP2. To directly test this hypothesis, WT- and a non-phosphorylatable CRMP2 (S522A) construct could be co-expressed with PINK1 in neurons. Spine number and morphology, along with dendritic arborization could be analyzed in these neurons.

CRMP2 was first identified as the mediator of axonal retraction and growth cone collapse induced by secretion of the neuronal guidance molecule semaphorin 3A. Conversely, semaphorin 3A signaling increases dendritic spine density and promotes activity-dependent dendritic arborization [261, 262]. Cdk5 phosphorylates CRMP2 at Ser522 following activation of

semaphorin 3A signaling. Phosphorylation of CRMP2 at Ser522 is a crucial regulator of dendritic field organization [196] and spine maintenance [195]. Cumulatively, these studies indicate that phosphorylation of CRMP2 at Ser522 likely has divergent effects in dendritic and axonal compartments. To begin to investigate this in the context of PINK1, localization of total- and phospho-CRMP2 (Ser522) could be evaluated in PINK1 overexpressing and knockout neurons.

It will also be important to determine whether PINK1 regulates the activity of kinases and phosphatases known to modulate the phosphorylation status of CRMP2. Interestingly, overexpression of G309D- but not WT-PINK1 promotes hyperphosphorylation of tau, another Cdk5 and GSK3- β target [209]. This accumulation of highly phosphorylated tau was largely attributed to over-activation of GSK3- β . To determine whether GSK3- β signaling also contributes to the phenotypes observed above, levels of GSK3- β phosphorylated at its inactivation site (Ser9) could be assayed in the ventral midbrain of WT and PINK1 KO mice, and neuronal cells overexpressing WT- and PD-associated PINK1 mutants. Additionally, these lysates could be probed for CRMP2 at known GSK3- β phosphorylation sites (Thr509 and Thr514). Protein phosphatase 2A (PP2A) also regulates CRMP2 phosphorylation [175, 212-214]. Intriguingly, the Cdk5 phosphorylation site (Ser522) of CRMP2 is relatively resistant to dephosphorylation by PP2A [212]. PINK1 knockdown inhibits PP2A activation [118] and PINK1-GFP pulled down the catalytic subunit of PP2A in our proteomic screen of PINK1 interacting proteins (Data not shown). To determine whether PINK1 contributes to regulation of PP2A activity, levels of phosphorylation at its inactivating site (Tyr307) could be assessed in the ventral midbrain of WT and PINK1 KO mice and neuronal cell lines expressing WT- or PD-associated PINK1 mutants. Additionally, commercially available kits could be used as a direct

measure of PP2A activity on lysates from neuronal cells expressing WT- or PD-associated PINK1. The effect of GSK3- β (6BIO) and PP2A (okadaic acid) inhibition on isoelectric focusing of CRMP2 in PINK1 overexpressing neuronal cells and knockout neurons could also be assessed.

Data shown here identify Ser522 as a PINK1 regulated phosphorylation site of CRMP, but it remains unknown whether PINK1 can directly phosphorylate this site. Further, the intensities of multiple spots are altered by loss or overexpression of PINK1, leaving open the possibility that PINK1 regulates more than one phosphorylation site. In vitro kinase assays coupled to mass spectrometric analysis could be employed to determine whether PINK1 can directly phosphorylate CRMP2 at Ser522 or other residues. Isoelectric focusing of CRMP2 and levels of CRMP2 phosphorylated at Ser522 could be analyzed in these lysates. Finally, phosphorylation of CRMP2 could be assessed in cells expressing These proposed studies would delineate the mechanism by which PINK1 modulates CRMP2 phosphorylation and regulates neuronal morphology.

6.3 PINK1 AND CRMP2 IN REGULATION OF MITOCHONDRIAL TRAFFICKING

Cytosolic PINK1 promotes anterograde trafficking of mitochondria in the dendrites [110] and inhibit retrograde transport of axonal mitochondrial [61]. Similarly, CRMP2 associates with kinesin to facilitate anterograde trafficking [182, 186] and dynein to inhibit retrograde transport [183]. It is possible that processed PINK1 modulates the phosphorylation status of Miro/Milton to regulate mitochondrial trafficking, as full-length PINK1 does following chemical

depolarization of mitochondria [108, 109]. However, given the interaction between PINK1 and CRMP2 reported here, it is reasonable to hypothesize that CRMP2 is a downstream mediator of PINK1 regulated mitochondrial trafficking.

To explore this possibility, dendritic mitochondrial content and distribution could be evaluated in primary neurons co-expressing Δ N-PINK1 and WT- or S522A-CRMP2. Particular attention should be paid to the distribution of mitochondria in dendritic spines, given the importance of the process to synapse maturation and maintenance [263]. Additionally, WAVE1, a protein whose axonal trafficking is regulated by CRMP2 [182], promotes activity-dependent trafficking of mitochondria into dendritic filopodia and spines [264]. Thus, live cell imaging could be employed to monitor the dynamics of mitochondrial entry into dendritic spines in PINK1 overexpressing and knockdown neurons treated with NMDAR agonists or inhibitors. Similar experiments could be conducted in neurons expressing WT- or S522A-CRMP2. More comprehensive measures of mitochondrial trafficking, such as the mobile fraction (fraction of total mitochondria that move during the course of the experiment), ratio of mitochondria moving anterograde versus retrograde, and mitochondrial velocity could also be assessed. These experiments would help to clarify whether the effects of cytosolic PINK1 on mitochondrial trafficking are mediated through CRMP2.

6.4 REGULATION OF UBIQUITINATED PROTEINS BY PINK1-VCP

Perhaps the most surprising finding of this project was that cytosolic PINK1 overexpression induces a dramatic accumulation of high molecular weight ubiquitination products in HEK293

cells. Interestingly, PINK1 overexpression alone did not cause this accrual in a neuronal cell line, but it was observed following treatment with a VCP inhibitor. Full-length PINK1 phosphorylates ubiquitin on the outer membrane of chemically depolarized mitochondria to activate parkin and promote mitophagy [4, 100, 101]. It remains unknown whether cytosolic PINK1 is also able to phosphorylate ubiquitin. To investigate this, levels of ubiquitin phosphorylated at Ser65 could be assessed in cells expressing Δ N-PINK1 and OMM-PINK1. Additionally, levels of phospho-ubiquitin (Ser65) could be evaluated in PINK1 overexpressing neuronal cells treated with a panel of cellular stressors, including a VCP inhibitor. Data from these experiments would provide insight into the types of stimuli that promote phosphorylation of ubiquitin by PINK1 in neuronal cells.

While the phosphorylation of ubiquitin by PINK1 at the mitochondrial surface promotes mitophagy [4, 100, 101], it is unclear whether Ser65 phosphorylation universally fosters autophagic degradation. To study this in the context of PINK1-VCP regulated autophagy, LC3 lipidation, puncta formation, and ubiquitination could be monitored in the PINK1 stable overexpression cell line co-transfected with WT- or a non-phosphorylatable ubiquitin mutant (S65A) following treatment with a VCP inhibitor. Additionally, WT- and S65A-ubiquitin could be immunoprecipitated from PINK1 overexpressing cells treated with a VCP inhibitor. The ability of these constructs to co-immunoprecipitate known autophagy receptors (p62, OPTN, NBR1, TOLLIP, Cue5) should also be analyzed.

Recently, it was reported that phosphorylation of ubiquitin at Ser65 impairs the hydrolytic activity of multiple deubiquitinating enzymes *in vitro*, including ataxin-3 [239]. VCP interacts with and promotes the activity of ataxin-3 [245]. Given that inhibition of VCP is required for accumulation of polyubiquitinated products in PINK1 overexpressing neuronal cells,

it is possible that inhibition of ataxin-3 activity contributes to this phenotype. To test this hypothesis, the PINK1 overexpressing neuronal cell line could be transfected with ataxin-3 siRNA and the levels of ubiquitin in the resulting lysates assessed. If ataxin-3 inactivation is a major contributor to this phenotype, the results from this experiment would be expected to closely parallel those found in Figure 30B.

Polyubiquitin chains have distinct functions depending on their linkage. For example, proteins destined for proteasomal degradation are often ubiquitinated with Lys48 linked chains, but Lys48 linkages promote the segregase activity of VCP [265]. Also potentially relevant to this project, Lys63 polyubiquitination promotes the selective clearance of inclusions through autophagic degradation [266]. Determining whether PINK1 preferentially promotes accumulation of ubiquitin chains with specific linkages may provide insight into biological consequence of this accrual. To investigate this possibility, linkage-specific polyubiquitin antibodies could be used to assess levels of the three most predominant linkages of polyubiquitin chains (Lys11, Lys48, and Lys63) in neuronal cells overexpressing PINK1. Levels of these polyubiquitin chains could also be assessed in cells overexpressing PINK1 following treatment with a VCP inhibitor, to determine whether VCP activity contributes to any observed differences. These proposed experiments build on the findings reported here to help elucidate the mechanism through which PINK1 and VCP cooperate to promote accumulation of polyubiquitination products.

6.5 CRMP2 PHOSPHORYLATION IN PD, IBMPFD, AND NEUROFIBROMATOSIS

In this project, we demonstrated that WT-PINK1 co-IPs CRMP2 and regulates its phosphorylation. Additionally, two PD-associated mutants were shown to pull down less endogenous VCP than WT-PINK1. Future studies should evaluate whether CRMP2 binding is reduced for any of these mutations. The possibility that PD-associated PINK1 mutants disrupt the interaction between NF1 and VCP or CRMP2 could also be investigated. Additionally, phosphorylation at Ser522 and isoelectric focusing of CRMP2 should be evaluated in neuronal cells expressing PD-associated PINK1 mutations.

Impaired dendritic spine maturation and/or maintenance have been reported in genetic [217, 267, 268] and toxin [218, 219, 269, 270] animal models of PD. It will be important to determine whether altered CRMP2 phosphorylation contributes to this pathology in response to a broad spectrum of parkinsonian injury, or if it is only observed in PINK1 models. To examine this, phosphorylation of CRMP2 could be evaluated in genetic (leucine-rich repeat kinase, parkin) and toxin (6-OHDA, MPTP) cell culture and/or animal models of PD. If altered CRMP2 phosphorylation is consistently observed, post-mortem samples from the individuals with idiopathic PD could also be examined.

Knockdown of VCP and NF1 impaired PINK1 induced neurite outgrowth and dendritic arborization. Therefore, it is reasonable to hypothesize that VCP or NF1 pathogenic mutants that disrupt associations between components of the PINK1-VCP-NF1-CRMP2 signaling hub may also perturb regulation of CRMP2 phosphorylation by PINK1. Initially, CRMP2 phosphorylation at Ser522 and isoelectric focusing of CRMP2 could be evaluated in neuronal cells expressing pathogenic VCP and NF1 mutants known to disrupt the NF1-VCP interaction. If differences are

observed, a panel of pathogenic NF1 and VCP mutants could be generated or obtained. The capacity of these mutants to disrupt interactions between PINK1 and VCP, VCP and NF1, NF1 and CRMP2, or CRMP2 and PINK1 could then be assessed. Phosphorylation of CRMP2 could then be monitored in cells expressing mutants that dissociate physical associations between members of the PINK1-VCP-NF1-CRMP2 signaling pathway. CRMP2 phosphorylation could also be assessed in the post-mortem brain of IBMPFD and neurofibromatosis patients, if samples are obtainable.

7.0 SUMMARY

The results presented here provide the first evidence that PINK1 physically associates with the cytosolic AAA+ ATPase VCP. PINK1 induced neurite outgrowth and dendritic arborization is impaired following disruption of this interaction by expression of the PINK1-binding domain of VCP, VCP knockdown, or expression of PD-associated PINK1 mutants. The ability of PINK1 to promote dendritic complexity is also contingent upon expression of NF1, a protein known to interact with VCP to promote spinogenesis [152]. Additionally, PINK1 was found to associate with another NF1 interacting protein, CRMP2, and regulate its phosphorylation at Ser522. Previous work has demonstrated that phosphorylation of CRMP2 at Ser522 is required for dendritic spine maintenance [195]. Consistent with this finding, reduced levels of phosphorylated CRMP2 and decreased expression of synaptic markers were observed in the ventral midbrain of PINK1 KO mice. Moreover, overexpression of PINK1 promotes maturation of dendritic spines in mouse cortical neurons. In summary, this project identified PINK1-VCP-NF1-CRMP2 as components of a signaling hub that regulates dendritic morphology and synaptic maturation and maintenance.

PINK1 and VCP were also shown to co-regulate autophagy. Expression of PINK1 modulates the sensitivity of neuronal and non-neuronal cells to autophagosome accumulation induced by VCP inhibition. Further, overexpression of VCP prevented accrual of LC3 puncta in

PINK1 deficient cells. Knockdown of an essential autophagy protein did not cause further extension of neurites, but it did abrogate the difference in neurite length between control and PINK1 overexpressing cells. Autophagy induced by expression of a LC3 mutant impaired the PINK1 induced neurite extension. These findings suggest that inhibition of autophagosome accumulation is not the sole mechanism of PINK1 induced neurite outgrowth, but is likely a contributing factor. Finally, inhibition of VCP promotes accumulation of high molecular weight ubiquitination products. The role of autophagy in this buildup is currently unknown.

This project has found that the PINK1-VCP interaction is important for dendritic arborization, synaptic maturation and maintenance, and autophagy regulation. Future studies will focus on elucidating the mechanisms by which PINK1 promotes accumulation of ubiquitination products and regulates CRMP2 phosphorylation and the downstream consequences of these processes.

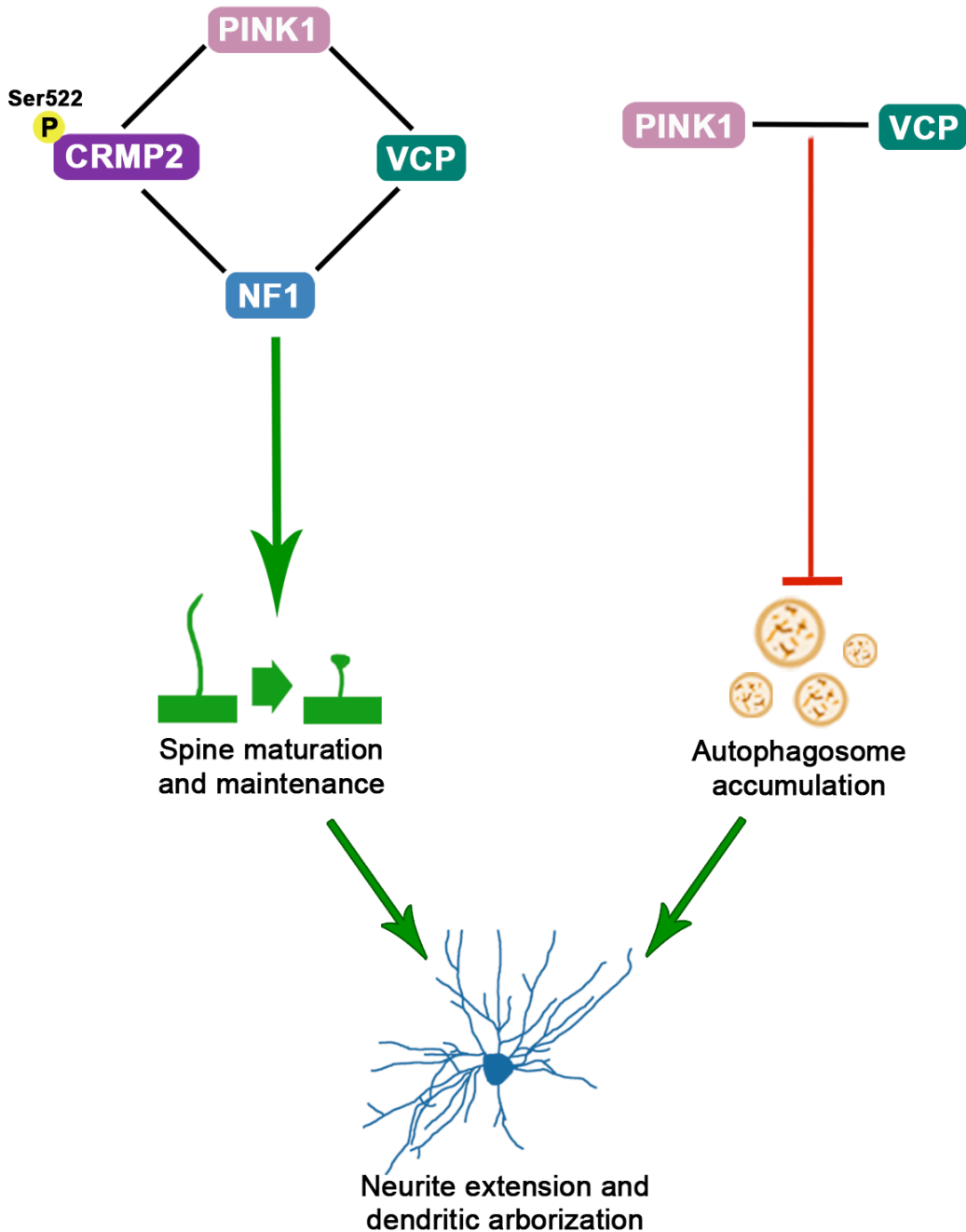


Figure 32: Proposed model of PINK1-VCP-NF1-CRMP2 signaling in regulation of neuronal morphology. This study identified two novel PINK1 interaction partners, VCP and CRMP2. The data shown here demonstrate that PINK1 and VCP cooperate to suppress autophagosome accumulation, with mild effects on neurite length. VCP and CRMP2 also share another binding partner, NF1. PINK1 and NF1 co-regulate CRMP2 phosphorylation at Ser522 to promote dendritic spine maturation and maintenance. Further, VCP and NF1 were shown to act downstream in PINK1 induced neurite outgrowth and dendritic arborization.

BIBLIOGRAPHY

1. Valente, E.M., et al., *Hereditary early-onset Parkinson's disease caused by mutations in PINK1*. Science (New York, N.Y.), 2004. **304**(5674): p. 1158-1160.
2. Jin, S.M., et al., *Mitochondrial membrane potential regulates PINK1 import and proteolytic destabilization by PARL*. The Journal of cell biology, 2010. **191**(5): p. 933-942.
3. Narendra, D.P., et al., *PINK1 is selectively stabilized on impaired mitochondria to activate Parkin*. PLoS biology, 2010. **8**(1).
4. Kane, L.A., et al., *PINK1 phosphorylates ubiquitin to activate Parkin E3 ubiquitin ligase activity*. The Journal of cell biology, 2014. **205**(2): p. 143-153.
5. Lazarou, M., et al., *Role of PINK1 binding to the TOM complex and alternate intracellular membranes in recruitment and activation of the E3 ligase Parkin*. Developmental cell, 2012. **22**(2): p. 320-333.
6. Dagda, R.K., et al., *Beyond the mitochondrion: cytosolic PINK1 remodels dendrites through protein kinase A*. Journal of neurochemistry, 2014. **128**(6): p. 864-877.
7. Haque, M.E., et al., *Cytoplasmic Pink1 activity protects neurons from dopaminergic neurotoxin MPTP*. Proceedings of the National Academy of Sciences of the United States of America, 2008. **105**(5): p. 1716-1721.
8. Contreras-Zárate, M.J.J., et al., *Silencing of PINK1 inhibits insulin-like growth factor-1-mediated receptor activation and neuronal survival*. Journal of molecular neuroscience : MN, 2015. **56**(1): p. 188-197.
9. Hirtz, D., et al., *How common are the "common" neurologic disorders?* Neurology, 2007. **68**(5): p. 326-337.

10. Damier, P., et al., *The substantia nigra of the human brain. II. Patterns of loss of dopamine-containing neurons in Parkinson's disease*. Brain : a journal of neurology, 1999. **122 (Pt 8)**: p. 1437-1448.
11. Galvan, A. and T. Wichmann, *Pathophysiology of parkinsonism*. Clinical neurophysiology : official journal of the International Federation of Clinical Neurophysiology, 2008. **119(7)**: p. 1459-1474.
12. Wirdefeldt, K., et al., *Epidemiology and etiology of Parkinson's disease: a review of the evidence*. European journal of epidemiology, 2011. **26 Suppl 1**: p. 58.
13. Goedert, M., et al., *100 years of Lewy pathology*. Nature reviews. Neurology, 2013. **9(1)**: p. 13-24.
14. Sulzer, D. and D.J. Surmeier, *Neuronal vulnerability, pathogenesis, and Parkinson's disease*. Movement disorders : official journal of the Movement Disorder Society, 2013. **28(6)**: p. 715-724.
15. Braak, H., et al., *Staging of brain pathology related to sporadic Parkinson's disease*. Neurobiology of aging, 2003. **24(2)**: p. 197-211.
16. Zgaljardic, D.J., N.S. Foldi, and J.C. Borod, *Cognitive and behavioral dysfunction in Parkinson's disease: neurochemical and clinicopathological contributions*. Journal of neural transmission (Vienna, Austria : 1996), 2004. **111(10-11)**: p. 1287-1301.
17. Dickson, D.W., et al., *Neuropathology of non-motor features of Parkinson disease*. Parkinsonism & related disorders, 2009. **15 Suppl 3**: p. 5.
18. Mercuri, N.B. and G. Bernardi, *The 'magic' of L-dopa: why is it the gold standard Parkinson's disease therapy?* Trends in pharmacological sciences, 2005. **26(7)**: p. 341-344.
19. Marsden, C.D. and J.D. Parkes, *"On-off" effects in patients with Parkinson's disease on chronic levodopa therapy*. Lancet (London, England), 1976. **1(7954)**: p. 292-296.
20. Fox, S.H., et al., *The Movement Disorder Society Evidence-Based Medicine Review Update: Treatments for the motor symptoms of Parkinson's disease*. Movement disorders : official journal of the Movement Disorder Society, 2011. **26 Suppl 3**: p. 41.
21. Lang, A.E. and C. Marras, *Initiating dopaminergic treatment in Parkinson's disease*. Lancet (London, England), 2014. **384(9949)**: p. 1164-1166.

22. Connolly, B.S. and A.E. Lang, *Pharmacological treatment of Parkinson disease: a review*. JAMA, 2014. **311**(16): p. 1670-1683.
23. Kalia, S.K., T. Sankar, and A.M. Lozano, *Deep brain stimulation for Parkinson's disease and other movement disorders*. Current opinion in neurology, 2013. **26**(4): p. 374-380.
24. Tröster, A.I. and J. Massano, *Changes in cognitive abilities after deep brain stimulation for Parkinson disease*. Neurology, 2015. **84**(13): p. 9.
25. Deuschl, G. and Y. Agid, *Subthalamic neurostimulation for Parkinson's disease with early fluctuations: balancing the risks and benefits*. The Lancet. Neurology, 2013. **12**(10): p. 1025-1034.
26. Peters, A. and I.R. Kaiserman-Abramof, *The small pyramidal neuron of the rat cerebral cortex. The perikaryon, dendrites and spines*. The American journal of anatomy, 1970. **127**(4): p. 321-355.
27. Miller, M. and A. Peters, *Maturation of rat visual cortex. II. A combined Golgi-electron microscope study of pyramidal neurons*. The Journal of comparative neurology, 1981. **203**(4): p. 555-573.
28. Fiala, J.C., et al., *Synaptogenesis via dendritic filopodia in developing hippocampal area CA1*. The Journal of neuroscience : the official journal of the Society for Neuroscience, 1998. **18**(21): p. 8900-8911.
29. Rochefort, N.L. and A. Konnerth, *Dendritic spines: from structure to in vivo function*. EMBO reports, 2012. **13**(8): p. 699-708.
30. Freund, T.F., J.F. Powell, and A.D. Smith, *Tyrosine hydroxylase-immunoreactive boutons in synaptic contact with identified striatonigral neurons, with particular reference to dendritic spines*. Neuroscience, 1984. **13**(4): p. 1189-1215.
31. Anglade, P., et al., *Synaptic plasticity in the caudate nucleus of patients with Parkinson's disease*. Neurodegeneration : a journal for neurodegenerative disorders, neuroprotection, and neuroregeneration, 1996. **5**(2): p. 121-128.
32. Stephens, B., et al., *Evidence of a breakdown of corticostriatal connections in Parkinson's disease*. Neuroscience, 2005. **132**(3): p. 741-754.
33. Zaja-Milatovic, S., et al., *Selective dendritic degeneration of medium spiny neurons in dementia with Lewy bodies*. Neurology, 2006. **66**(10): p. 1591-1593.

34. Deutch, A.Y., R.J. Colbran, and D.J. Winder, *Striatal plasticity and medium spiny neuron dendritic remodeling in parkinsonism*. Parkinsonism & related disorders, 2007. **13 Suppl 3**: p. 8.
35. Zaja-Milatovic, S., et al., *Dendritic degeneration in neostriatal medium spiny neurons in Parkinson disease*. Neurology, 2005. **64**(3): p. 545-547.
36. Patt, S., et al., *Pathological changes in dendrites of substantia nigra neurons in Parkinson's disease: a Golgi study*. Histology and histopathology, 1991. **6**(3): p. 373-380.
37. Villalba, R.M. and Y. Smith, *Differential striatal spine pathology in Parkinson's disease and cocaine addiction: a key role of dopamine?* Neuroscience, 2013. **251**: p. 2-20.
38. Boya, P., F. Reggiori, and P. Codogno, *Emerging regulation and functions of autophagy*. Nature cell biology, 2013. **15**(7): p. 713-720.
39. Kim, Y.C. and K.-L.L. Guan, *mTOR: a pharmacologic target for autophagy regulation*. The Journal of clinical investigation, 2015. **125**(1): p. 25-32.
40. Yang, Z. and D.J. Klionsky, *Mammalian autophagy: core molecular machinery and signaling regulation*. Current opinion in cell biology, 2010. **22**(2): p. 124-131.
41. Shibutani, S.T. and T. Yoshimori, *A current perspective of autophagosome biogenesis*. Cell research, 2014. **24**(1): p. 58-68.
42. Suzuki, H., et al., *Structure of the Atg101-Atg13 complex reveals essential roles of Atg101 in autophagy initiation*. Nature structural & molecular biology, 2015. **22**(7): p. 572-580.
43. Rubinsztein, D.C., et al., *Dyneins, autophagy, aggregation and neurodegeneration*. Autophagy, 2005. **1**(3): p. 177-178.
44. Moreau, K., et al., *Autophagosome precursor maturation requires homotypic fusion*. Cell, 2011. **146**(2): p. 303-317.
45. Kim, H.J., et al., *Beclin-1-interacting autophagy protein Atg14L targets the SNARE-associated protein Snapin to coordinate endocytic trafficking*. Journal of cell science, 2012. **125**(Pt 20): p. 4740-4750.
46. Khaminets, A., C. Behl, and I. Dikic, *Ubiquitin-Dependent And Independent Signals In Selective Autophagy*. Trends in cell biology, 2015.

47. Pankiv, S., et al., *p62/SQSTM1 binds directly to Atg8/LC3 to facilitate degradation of ubiquitinated protein aggregates by autophagy*. The Journal of biological chemistry, 2007. **282**(33): p. 24131-24145.
48. Kirkin, V., et al., *A role for NBR1 in autophagosomal degradation of ubiquitinated substrates*. Molecular cell, 2009. **33**(4): p. 505-516.
49. Korac, J., et al., *Ubiquitin-independent function of optineurin in autophagic clearance of protein aggregates*. Journal of cell science, 2013. **126**(Pt 2): p. 580-592.
50. Lu, W., et al., *Dual proteolytic pathways govern glycolysis and immune competence*. Cell, 2014. **159**(7): p. 1578-1590.
51. Anglade, P., et al., *Apoptosis in dopaminergic neurons of the human substantia nigra during normal aging*. Histology and histopathology, 1997. **12**(3): p. 603-610.
52. Zhu, J.-H.H., et al., *Localization of phosphorylated ERK/MAP kinases to mitochondria and autophagosomes in Lewy body diseases*. Brain pathology (Zurich, Switzerland), 2003. **13**(4): p. 473-481.
53. Boland, B., et al., *Autophagy induction and autophagosome clearance in neurons: relationship to autophagic pathology in Alzheimer's disease*. The Journal of neuroscience : the official journal of the Society for Neuroscience, 2008. **28**(27): p. 6926-6937.
54. Ibáñez, P., et al., *Mutational analysis of the PINK1 gene in early-onset parkinsonism in Europe and North Africa*. Brain : a journal of neurology, 2006. **129**(Pt 3): p. 686-694.
55. Valente, E., et al., *Hereditary early-onset Parkinson's disease caused by mutations in PINK1*. Science (New York, N.Y.), 2004. **304**(5674): p. 1158-1160.
56. Bonifati, V., et al., *Early-onset parkinsonism associated with PINK1 mutations: frequency, genotypes, and phenotypes*. Neurology, 2005. **65**(1): p. 87-95.
57. Leutenegger, A.-L., et al., *Juvenile-onset Parkinsonism as a result of the first mutation in the adenosine triphosphate orientation domain of PINK1*. Archives of neurology, 2006. **63**(9): p. 1257-1261.
58. Klein, C., et al., *PINK1, Parkin, and DJ-1 mutations in Italian patients with early-onset parkinsonism*. European journal of human genetics : EJHG, 2005. **13**(9): p. 1086-1093.

59. Silvestri, L., et al., *Mitochondrial import and enzymatic activity of PINK1 mutants associated to recessive parkinsonism*. Human molecular genetics, 2005. **14**(22): p. 3477-3492.
60. Aerts, L., et al., *PINK1 kinase catalytic activity is regulated by phosphorylation on serines 228 and 402*. The Journal of biological chemistry, 2015. **290**(5): p. 2798-2811.
61. Matenia, D., et al., *Microtubule affinity-regulating kinase 2 (MARK2) turns on phosphatase and tensin homolog (PTEN)-induced kinase 1 (PINK1) at Thr-313, a mutation site in Parkinson disease: effects on mitochondrial transport*. The Journal of biological chemistry, 2012. **287**(11): p. 8174-8186.
62. Dudek, J., P. Rehling, and M. van der Laan, *Mitochondrial protein import: common principles and physiological networks*. Biochimica et biophysica acta, 2013. **1833**(2): p. 274-285.
63. Lazarou, M., et al., *Role of PINK1 binding to the TOM complex and alternate intracellular membranes in recruitment and activation of the E3 ligase Parkin*. Developmental cell, 2012. **22**(2): p. 320-333.
64. Kato, H., et al., *Tom70 is essential for PINK1 import into mitochondria*. PloS one, 2013. **8**(3).
65. Zara, V., et al., *Mitochondrial carrier protein biogenesis: role of the chaperones Hsc70 and Hsp90*. The Biochemical journal, 2009. **419**(2): p. 369-375.
66. Becker, D., et al., *Pink1 kinase and its membrane potential ($\Delta\psi$)-dependent cleavage product both localize to outer mitochondrial membrane by unique targeting mode*. The Journal of biological chemistry, 2012. **287**(27): p. 22969-22987.
67. Zhou, C., et al., *The kinase domain of mitochondrial PINK1 faces the cytoplasm*. Proceedings of the National Academy of Sciences of the United States of America, 2008. **105**(33): p. 12022-12027.
68. Lin, W. and U.J. Kang, *Structural determinants of PINK1 topology and dual subcellular distribution*. BMC cell biology, 2010. **11**: p. 90.
69. Weihofen, A., et al., *Pink1 Parkinson mutations, the Cdc37/Hsp90 chaperones and Parkin all influence the maturation or subcellular distribution of Pink1*. Human molecular genetics, 2008. **17**(4): p. 602-616.

70. Sim, C., et al., *Analysis of the regulatory and catalytic domains of PTEN-induced kinase-1 (PINK1)*. Human mutation, 2012. **33**(10): p. 1408-1422.
71. Greene, A., et al., *Mitochondrial processing peptidase regulates PINK1 processing, import and Parkin recruitment*. EMBO reports, 2012. **13**(4): p. 378-385.
72. Meissner, C., et al., *The mitochondrial intramembrane protease PARL cleaves human PINK1 to regulate Pink1 trafficking*. Journal of neurochemistry, 2011. **117**(5): p. 856-867.
73. Jin, S., et al., *Mitochondrial membrane potential regulates PINK1 import and proteolytic destabilization by PARL*. The Journal of cell biology, 2010. **191**(5): p. 933-942.
74. Deas, E., et al., *PINK1 cleavage at position A103 by the mitochondrial protease PARL*. Human molecular genetics, 2011. **20**(5): p. 867-879.
75. Yamano, K. and R.J. Youle, *PINK1 is degraded through the N-end rule pathway*. Autophagy, 2013. **9**(11): p. 1758-1769.
76. Pridgeon, J., et al., *PINK1 protects against oxidative stress by phosphorylating mitochondrial chaperone TRAP1*. PLoS biology, 2007. **5**(7).
77. Arena, G., et al., *PINK1 protects against cell death induced by mitochondrial depolarization, by phosphorylating Bcl-xL and impairing its pro-apoptotic cleavage*. Cell death and differentiation, 2013. **20**(7): p. 920-930.
78. Haque, M., et al., *Cytoplasmic Pink1 activity protects neurons from dopaminergic neurotoxin MPTP*. Proceedings of the National Academy of Sciences of the United States of America, 2008. **105**(5): p. 1716-1721.
79. Deng, H., et al., *Small interfering RNA targeting the PINK1 induces apoptosis in dopaminergic cells SH-SY5Y*. Biochemical and biophysical research communications, 2005. **337**(4): p. 1133-1138.
80. Celardo, I., L. Martins, and S. Gandhi, *Unravelling mitochondrial pathways to Parkinson's disease*. British journal of pharmacology, 2013.
81. Chaturvedi, R. and M. Flint Beal, *Mitochondrial diseases of the brain*. Free radical biology & medicine, 2013. **63**: p. 1-29.

82. Amo, T., et al., *Mitochondrial membrane potential decrease caused by loss of PINK1 is not due to proton leak, but to respiratory chain defects*. *Neurobiology of disease*, 2011. **41**(1): p. 111-118.
83. Morais, V., et al., *Parkinson's disease mutations in PINK1 result in decreased Complex I activity and deficient synaptic function*. *EMBO molecular medicine*, 2009. **1**(2): p. 99-111.
84. Gautier, C., T. Kitada, and J. Shen, *Loss of PINK1 causes mitochondrial functional defects and increased sensitivity to oxidative stress*. *Proceedings of the National Academy of Sciences of the United States of America*, 2008. **105**(32): p. 11364-11369.
85. Gautier, C., et al., *Regulation of mitochondrial permeability transition pore by PINK1*. *Molecular neurodegeneration*, 2012. **7**: p. 22.
86. Gandhi, S., et al., *PINK1-associated Parkinson's disease is caused by neuronal vulnerability to calcium-induced cell death*. *Molecular cell*, 2009. **33**(5): p. 627-638.
87. Kostic, M., et al., *PKA Phosphorylation of NCLX Reverses Mitochondrial Calcium Overload and Depolarization, Promoting Survival of PINK1-Deficient Dopaminergic Neurons*. *Cell reports*, 2015. **13**(2): p. 376-386.
88. Vos, M., et al., *Vitamin K2 is a mitochondrial electron carrier that rescues pink1 deficiency*. *Science (New York, N.Y.)*, 2012. **336**(6086): p. 1306-1310.
89. Chan, C., T. Gertler, and D. Surmeier, *Calcium homeostasis, selective vulnerability and Parkinson's disease*. *Trends in neurosciences*, 2009. **32**(5): p. 249-256.
90. De Stefani, D., et al., *A forty-kilodalton protein of the inner membrane is the mitochondrial calcium uniporter*. *Nature*, 2011. **476**(7360): p. 336-340.
91. Palty, R., et al., *NCLX is an essential component of mitochondrial Na⁺/Ca²⁺ exchange*. *Proceedings of the National Academy of Sciences of the United States of America*, 2010. **107**(1): p. 436-441.
92. Heeman, B., et al., *Depletion of PINK1 affects mitochondrial metabolism, calcium homeostasis and energy maintenance*. *Journal of cell science*, 2011. **124**(Pt 7): p. 1115-1125.
93. Chan, D.C., *Mitochondrial fusion and fission in mammals*. *Annu Rev Cell Dev Biol*, 2006. **22**: p. 79-99.

94. Twig, G., B. Hyde, and O.S. Shirihai, *Mitochondrial fusion, fission and autophagy as a quality control axis: the bioenergetic view*. *Biochim Biophys Acta*, 2008. **1777**(9): p. 1092-7.
95. Twig, G., et al., *Fission and selective fusion govern mitochondrial segregation and elimination by autophagy*. *EMBO J*, 2008. **27**(2): p. 433-46.
96. Narendra, D., et al., *PINK1 is selectively stabilized on impaired mitochondria to activate Parkin*. *PLoS biology*, 2010. **8**(1).
97. Matsuda, N., et al., *PINK1 stabilized by mitochondrial depolarization recruits Parkin to damaged mitochondria and activates latent Parkin for mitophagy*. *The Journal of cell biology*, 2010. **189**(2): p. 211-221.
98. Narendra, D., et al., *Parkin is recruited selectively to impaired mitochondria and promotes their autophagy*. *J Cell Biol*, 2008. **183**(5): p. 795-803.
99. Greene, A.W., et al., *Mitochondrial processing peptidase regulates PINK1 processing, import and Parkin recruitment*. *EMBO Rep*, 2012. **13**(4): p. 378-85.
100. Kazlauskaitė, A., et al., *Parkin is activated by PINK1-dependent phosphorylation of ubiquitin at Ser65*. *The Biochemical journal*, 2014. **460**(1): p. 127-139.
101. Koyano, F., et al., *Ubiquitin is phosphorylated by PINK1 to activate parkin*. *Nature*, 2014. **510**(7503): p. 162-166.
102. Lazarou, M., et al., *The ubiquitin kinase PINK1 recruits autophagy receptors to induce mitophagy*. *Nature*, 2015. **524**(7565): p. 309-314.
103. Heo, J.-M.M., et al., *The PINK1-PARKIN Mitochondrial Ubiquitylation Pathway Drives a Program of OPTN/NDP52 Recruitment and TBK1 Activation to Promote Mitophagy*. *Molecular cell*, 2015. **60**(1): p. 7-20.
104. Van Laar, V.S. and S.B. Berman, *The interplay of neuronal mitochondrial dynamics and bioenergetics: implications for Parkinson's disease*. *Neurobiol Dis*, 2013. **51**: p. 43-55.
105. Cai, Q., et al., *Spatial parkin translocation and degradation of damaged mitochondria via mitophagy in live cortical neurons*. *Curr Biol*, 2012. **22**(6): p. 545-52.

106. Chu, C.T., et al., *Cardiolipin externalization to the outer mitochondrial membrane acts as an elimination signal for mitophagy in neuronal cells*. *Nature cell biology*, 2013. **15**(10): p. 1197-1205.
107. Dagda, R.K., et al., *Loss of PINK1 function promotes mitophagy through effects on oxidative stress and mitochondrial fission*. *J Biol Chem*, 2009. **284**(20): p. 13843-55.
108. Weihofen, A., et al., *Pink1 forms a multiprotein complex with Miro and Milton, linking Pink1 function to mitochondrial trafficking*. *Biochemistry*, 2009. **48**(9): p. 2045-52.
109. Liu, S., et al., *Parkinson's disease-associated kinase PINK1 regulates Miro protein level and axonal transport of mitochondria*. *PLoS Genet*, 2012. **8**(3): p. e1002537.
110. Dagda, R., et al., *Beyond the mitochondrion: cytosolic PINK1 remodels dendrites through Protein Kinase A*. *Journal of neurochemistry*, 2013.
111. Gispert, S., et al., *Parkinson phenotype in aged PINK1-deficient mice is accompanied by progressive mitochondrial dysfunction in absence of neurodegeneration*. *PloS one*, 2009. **4**(6).
112. Sanchez, G., et al., *Unaltered striatal dopamine release levels in young Parkin knockout, Pink1 knockout, DJ-1 knockout and LRRK2 R1441G transgenic mice*. *PloS one*, 2014. **9**(4).
113. Kitada, T., et al., *Impaired dopamine release and synaptic plasticity in the striatum of PINK1-deficient mice*. *Proceedings of the National Academy of Sciences of the United States of America*, 2007. **104**(27): p. 11441-11446.
114. Madeo, G., et al., *PINK1 heterozygous mutations induce subtle alterations in dopamine-dependent synaptic plasticity*. *Movement disorders : official journal of the Movement Disorder Society*, 2014. **29**(1): p. 41-53.
115. Sun, J., et al., *Regulation of dopamine presynaptic markers and receptors in the striatum of DJ-1 and Pink1 knockout rats*. *Neuroscience letters*, 2013. **557 Pt B**: p. 123-128.
116. Michiorri, S., et al., *The Parkinson-associated protein PINK1 interacts with Beclin1 and promotes autophagy*. *Cell death and differentiation*, 2010. **17**(6): p. 962-974.
117. Dagda, R.K., et al., *Loss of PINK1 function promotes mitophagy through effects on oxidative stress and mitochondrial fission*. *The Journal of biological chemistry*, 2009. **284**(20): p. 13843-13855.

118. Qi, Z., et al., *Loss of PINK1 function decreases PP2A activity and promotes autophagy in dopaminergic cells and a murine model*. *Neurochemistry international*, 2011. **59**(5): p. 572-581.
119. Murata, H., et al., *A new cytosolic pathway from a Parkinson disease-associated kinase, BRPK/PINK1: activation of AKT via mTORC2*. *The Journal of biological chemistry*, 2011. **286**(9): p. 7182-7189.
120. Noguchi, M., N. Hirata, and F. Suizu, *The links between AKT and two intracellular proteolytic cascades: ubiquitination and autophagy*. *Biochimica et biophysica acta*, 2014. **1846**(2): p. 342-352.
121. Fiesel, F.C. and W. Springer, *Disease relevance of phosphorylated ubiquitin (p-S65-Ub)*. *Autophagy*, 2015.
122. Meyer, H., M. Bug, and S. Bremer, *Emerging functions of the VCP/p97 AAA-ATPase in the ubiquitin system*. *Nature cell biology*, 2012. **14**(2): p. 117-123.
123. Zhang, X., et al., *Structure of the AAA ATPase p97*. *Molecular cell*, 2000. **6**(6): p. 1473-1484.
124. Huyton, T., et al., *The crystal structure of murine p97/VCP at 3.6Å*. *Journal of structural biology*, 2003. **144**(3): p. 337-348.
125. Wang, Q., et al., *D1 ring is stable and nucleotide-independent, whereas D2 ring undergoes major conformational changes during the ATPase cycle of p97-VCP*. *The Journal of biological chemistry*, 2003. **278**(35): p. 32784-32793.
126. Buchberger, A., H. Schindelin, and P. Hänzelmann, *Control of p97 function by cofactor binding*. *FEBS letters*, 2015. **589**(19 Pt A): p. 2578-2589.
127. Watts, G.D., et al., *Inclusion body myopathy associated with Paget disease of bone and frontotemporal dementia is caused by mutant valosin-containing protein*. *Nature genetics*, 2004. **36**(4): p. 377-381.
128. Johnson, J.O., et al., *Exome sequencing reveals VCP mutations as a cause of familial ALS*. *Neuron*, 2010. **68**(5): p. 857-864.
129. Meyer, H. and C.C. Wehl, *The VCP/p97 system at a glance: connecting cellular function to disease pathogenesis*. *Journal of cell science*, 2014. **127**(Pt 18): p. 3877-3883.

130. Niwa, H., et al., *The role of the N-domain in the ATPase activity of the mammalian AAA ATPase p97/VCP*. The Journal of biological chemistry, 2012. **287**(11): p. 8561-8570.
131. Guyant-Maréchal, L., et al., *Valosin-containing protein gene mutations: clinical and neuropathologic features*. Neurology, 2006. **67**(4): p. 644-651.
132. Forman, M.S., et al., *Novel ubiquitin neuropathology in frontotemporal dementia with valosin-containing protein gene mutations*. Journal of neuropathology and experimental neurology, 2006. **65**(6): p. 571-581.
133. Tresse, E., et al., *VCP/p97 is essential for maturation of ubiquitin-containing autophagosomes and this function is impaired by mutations that cause IBMPFD*. Autophagy, 2010. **6**(2): p. 217-227.
134. Ritz, D., et al., *Endolysosomal sorting of ubiquitylated caveolin-1 is regulated by VCP and UBXD1 and impaired by VCP disease mutations*. Nature cell biology, 2011. **13**(9): p. 1116-1123.
135. Weihl, C.C., et al., *Inclusion body myopathy-associated mutations in p97/VCP impair endoplasmic reticulum-associated degradation*. Human molecular genetics, 2006. **15**(2): p. 189-199.
136. Janiesch, P.C., et al., *The ubiquitin-selective chaperone CDC-48/p97 links myosin assembly to human myopathy*. Nature cell biology, 2007. **9**(4): p. 379-390.
137. Ju, J.-S.S., et al., *Valosin-containing protein (VCP) is required for autophagy and is disrupted in VCP disease*. The Journal of cell biology, 2009. **187**(6): p. 875-888.
138. Ju, J.-S.S., et al., *Impaired protein aggregate handling and clearance underlie the pathogenesis of p97/VCP-associated disease*. The Journal of biological chemistry, 2008. **283**(44): p. 30289-30299.
139. Mori, F., et al., *Valosin-containing protein immunoreactivity in tauopathies, synucleinopathies, polyglutamine diseases and intranuclear inclusion body disease*. Neuropathology : official journal of the Japanese Society of Neuropathology, 2013. **33**(6): p. 637-644.
140. Nalbandian, A., et al., *The homozygote VCP(R¹⁵⁵H/R¹⁵⁵H) mouse model exhibits accelerated human VCP-associated disease pathology*. PloS one, 2012. **7**(9).

141. Nalbandian, A., et al., *A progressive translational mouse model of human valosin-containing protein disease: the VCP(R155H/+) mouse*. Muscle & nerve, 2013. **47**(2): p. 260-270.
142. Bartolome, F., et al., *Pathogenic VCP mutations induce mitochondrial uncoupling and reduced ATP levels*. Neuron, 2013. **78**(1): p. 57-64.
143. Nalbandian, A., et al., *In vitro studies in VCP-associated multisystem proteinopathy suggest altered mitochondrial bioenergetics*. Mitochondrion, 2015. **22**: p. 1-8.
144. Heo, J.-M.M., et al., *Intramolecular interactions control Vms1 translocation to damaged mitochondria*. Molecular biology of the cell, 2013. **24**(9): p. 1263-1273.
145. Heo, J.-M.M., et al., *A stress-responsive system for mitochondrial protein degradation*. Molecular cell, 2010. **40**(3): p. 465-480.
146. Tanaka, A., et al., *Proteasome and p97 mediate mitophagy and degradation of mitofusins induced by Parkin*. The Journal of cell biology, 2010. **191**(7): p. 1367-1380.
147. Kim, N.C., et al., *VCP is essential for mitochondrial quality control by PINK1/Parkin and this function is impaired by VCP mutations*. Neuron, 2013. **78**(1): p. 65-80.
148. Custer, S.K., et al., *Transgenic mice expressing mutant forms VCP/p97 recapitulate the full spectrum of IBMPFD including degeneration in muscle, brain and bone*. Human molecular genetics, 2010. **19**(9): p. 1741-1755.
149. Rodriguez-Ortiz, C.J., et al., *Neuronal-specific overexpression of a mutant valosin-containing protein associated with IBMPFD promotes aberrant ubiquitin and TDP-43 accumulation and cognitive dysfunction in transgenic mice*. The American journal of pathology, 2013. **183**(2): p. 504-515.
150. Rumpf, S., et al., *Neuronal remodeling and apoptosis require VCP-dependent degradation of the apoptosis inhibitor DIAP1*. Development (Cambridge, England), 2011. **138**(6): p. 1153-1160.
151. Rumpf, S., et al., *Drosophila Valosin-Containing Protein is required for dendrite pruning through a regulatory role in mRNA metabolism*. Proceedings of the National Academy of Sciences of the United States of America, 2014. **111**(20): p. 7331-7336.
152. Wang, H.-F.F., et al., *Valosin-containing protein and neurofibromin interact to regulate dendritic spine density*. The Journal of clinical investigation, 2011. **121**(12): p. 4820-4837.

153. Ratner, N. and S.J. Miller, *A RASopathy gene commonly mutated in cancer: the neurofibromatosis type 1 tumour suppressor*. Nature reviews. Cancer, 2015. **15**(5): p. 290-301.
154. Evans, D.G., et al., *Birth incidence and prevalence of tumor-prone syndromes: estimates from a UK family genetic register service*. American journal of medical genetics. Part A, 2010. **152A**(2): p. 327-332.
155. Hsueh, Y.-P.P., *From neurodevelopment to neurodegeneration: the interaction of neurofibromin and valosin-containing protein/p97 in regulation of dendritic spine formation*. Journal of biomedical science, 2012. **19**: p. 33.
156. Hyman, S.L., A. Shores, and K.N. North, *The nature and frequency of cognitive deficits in children with neurofibromatosis type 1*. Neurology, 2005. **65**(7): p. 1037-1044.
157. Lehtonen, A., et al., *Behaviour in children with neurofibromatosis type 1: cognition, executive function, attention, emotion, and social competence*. Developmental medicine and child neurology, 2013. **55**(2): p. 111-125.
158. Hyman, S.L., E. Arthur Shores, and K.N. North, *Learning disabilities in children with neurofibromatosis type 1: subtypes, cognitive profile, and attention-deficit-hyperactivity disorder*. Developmental medicine and child neurology, 2006. **48**(12): p. 973-977.
159. Altarac, M. and E. Saroha, *Lifetime prevalence of learning disability among US children*. Pediatrics, 2007. **119 Suppl 1**: p. 83.
160. Costa, R.M., et al., *Mechanism for the learning deficits in a mouse model of neurofibromatosis type 1*. Nature, 2002. **415**(6871): p. 526-530.
161. Hegedus, B., et al., *Neurofibromatosis-1 regulates neuronal and glial cell differentiation from neuroglial progenitors in vivo by both cAMP- and Ras-dependent mechanisms*. Cell stem cell, 2007. **1**(4): p. 443-457.
162. Brown, J.A., et al., *Reduced striatal dopamine underlies the attention system dysfunction in neurofibromatosis-1 mutant mice*. Human molecular genetics, 2010. **19**(22): p. 4515-4528.
163. Mautner, V.-F.F., et al., *Treatment of ADHD in neurofibromatosis type 1*. Developmental medicine and child neurology, 2002. **44**(3): p. 164-170.
164. Brambilla, R., et al., *A role for the Ras signalling pathway in synaptic transmission and long-term memory*. Nature, 1997. **390**(6657): p. 281-286.

165. Stornetta, R.L. and J.J. Zhu, *Ras and Rap signaling in synaptic plasticity and mental disorders*. The Neuroscientist : a review journal bringing neurobiology, neurology and psychiatry, 2011. **17**(1): p. 54-78.
166. Oliveira, A.F. and R. Yasuda, *Neurofibromin is the major ras inactivator in dendritic spines*. The Journal of neuroscience : the official journal of the Society for Neuroscience, 2014. **34**(3): p. 776-783.
167. Yunoue, S., et al., *Neurofibromatosis type I tumor suppressor neurofibromin regulates neuronal differentiation via its GTPase-activating protein function toward Ras*. The Journal of biological chemistry, 2003. **278**(29): p. 26958-26969.
168. Brown, J.A., S.M. Gianino, and D.H. Gutmann, *Defective cAMP generation underlies the sensitivity of CNS neurons to neurofibromatosis-1 heterozygosity*. The Journal of neuroscience : the official journal of the Society for Neuroscience, 2010. **30**(16): p. 5579-5589.
169. Brown, J.A., et al., *Neurofibromatosis-1 heterozygosity impairs CNS neuronal morphology in a cAMP/PKA/ROCK-dependent manner*. Molecular and cellular neurosciences, 2012. **49**(1): p. 13-22.
170. Lin, Y.-L.L., et al., *Syndecan-2 induces filopodia and dendritic spine formation via the neurofibromin-PKA-Ena/VASP pathway*. The Journal of cell biology, 2007. **177**(5): p. 829-841.
171. Kwon, H.-B.B. and B.L. Sabatini, *Glutamate induces de novo growth of functional spines in developing cortex*. Nature, 2011. **474**(7349): p. 100-104.
172. Patrakitkomjorn, S., et al., *Neurofibromatosis type 1 (NF1) tumor suppressor, neurofibromin, regulates the neuronal differentiation of PC12 cells via its associating protein, CRMP-2*. The Journal of biological chemistry, 2008. **283**(14): p. 9399-9413.
173. Lin, Y.-L.L. and Y.-P.P. Hsueh, *Neurofibromin interacts with CRMP-2 and CRMP-4 in rat brain*. Biochemical and biophysical research communications, 2008. **369**(2): p. 747-752.
174. Uchida, Y., et al., *Semaphorin3A signalling is mediated via sequential Cdk5 and GSK3beta phosphorylation of CRMP2: implication of common phosphorylating mechanism underlying axon guidance and Alzheimer's disease*. Genes to cells : devoted to molecular & cellular mechanisms, 2005. **10**(2): p. 165-179.

175. Cole, A.R., et al., *Distinct priming kinases contribute to differential regulation of collapsin response mediator proteins by glycogen synthase kinase-3 in vivo*. The Journal of biological chemistry, 2006. **281**(24): p. 16591-16598.
176. Charrier, E., et al., *Collapsin response mediator proteins (CRMPs): involvement in nervous system development and adult neurodegenerative disorders*. Molecular neurobiology, 2003. **28**(1): p. 51-64.
177. Ponnusamy, R. and B. Lohkamp, *Insights into the oligomerization of CRMPs: crystal structure of human collapsin response mediator protein 5*. Journal of neurochemistry, 2013. **125**(6): p. 855-868.
178. Hensley, K., et al., *Collapsin response mediator protein-2: an emerging pathologic feature and therapeutic target for neurodegeneration indications*. Molecular neurobiology, 2011. **43**(3): p. 180-191.
179. Majava, V., et al., *Crystal and solution structure, stability and post-translational modifications of collapsin response mediator protein 2*. The FEBS journal, 2008. **275**(18): p. 4583-4596.
180. Inagaki, N., et al., *CRMP-2 induces axons in cultured hippocampal neurons*. Nature neuroscience, 2001. **4**(8): p. 781-782.
181. Deo, R.C., et al., *Structural bases for CRMP function in plexin-dependent semaphorin3A signaling*. The EMBO journal, 2004. **23**(1): p. 9-22.
182. Kawano, Y., et al., *CRMP-2 is involved in kinesin-1-dependent transport of the Sra-1/WAVE1 complex and axon formation*. Molecular and cellular biology, 2005. **25**(22): p. 9920-9935.
183. Arimura, N., et al., *CRMP-2 directly binds to cytoplasmic dynein and interferes with its activity*. Journal of neurochemistry, 2009. **111**(2): p. 380-390.
184. Rahajeng, J., et al., *Collapsin response mediator protein-2 (Crmp2) regulates trafficking by linking endocytic regulatory proteins to dynein motors*. The Journal of biological chemistry, 2010. **285**(42): p. 31918-31922.
185. Kimura, T., et al., *Tubulin and CRMP-2 complex is transported via Kinesin-1*. Journal of neurochemistry, 2005. **93**(6): p. 1371-1382.
186. Arimura, N., et al., *Anterograde transport of TrkB in axons is mediated by direct interaction with Slp1 and Rab27*. Developmental cell, 2009. **16**(5): p. 675-686.

187. Xia, Z. and D.R. Storm, *The role of calmodulin as a signal integrator for synaptic plasticity*. Nature reviews. Neuroscience, 2005. **6**(4): p. 267-276.
188. Zhang, Z., et al., *Collapsin response mediator protein-2 is a calmodulin-binding protein*. Cellular and molecular life sciences : CMLS, 2009. **66**(3): p. 526-536.
189. Yin, Y., et al., *Tat-collapsin response mediator protein 2 (CRMP2) increases the survival of neurons after NMDA excitotoxicity by reducing the cleavage of CRMP2*. Neurochemical research, 2013. **38**(10): p. 2095-2104.
190. Brustovetsky, T., et al., *Collapsin response mediator protein 2 (CRMP2) interacts with N-methyl-D-aspartate (NMDA) receptor and Na⁺/Ca²⁺ exchanger and regulates their functional activity*. The Journal of biological chemistry, 2014. **289**(11): p. 7470-7482.
191. Brittain, J.M., et al., *Suppression of inflammatory and neuropathic pain by uncoupling CRMP-2 from the presynaptic Ca²⁺ channel complex*. Nature medicine, 2011. **17**(7): p. 822-829.
192. Wilson, S.M., et al., *Inhibition of transmitter release and attenuation of anti-retroviral-associated and tibial nerve injury-related painful peripheral neuropathy by novel synthetic Ca²⁺ channel peptides*. The Journal of biological chemistry, 2012. **287**(42): p. 35065-35077.
193. Catterall, W.A., *Structure and regulation of voltage-gated Ca²⁺ channels*. Annual review of cell and developmental biology, 2000. **16**: p. 521-555.
194. Brittain, J.M., et al., *Cdk5-mediated phosphorylation of CRMP-2 enhances its interaction with CaV2.2*. FEBS letters, 2012. **586**(21): p. 3813-3818.
195. Jin, X., et al., *Phosphorylation of CRMP2 by Cdk5 Regulates Dendritic Spine Development of Cortical Neuron in the Mouse Hippocampus*. Neural ..., 2015.
196. Yamashita, N., et al., *Phosphorylation of CRMP2 (collapsin response mediator protein 2) is involved in proper dendritic field organization*. The Journal of neuroscience : the official journal of the Society for Neuroscience, 2012. **32**(4): p. 1360-1365.
197. Tan, M., et al., *GSK-3 α / β -mediated phosphorylation of CRMP-2 regulates activity-dependent dendritic growth*. Journal of neurochemistry, 2013. **125**(5): p. 685-697.
198. Dagda, R.K., et al., *Mitochondrially localized PKA reverses mitochondrial pathology and dysfunction in a cellular model of Parkinson's disease*. Cell death and differentiation, 2011. **18**(12): p. 1914-1923.

199. Cherra, S.J., et al., *Regulation of the autophagy protein LC3 by phosphorylation*. The Journal of cell biology, 2010. **190**(4): p. 533-539.
200. Degasperis, A., et al., *Evaluating strategies to normalise biological replicates of Western blot data*. PloS one, 2014. **9**(1).
201. Ferreira, T.A., et al., *Neuronal morphometry directly from bitmap images*. Nature methods, 2014. **11**(10): p. 982-984.
202. Kulkarni, V.A. and B.L. Firestein, *The dendritic tree and brain disorders*. Molecular and cellular neurosciences, 2012. **50**(1): p. 10-20.
203. Braak, H. and E. Braak, *Nuclear configuration and neuronal types of the nucleus nigra in the brain of the human adult*. Human neurobiology, 1986. **5**(2): p. 71-82.
204. Petit, A., et al., *Wild-type PINK1 prevents basal and induced neuronal apoptosis, a protective effect abrogated by Parkinson disease-related mutations*. The Journal of biological chemistry, 2005. **280**(40): p. 34025-34032.
205. Triplett, J.C., et al., *Quantitative expression proteomics and phosphoproteomics profile of brain from PINK1 knockout mice: insights into mechanisms of familial Parkinson's disease*. Journal of neurochemistry, 2015. **133**(5): p. 750-765.
206. Chou, T.-F.F., et al., *Reversible inhibitor of p97, DBeQ, impairs both ubiquitin-dependent and autophagic protein clearance pathways*. Proceedings of the National Academy of Sciences of the United States of America, 2011. **108**(12): p. 4834-4839.
207. Buchan, J.R., et al., *Eukaryotic stress granules are cleared by autophagy and Cdc48/VCP function*. Cell, 2013. **153**(7): p. 1461-1474.
208. Plowey, E.D., et al., *Role of autophagy in G2019S-LRRK2-associated neurite shortening in differentiated SH-SY5Y cells*. Journal of neurochemistry, 2008. **105**(3): p. 1048-1056.
209. Ye, M., et al., *Parkinson's disease-associated PINK1 G309D mutation increases abnormal phosphorylation of Tau*. IUBMB life, 2015. **67**(4): p. 286-290.
210. Matsuo, E.S., et al., *Biopsy-derived adult human brain tau is phosphorylated at many of the same sites as Alzheimer's disease paired helical filament tau*. Neuron, 1994. **13**(4): p. 989-1002.

211. Sontag, E., et al., *Regulation of the phosphorylation state and microtubule-binding activity of Tau by protein phosphatase 2A*. *Neuron*, 1996. **17**(6): p. 1201-1207.
212. Cole, A.R., et al., *Relative resistance of Cdk5-phosphorylated CRMP2 to dephosphorylation*. *The Journal of biological chemistry*, 2008. **283**(26): p. 18227-18237.
213. Zhu, L.-Q.Q., et al., *Protein phosphatase 2A facilitates axonogenesis by dephosphorylating CRMP2*. *The Journal of neuroscience : the official journal of the Society for Neuroscience*, 2010. **30**(10): p. 3839-3848.
214. Wilson, S.M., et al., *Differential regulation of collapsin response mediator protein 2 (CRMP2) phosphorylation by GSK3 β and CDK5 following traumatic brain injury*. *Frontiers in cellular neuroscience*, 2014. **8**: p. 135.
215. Ohama, T. and D.L. Brautigan, *Endotoxin conditioning induces VCP/p97-mediated and inducible nitric-oxide synthase-dependent Tyr284 nitration in protein phosphatase 2A*. *The Journal of biological chemistry*, 2010. **285**(12): p. 8711-8718.
216. McNeill, T.H., et al., *Atrophy of medium spiny I striatal dendrites in advanced Parkinson's disease*. *Brain research*, 1988. **455**(1): p. 148-152.
217. Parisiadou, L., et al., *LRRK2 regulates synaptogenesis and dopamine receptor activation through modulation of PKA activity*. *Nature neuroscience*, 2014. **17**(3): p. 367-376.
218. Solis, O., et al., *Alterations in dendritic morphology of the prefrontal cortical and striatum neurons in the unilateral 6-OHDA-rat model of Parkinson's disease*. *Synapse (New York, N.Y.)*, 2007. **61**(6): p. 450-458.
219. Villalba, R.M., H. Lee, and Y. Smith, *Dopaminergic denervation and spine loss in the striatum of MPTP-treated monkeys*. *Experimental neurology*, 2009. **215**(2): p. 220-227.
220. Neely, M.D., D.E. Schmidt, and A.Y. Deutch, *Cortical regulation of dopamine depletion-induced dendritic spine loss in striatal medium spiny neurons*. *Neuroscience*, 2007. **149**(2): p. 457-464.
221. Garcia, B.G., M.D. Neely, and A.Y. Deutch, *Cortical regulation of striatal medium spiny neuron dendritic remodeling in parkinsonism: modulation of glutamate release reverses dopamine depletion-induced dendritic spine loss*. *Cerebral cortex (New York, N.Y. : 1991)*, 2010. **20**(10): p. 2423-2432.
222. Skeberdis, V.A., et al., *Protein kinase A regulates calcium permeability of NMDA receptors*. *Nature neuroscience*, 2006. **9**(4): p. 501-510.

223. Brittain, J.M., et al., *Neuroprotection against traumatic brain injury by a peptide derived from the collapsin response mediator protein 2 (CRMP2)*. The Journal of biological chemistry, 2011. **286**(43): p. 37778-37792.
224. Gambrill, A.C. and A. Barria, *NMDA receptor subunit composition controls synaptogenesis and synapse stabilization*. Proceedings of the National Academy of Sciences of the United States of America, 2011. **108**(14): p. 5855-5860.
225. François-Moutal, L., et al., *A membrane-delimited N-myristoylated CRMP2 peptide aptamer inhibits CaV2.2 trafficking and reverses inflammatory and postoperative pain behaviors*. Pain, 2015. **156**(7): p. 1247-1264.
226. Pravettoni, E., et al., *Different localizations and functions of L-type and N-type calcium channels during development of hippocampal neurons*. Developmental biology, 2000. **227**(2): p. 581-594.
227. Harris, J.J., R. Jolivet, and D. Attwell, *Synaptic energy use and supply*. Neuron, 2012. **75**(5): p. 762-777.
228. Gautier, C.A., T. Kitada, and J. Shen, *Loss of PINK1 causes mitochondrial functional defects and increased sensitivity to oxidative stress*. Proceedings of the National Academy of Sciences of the United States of America, 2008. **105**(32): p. 11364-11369.
229. Pivovarova, N.B. and S.B. Andrews, *Calcium-dependent mitochondrial function and dysfunction in neurons*. The FEBS journal, 2010. **277**(18): p. 3622-3636.
230. Tang, G., et al., *Loss of mTOR-dependent macroautophagy causes autistic-like synaptic pruning deficits*. Neuron, 2014. **83**(5): p. 1131-1143.
231. Hernandez, D., et al., *Regulation of presynaptic neurotransmission by macroautophagy*. Neuron, 2012. **74**(2): p. 277-284.
232. Oakhill, J.S., et al., *AMPK is a direct adenylate charge-regulated protein kinase*. Science (New York, N.Y.), 2011. **332**(6036): p. 1433-1435.
233. Drake, K.R., M. Kang, and A.K. Kenworthy, *Nucleocytoplasmic distribution and dynamics of the autophagosome marker EGFP-LC3*. PloS one, 2010. **5**(3).
234. Kraft, L.J., et al., *Size, stoichiometry, and organization of soluble LC3-associated complexes*. Autophagy, 2014. **10**(5): p. 861-877.

235. Rock, K.L., et al., *Inhibitors of the proteasome block the degradation of most cell proteins and the generation of peptides presented on MHC class I molecules*. Cell, 1994. **78**(5): p. 761-771.
236. McKinnon, C. and S.J. Tabrizi, *The ubiquitin-proteasome system in neurodegeneration. Antioxidants & redox signaling*, 2014. **21**(17): p. 2302-2321.
237. Korolchuk, V.I., F.M. Menzies, and D.C. Rubinsztein, *Mechanisms of cross-talk between the ubiquitin-proteasome and autophagy-lysosome systems*. FEBS letters, 2010. **584**(7): p. 1393-1398.
238. Martinez-Vicente, M., et al., *Cargo recognition failure is responsible for inefficient autophagy in Huntington's disease*. Nature neuroscience, 2010. **13**(5): p. 567-576.
239. Wauer, T., et al., *Ubiquitin Ser65 phosphorylation affects ubiquitin structure, chain assembly and hydrolysis*. The EMBO journal, 2015. **34**(3): p. 307-325.
240. Seidel, K., et al., *Axonal inclusions in spinocerebellar ataxia type 3*. Acta neuropathologica, 2010. **120**(4): p. 449-460.
241. Paulson, H.L., et al., *Intranuclear inclusions of expanded polyglutamine protein in spinocerebellar ataxia type 3*. Neuron, 1997. **19**(2): p. 333-344.
242. Wang, H., Z. Ying, and G. Wang, *Ataxin-3 regulates aggresome formation of copper-zinc superoxide dismutase (SOD1) by editing K63-linked polyubiquitin chains*. The Journal of biological chemistry, 2012. **287**(34): p. 28576-28585.
243. Ouyang, H., et al., *Protein aggregates are recruited to aggresome by histone deacetylase 6 via unanchored ubiquitin C termini*. The Journal of biological chemistry, 2012. **287**(4): p. 2317-2327.
244. Kawaguchi, Y., et al., *The deacetylase HDAC6 regulates aggresome formation and cell viability in response to misfolded protein stress*. Cell, 2003. **115**(6): p. 727-738.
245. Laço, M.N.N., et al., *Valosin-containing protein (VCP/p97) is an activator of wild-type ataxin-3*. PloS one, 2012. **7**(9).
246. Nadeau, M.-È.È., et al., *Pharmacological targeting of valosin containing protein (VCP) induces DNA damage and selectively kills canine lymphoma cells*. BMC cancer, 2015. **15**: p. 479.

247. Aredia, F. and A.I. Scovassi, *Poly(ADP-ribose): a signaling molecule in different paradigms of cell death*. Biochemical pharmacology, 2014. **92**(1): p. 157-163.
248. Huang, Q. and H.-M.M. Shen, *To die or to live: the dual role of poly(ADP-ribose) polymerase-1 in autophagy and necrosis under oxidative stress and DNA damage*. Autophagy, 2009. **5**(2): p. 273-276.
249. Rodríguez-Vargas, J.M.M., et al., *ROS-induced DNA damage and PARP-1 are required for optimal induction of starvation-induced autophagy*. Cell research, 2012. **22**(7): p. 1181-1198.
250. Zong, W.-X.X., et al., *Alkylating DNA damage stimulates a regulated form of necrotic cell death*. Genes & development, 2004. **18**(11): p. 1272-1282.
251. Morais, V.A., et al., *PINK1 loss-of-function mutations affect mitochondrial complex I activity via NdufA10 ubiquinone uncoupling*. Science (New York, N.Y.), 2014. **344**(6180): p. 203-207.
252. Shvets, E. and Z. Elazar, *Autophagy-independent incorporation of GFP-LC3 into protein aggregates is dependent on its interaction with p62/SQSTM1*. Autophagy, 2008. **4**(8): p. 1054-1056.
253. Mizushima, N., T. Yoshimori, and B. Levine, *Methods in mammalian autophagy research*. Cell, 2010. **140**(3): p. 313-326.
254. Nakai, J., M. Ohkura, and K. Imoto, *A high signal-to-noise Ca(2+) probe composed of a single green fluorescent protein*. Nature biotechnology, 2001. **19**(2): p. 137-141.
255. Sobczyk, A., V. Scheuss, and K. Svoboda, *NMDA receptor subunit-dependent [Ca2+] signaling in individual hippocampal dendritic spines*. The Journal of neuroscience : the official journal of the Society for Neuroscience, 2005. **25**(26): p. 6037-6046.
256. Williams, J.M., et al., *Biphasic changes in the levels of N-methyl-D-aspartate receptor-2 subunits correlate with the induction and persistence of long-term potentiation*. Brain research. Molecular brain research, 1998. **60**(1): p. 21-27.
257. Hrabetova, S., et al., *Distinct NMDA receptor subpopulations contribute to long-term potentiation and long-term depression induction*. The Journal of neuroscience : the official journal of the Society for Neuroscience, 2000. **20**(12).

258. Kirchner, P., M. Bug, and H. Meyer, *Ubiquitination of the N-terminal region of caveolin-1 regulates endosomal sorting by the VCP/p97 AAA-ATPase*. The Journal of biological chemistry, 2013. **288**(10): p. 7363-7372.
259. Roche, K.W., et al., *Molecular determinants of NMDA receptor internalization*. Nature neuroscience, 2001. **4**(8): p. 794-802.
260. Gandini, M.A.A., et al., *The MAP1B-LC1/UBE2L3 complex catalyzes degradation of cell surface CaV2.2 channels*. Channels (Austin, Tex.), 2014. **8**(5): p. 452-457.
261. Morita, A., et al., *Regulation of dendritic branching and spine maturation by semaphorin3A-Fyn signaling*. The Journal of neuroscience : the official journal of the Society for Neuroscience, 2006. **26**(11): p. 2971-2980.
262. Cheadle, L. and T. Biederer, *Activity-dependent regulation of dendritic complexity by semaphorin 3A through Farp1*. The Journal of neuroscience : the official journal of the Society for Neuroscience, 2014. **34**(23): p. 7999-8009.
263. Li, Z., et al., *The importance of dendritic mitochondria in the morphogenesis and plasticity of spines and synapses*. Cell, 2004. **119**(6): p. 873-887.
264. Sung, J.Y., et al., *WAVE1 controls neuronal activity-induced mitochondrial distribution in dendritic spines*. Proceedings of the National Academy of Sciences of the United States of America, 2008. **105**(8): p. 3112-3116.
265. Ramadan, K., *p97/VCP- and Lys48-linked polyubiquitination form a new signaling pathway in DNA damage response*. Cell cycle (Georgetown, Tex.), 2012. **11**(6): p. 1062-1069.
266. Tan, J.M.M., et al., *Lysine 63-linked ubiquitination promotes the formation and autophagic clearance of protein inclusions associated with neurodegenerative diseases*. Human molecular genetics, 2008. **17**(3): p. 431-439.
267. Winner, B., et al., *Adult neurogenesis and neurite outgrowth are impaired in LRRK2 G2019S mice*. Neurobiology of disease, 2011. **41**(3): p. 706-716.
268. Helton, T.D., et al., *Pruning and loss of excitatory synapses by the parkin ubiquitin ligase*. Proceedings of the National Academy of Sciences of the United States of America, 2008. **105**(49): p. 19492-19497.

269. Amini, M., et al., *Conditional disruption of calpain in the CNS alters dendrite morphology, impairs LTP, and promotes neuronal survival following injury*. The Journal of neuroscience : the official journal of the Society for Neuroscience, 2013. **33**(13): p. 5773-5784.
270. Day, M., et al., *Selective elimination of glutamatergic synapses on striatopallidal neurons in Parkinson disease models*. Nature neuroscience, 2006. **9**(2): p. 251-259.